STRUCTURAL RELIABILITY OF JACKET PLATFORMS USING SECOND ORDER RELIABILITY METHOD

WAN YIN HUAN

UNIVERSITI TUNKU ABDUL RAHMAN

STRUCTURAL RELIABILITY OF JACKET PLATFORMS USING SECOND ORDER RELIABILITY METHOD

WAN YIN HUAN

A project report submitted in partial fulfilment of the requirements for the award of Bachelor of Engineering (Hons.) Environmental Engineering

Faculty of Engineering and Green Technology
Universiti Tunku Abdul Rahman

April 2015

DECLARATION

I hereby declare that this project is based on my original work except for citations and quotations which have been duly acknowledged. I also declare that it had not been previously and concurrently submitted for any other degree or award at UTAR or other institutions.

Signature : ________________________

Name : ________________________

ID No. : ________________________

Date : ________________________

APPROVAL OF SUBMISSION

I certify that this project report entitled **"STRUCTURAL RELIABILITY OF JACKET PLATFORMS USING SECOND ORDER RELIABILITY METHOD"** was prepared by **WAN YIN HUAN** has met the required standard for submission in partial fulfilment of the requirements for the award of Bachelor of Engineering (Hons.) Environmental Engineering at Universiti Tunku Abdul Rahman.

Approved by,

Signature : ________________________

Supervisor : Dr. Zafarullah Nizamani

Date : ________________________

ACKNOWLEDGEMENTS

I would like to thank everyone who had contributed to the successful completion of this project. I would like to express my gratitude to my research supervisor, Dr. Zafarullah Nizamani for his invaluable advice guidance and his enormous patience throughout the development of the research.

Besides that, I would also like to express my gratitude to my friends and family who supported and encouraged me throughout the completion of this paper.

STRUCTURAL RELIABILITY OF JACKET PLATFORMS USING SECOND ORDER RELIABILITY METHOD

ABSTRACT

Jacket platform is the base structure for offshore oil processing topside structure which is used for continuous processing of crude oil. However, jacket platforms are subject to very harsh environments, subjected to extreme and operational conditions. Seawater comprises of salty and oxygenated water with high pH level that accelerates the process of corrosion and constant wave and current striking the jacket causes fatigue. This decreases the reliability index of the structure and increases the probability of failure of the structure at the same time. Due to the importance of the safety of structures, methods for the reliability assessment such as First-order Reliability Method (FORM), Second-order Reliability Method (SORM) and Monte Carlo Simulation (MCS) have been developed. This research will check the reliability of jacket elements under isolated and combined stresses by using Second Order Reliability Method which has not been used in previous studies.

TABLE OF CONTENTS

LIST OF TABLES

LIST OF FIGURES

LIST OF SYMBOLS/ABBREVATIONS

A	cross-sectional area
C_h	critical hoop buckling coefficient
C_x	elastic critical buckling coefficient
d	still water depth
D	outside diameter of the member
D_r	diameter of the centroid of the composite ring section
D_l	dead load
D_{l_n}	nominal dead load
E	Young's modulus of elasticity
E_l	environmental load
E_{l_n}	nominal environmental load (100-year extreme)
f_b	representative bending strength
f_c	representative axial compressive strength
f_h	hoop stress due to hydrostatic pressure
f_t	tensile strength
F_{xc}	representative inelastic local buckling strength
F_{xe}	representative elastic local buckling strength
f_{yc}	representative local buckling strength

f_v	representative shear strength
F_b	allowable bending strength
F_{he}	representative elastic critical hop buckling strength
F_t	tensile stress
F_y	yield strength
FS	factor of safety
G	acceleration due to gravity
H_w	wave height
H_z	effective hydrostatic head
I_p	polar moment of inertia
I_c	required moment of inertia for the composite ring section
k	wave number
k_i	principal curvatures of the limit state at the minimum distance point
K	effective length factor in the y- or z- direction selected
L_l	live load
L_{l_n}	nominal live load
L	unbraced length in y- or z- direction
L_r	length of cylinder between cylinder rings
L_s	ring spacing
$M_{v,t}$	torsional moment due to factored actions
n	number/ type of load components
N_f	number of trials
p	hydrostatic pressure
P_f	probability of failure

Q	load
Q_i	nominal/ characteristic value of load
r	radius of gyration, $r = \sqrt(l/A)$
R	resistance normal variable
R_n	nominal resistance
S	Elastic modulus
SF_{hc}	safety factor against hydrostatic collapse
t	wall thickness of the member
V	beam shear due to factored actions, in force units
X_i	random variable in the original space
Y_i	random variable in the equivalent uncorrelated standard normal space
z	depth below still water including tide
Z	Plastic modulus
∅	resistance factor
$\emptyset_b$	partial resistance safety factor for bending strength
Φ	cumulative distribution function for a standard normal variable
β	safety index / reliability index
β_{FORM}	reliability index using FORM
λ	column slenderness parameter
ρ_w	density of sea water, $1025 kg/m^3$
${\sigma_{X_i}}^N$	equivalent normal standard deviation of X_i at the design point ${x_1}^*$
σ_z	standard deviation of the variable Z
τ_b	maximum beam shear stress due to forces from factored actions
τ_t	torsional shear stress due to forces in factored actions

${\mu_{X_i}}^N$	equivalent normal mean of X_i at the design point ${x_1}^*$
μ_z	mean of the variable Z
γ_D	dead load factor
$\gamma_{f,G1}$	partial action factor for permanent actions
γ_i	load factor (for uncertainty in load)
γ_L	live load factor
γ_w	environmental load factor
γ_{Rb}	partial resistance factor for bending strength
$\gamma_{R,v}$	partial resistance factor for shear strength
γ_t	load factor for axial tension
$\frac{\partial Z}{\partial X}$	partial derivative of a random variable X

API	American Petroleum Institution
C.O.V.	Coefficient of Variance
FORM	First Order Reliability Method
ISO	International Organization for Standard
LRFD	Load and Resistance Factor Design
MCS	Monte Carlo Simulation
SI	sensitivity index
SORM	Second Order Reliability Method
WSD	Work Stress Design

CHAPTER 1

INTRODUCTION

1.1 Background

Offshore platforms are structures made of materials such as steel and concrete (Sadeghi, 2007). They provide base for exploration and extraction of oil and gas from the earth crust. In general, the oil and gas platforms are built using numerous grades of high strength steel. There are several type of steel platforms and are categorized according to the function and also the water depth in which they will be functioning.

Offshore platforms are designed for installation in places far away from shoreline such as the open sea, lakes, and gulfs. Other than providing support to offshore oil production facilities, there are also many uses of offshore platforms which include oil exploration, support bridges and causeways, and ship loading and unloading. Among these applications, one of the most visible ones is provision of foundation for offshore oil production. At the platform, oil and gas extracted are separated at topside and then transported by tankers or through pipelines to shore for processing (Sadeghi, 2007).

Jacket platform, which is also known as template platform, is chosen in this study. This is because the total number of offshore platform in various gulf, bays, and oceans of the world is increasing annually, and most of the offshore platforms are of fixed jacket type platforms located in 32m to 200m depth for oil and gas exploration purposes (Raheem, 2013). Jacket platform consists mainly of jacket, decks, and piles (Sadeghi, 2007). There are more than 250 jacket platforms in Malaysia and this study will contribute to the economic development and life extension assessment process.

Structural reliability is associated with the calculation and prediction of the probability of limit-state violations at any stage throughout the lifetime of a structure. The probability of structural failure can be evaluated through determination of whether the limit-state functions are exceeded. After determination of the probability of failure, the next step is to choose design alternatives which will increase structural reliability and reduce the risk of failure (Choi, et al., 2007). Structural reliability methods can also be used to find the members which are truly critical and also if additional member can improve structural system reliability due to redistribution of load to adjacent members (Bucher & Bourgund, 1990).

Among reliability measures, both probability of failure and safety index are the significant ones. In order to calculate these measures, the use of limit-state function approximations is required, and Second-order Reliability Method (SORM) is chosen in this study. In previous studies First-order Reliability Method are used to find out reliability of jacket platform.

Codes which are applicable to jacket platforms include API LRFD, API WSD, and ISO 19902. These codes are based on component and joint reliability design. The assumption that the capacity of the platform has reached its limit when one component of jacket platform has failed is incorrect. Hence, the reassessment of old platforms component based approach is not feasible. However because all design codes are based on component reliability and due to this reason, in this study it will be determined for single stresses and combined stresses.

1.2 Problem Statements

Jacket platform is the base structure for offshore oil processing topside structure which is used for continuous processing of crude oil. However, jacket platforms are subjected to very harsh environments. Seawater comprises of salty and oxygenated water. Besides that, seawater also has high pH level which makes the process of corrosion become faster. Other than that, constant wave and current striking on the jacket causes fatigue. This decreases the reliability index of the structure and increases the probability of failure of the structure at the same time (Salau et al., 2011). In addition, due to high cost of replacement, a large number of existing jacket platforms are operating beyond their design life.

However, a structure or a part of the structure will not be able to perform as required if a part of the structure exceeds a specific limit which is known as limit-state. A structure is considered as unreliable when the probability of failure of the structure limit-state is larger than the required value (Choi, et al., 2007). Hence, in order to prevent unexpected failure, there is a need to closely monitor the structural reliability of the platforms. The safety of offshore platforms is important and due to this, the development of effective methods for reliability assessment of jacket structures are needed (Salau, et al., 2011).

Besides that, ISO code requires that environmental load factors for offshore structures should be developed for each region as the international codes of API LRFD and API WSD have been developed using calibration of North Sea and Gulf of Mexico. Hence, develop of environmental load factors for offshore structure in each region is necessary (ISO 19902, ISO 19901).

1.3 Aims and Objectives

The objectives of this study are as follows:

1) To determine the structural reliability of Jacket platform in Malaysia for isolated and combined stresses
2) To determine the environmental load factor of Jacket platform in Malaysia by using Second Order Reliability Method analysis to compare the results with the FORM analysis

1.4 Variables of Reliability

In order carry out reliability analysis of jacket platform, the first procedure is to carry out uncertainty modelling. According to Marlet et al., this is because the reliability analysis is remarkably dependent on the uncertainty modelling. Structural reliability depends on resistance uncertainties and also load uncertainties. Load uncertainty is more specifically linked to environmental loads and it is more severe compared to live load and dead load because of the unpredictable weather conditions. Wind, wave and current are the primary environmental load uncertainty parameters, and wave is the dominating load among them. In general, as time increases, loads uncertainty tends to increase, while resistance uncertainties tends to decrease. Hence, load and resistance uncertainties increases with time (Nizamani et al., 2014).

1.4.1 Resistance

Uncertainties of resistance are yield strength, diameter of component and thickness of member. The collected data is statistically analyzed for resistance uncertainty and the parameters to be analyzed are the material and geometric variables. Modelling uncertainty is predicted and the model uncertainty relies on the statistical parameters for basic variables such as diameter of component, thickness of member and yield strength (Nizamani et al., 2014).

1.4.2 Load

Basic random variable variations modelled for reliability analysis are related to load. The load can be a single load or combined loads. The service lifecycle of offshore structures are exposed to two conditions, namely the environmental condition and also the functional condition. Both of the conditions may lead to serious consequences, varying from the fatigue of structural members, up to the collapse of the entire structure. There are several types of loads, which include the environmental loads, gravity loads which include permanent and variable live loads and accidental loads. For load uncertainties, due to unpredictable weather conditions, environmental loads are more severe compared to other type of loads. Both individual and combined actions of environmental loads, which are wind, wave and current, are considered especially in extreme conditions analysis (Abayomi, 2012).

1.5 Outline of Report

In this report first chapter introduces the research study and its significance. The second chapter is about literature review. Here in this chapter overview of relevant and latest literature available has been made and gaps in the research work are highlighted. The third chapter describes methodology of the research. In this chapter outline of the methodology is explained which is to be applied for this research is explained. Fourth chapter provides results and discussion of the research. Fifth and last chapter provides conclusion and major findings of this study.

CHAPTER 2

LITERATURE REVIEW

2.1 Introduction

This chapter provides a literature review for the past research made for the reliability analysis. The reliability analysis can be made for different types of sensitive structures such as bridges, dams, nuclear power plants and offshore structures. The available gaps in the literature have been mentioned briefly.

2.2 Types of Offshore Structures

In order to obtain oil and gas in locations with greater water depth, different types of offshore structural system are developed to deal with the requirement. Offshore platforms can be divided into two types, which are the movable or floating offshore platforms that can move from place to place, and fixed platforms which is able to physically attach to the seafloor in shallow water, whereby the ‘legs’ which can be made of steel or concrete extending to the bottom and fixed to the seafloor by using piles from the platform. Moveable offshore drilling platforms are usually used for exploratory purpose. This is due to the reason that compared to permanent platform, usage of moveable offshore drilling platforms are much lower in term of cost. When large deposits of petroleum and natural gas are discovered, a fixed platform is then built to extract the petroleum and natural gas (Speight, 2014). Some of important platforms are discussed in following sections.

There are various types of offshore structures which include jack-up platform, submersible rig, semi-submersible rig and compliant tower. Jack-up platform is moved to the drilling site through towing, and the legs are then lowered until they positioned on the bottom of the sea and the continued jacking down of the legs once the seafloor has been reached will then results in the raising the jacket mechanism and the entire barge and drilling structures will then be slowly elevated beyond the water surface up to a height which is predetermined. Submersible rig and semi-submersible rig works through inflating and deflating of their lower hull, whereby the lower hull is occupied with air, and results in the buoyancy of the entire rig when the platform is to be moved from one location to another location. The air in the lower hull is then let out after the rig is placed at the drill site, and the rig will submerge to the lake or ocean floor. The main difference is that the rig does not submerge to the seafloor when the air in the hull is released out. Compliant tower consists of a narrow, flexible tower and a piled foundation which can support a conventional deck for drilling and production operations. The use of flex elements deamplifies wave forces and reduces resonance. (Speight, 2014)

2.2.1 Template (Jacket) Platform

The most common type of production platform in shallow water is the fixed piled structure known as jacket. These are steel framed tubular structures fixed to the seafloor by the means of drilled or driven and grouted piles. If water depth exceeds the limit, floating production platform and compliant tower are more functional and efficient (Speight, 2014).

The top side structure consist of drilling equipment, production equipment, crew quarters, eating facilities, revolving cranes, gas flare stacks, survival craft, and a helicopter landing pad. Within the jacket framing, there are conductor guides in which the drill pipes and production pipes are conveyed from bottom to the topside in order to transfer the crude oil and natural gas, in which the crude oil and natural gas travel from the reservoir which situated at the bottom of the seafloor, through the production riser and transferred to topside for processing prior to transporting to onshore refinery or a storage facility. The design life of this structure is typically twenty five years followed by the requirement to remove and dispose of the platform once the reservoir is depleted (Speight, 2014).

2.3 Types of Uncertainties

2.3.1 General Types of Uncertainties

Uncertainties create variations in resistance which will then eventually leads to major effect on the reliability analysis of jacket platform. Uncertainties can be divided into four types in offshore engineering, which are the aleatory, epistemic, model-related and human error based (Nizamani, 2015).

2.3.1.1 Aleatory Uncertainties

The aleatory type of uncertainties are related to inherent or physical randomness Physical randomness is always present in the nature such as wind, wave and current and it is very difficult to be forecasted (Nizamani, 2015).

2.3.1.2 Epistemic Uncertainties

The epistemic type of uncertainties is related to statistical or lack of knowledge. It is related to the limited amount of available data to be analyzed such as yield stress, diameter and thickness of member. Epistemic uncertainties can be improved by increasing the amount of data (Nizamani, 2015). Besides that, since epistemic uncertainty is related to the lack of knowledge, in other words, it can also be reduced by increasing the knowledge of the profession about the area of interest (Bulleit, 2008).

2.3.1.3 Model Uncertainties

Model uncertainties are related to the shortage of understanding and simplification of the equation given by the codes for the calculation of the stresses or forces in the element (Nizamani, 2015).

2.3.1.4 Human Uncertainties

Human error uncertainties are based on knowledge of a person upon designing, construction and operation of the structure (Nizamani, 2015).

2.3.2 Uncertainties for Reliability Analysis

Uncertainties deal with loading which shall be considered for design, and also resistance, which is about the amount of load in which the structure is able to withstand. Due to the variation of geographic location and design life of jacket, the largest waves in which the jacket will be exposed to during the expected design life of the jacket are different. This extreme and rare wave height for jacket design is assumed to take place once every 100 years. In other words, the probability of occurrence is 0.01 in one year (Nizamani, 2015).

Structure fails if the characteristic value of load surpasses the characteristic load carrying capacity. In general, load tends to increase as time passes while resistance tends to decrease as time passes. In other words, load and resistance uncertainty increases with time. The uncertainty of load and material needs to be taken into consideration in order to utilize the component, joint and the overall system of jacket platform effectively. The stochastic or probabilistic analysis method is required for randomness of load and uncertainty in structural materials (Nizamani, 2015). For reliability analysis, uncertainties can be categorized into three categories which are the resistance, load and stress model uncertainties. Resistance uncertainty can then be subdivided into material and geometric, load uncertainty is subdivided into wave, wind and current, while stress model uncertainty is subdivided into component and joint.

2.3.2.1 Resistance Uncertainty

Material or geometric variability results in uncertainties in capacity or member strength. Due to limitation in engineering theories to anticipate the component and system response and capacity, material uncertainties are used to measure statistical spread, and are evaluated by using the data obtained from fabrication yard and mill test reports. The load and resistance model uncertainties lead to safety factor which can accommodate for these uncertainties and results in a safe structure, by providing increased safety margin against structural deterioration and damage in the future (Nizamani, 2015).

Models of limit states are also prone to uncertainty. Limit states define the failure or safe region of a member. There are single or combined failure modes. For example, single failure mode is compression, while combined failure mode is compression along with bending. A component fails when it is incapable of resisting the loads. It can be due to deflection, yielding, or buckling. Statistics for resistance include the characteristics of material and geometrical properties.

Table 2.1 shows the type of resistance uncertainties for jacket platforms, which include material, geometric, fatigue and corrosion uncertainties together with some examples. However, types of uncertainty used for reliability analysis only include material and geometric uncertainties which are discussed in the following section.

Table 2.1 Type of resistance uncertainties for jacket platforms

Types of resistance uncertainty	Example
Material uncertainty	Yield strength, modulus of elasticity, elongation, tensile strength
Geometric uncertainty	Diameter, thickness
Fatigue uncertainty	Degradation of material
Corrosion uncertainty	Degradation of material

2.3.2.1.1 Material Uncertainty

Material uncertainties relates to the randomness due to material variations. Elongation, modulus of elasticity, yield strength and tensile strength are considered as material uncertainty. Material uncertainty can be dealt properly through application of controlled manufacturing and fabrication of material by using international standards and quality control.

2.3.2.1.2 Geometric Uncertainty

Geometric uncertainty relates to the randomness due to geometrical variations. Geometrical uncertainty includes diameter, thickness, length and effective length ratio (Nizamani, 2015).

2.3.2.2 Physical Stress Model

Model uncertainty is due to deviation of material strength, from component or joint stress bias with respect to actual strength acquired from tests results. Model uncertainty accounts for possible deviation of model assumptions of the resistance of a given section from the actual resistance of geometrical properties. The load model may also show variation due to natural variation in loads.

Model uncertainty is relate to the lack of knowledge, information or unavailability of software, and can be reduced by applying more detailed methods. Table 2.2 shows the uncertainties in model predictions.

Table 2.2: Uncertainties in model predictions

Component		Joint
Tension	Tension and bending	Tension
Compression column buckling	Compression (column buckling) and bending	Compression
Compression local buckling	Compression (local buckling) and bending	In-plane bending
Shear	Tension and bending and hydrostatic pressure	Out-plane bending
Bending	Compression (column buckling), bending and hydrostatic pressure	
Hydrostatic	Compression (local buckling) and hydrostatic pressure	

2.3.2.3 Load Uncertainty

The characteristics of structural design are reliant on load uncertainty, or environmental loads to be more specific. Platforms are designed to resist three types of loads to which they are subjected to, which are the environmental loads such as wind, wave and currents, dead loads such as weight of structure, and live loads such as weight of consumable supplies and the weight of fluid in the pipes and also tanks.

2.3.2.3.1 Wave

Jacket platforms are inherently more sensitive to waves compared to wind and current. This is because peak response always occurs at the time of maximum wave height (Grant et al., 1995). Significant wave height, which is the average wave height of the highest one-third of the waves, is the most important measure during a conventionally short time period of 20 minutes for a sea state to be considered as statistically stationary.

2.3.2.3.2 Wind

Wind could have significant effect on the design of jacket platforms, and it could induce large amount of forces on exposed parts during storm condition. Wind force arises from drag of air on component and from the difference in pressure on windward and leeward sides. The effect of wind force depends on size and shape of structural members and also on wind speed (University of Surrey, 2000). Wind load can be modelled as deterministic quantity for jacket platforms (Petrauskas, 1994) (Fugro GEOS, 2001). This is due to the reason that wind force is a small part, which is less than 5-10% of wave force (Fugro GEOS, 2001) (Grant et al., 1995). Wind is responsible for the generation of surface waves (Johannessen, K., et al., 2002), and influences the build-up of waves which can take significant time, for example many hours. This shows that short-term variation of wind speed and sea-elevation may be considered independently (Moses, 1981).

2.3.2.3.3 Current

Currents can play a significant role in the total forces acting on jacket platform. Current refers to motion of water which arises from sources other than surface waves, in which tidal currents arise from astronomical forces, while wind-drift currents arise from the drag of local wind on water surface (Heideman, et al., 1989). When extreme waves along with superimposed current occur in the same direction, velocities from both wind and waves can combine and produce large wave pressure (Thomas, et al., 1976).

2.4 Methods of Structural Reliability

2.4.1 First-order Reliability Method (FORM)

First-order Reliability Method (FORM) usually works well when the limit-state surface has only one minimal distance point and the function is nearly linear in the neighborhood of the design point. Nevertheless, probability of failure estimated using FORMs safety index may be unreasonable and inaccurate if the failure surface has large curvature or high nonlinearity (Lee and Kim, 2007).

FORM is one of the methods which is using reliability index and can be used to calculate the probability of failure. This method is according to the first-order Taylor series approximation of a limit state function, in which it is defined as in Equation 2.1.

$$Z = R - Q \tag{2.1}$$

Where:

R = Resistance normal variable

Q = load normal variable

By the assumption of resistance and load are statistically independent, normally distributed and random variables, and the variable Z is also normally distributed, the failure occurs when resistance is smaller than load and results in the variable Z to be less than 0. The failure probability given is as shown is Equation (2.2).

$$PF = P[Z < 0] \tag{2.2}$$

$$= \int_{-\infty}^{0} \frac{1}{\sigma_z\sqrt{2\pi}} \exp\{-\frac{1}{2}\left(\frac{Z-\mu_z}{\sigma_z}\right)^2\}dZ$$

$$= \int_{-\infty}^{-\beta} \frac{1}{\sqrt{2\pi}} \exp\{-\frac{U^2}{2}\}dU = \Phi(-\beta)$$

Where:

μ_z = mean of the variable Z

σ_z = standard deviation of the variable Z

Φ = cumulative distribution function for a standard normal variable

β = safety index / reliability index

The coefficient of variation is denoted as below:

$$\beta = \frac{\mu_z}{\sigma_z} = \frac{\mu_R - \mu_L}{\sqrt{{\sigma_R}^2 + {\sigma_L}^2}}, \qquad C.O.V = \frac{\sigma_x}{\mu_x} \tag{2.3}$$

Equation 2.3 can be used when the system has a linear limit state function. However, most real systems and cases do not have a linear limit state function, but a nonlinear state function. Hence, for systems with nonlinear state function cannot be used to calculate the reliability index (Lee and Kim, 2007).

Rackwitz and Fiessler proposed a method to estimate reliability index for a system having a nonlinear limit state function, where the loop is to be iterated to determine reliability index until the reliability index converges to a desired value, which can be less than or equal to 0.001 (Lee and Kim, 2007).

The sensitivity index which is used to evaluate the effect of random variables on the probability of failure is denoted as below:

$$SI = \frac{(\frac{\partial Z}{\partial X})}{\left(\sqrt{\Sigma(\frac{\partial Z}{\partial X})^2}\right)} \tag{2.4}$$

Where:

$\frac{\partial z}{\partial x}$ = partial derivative of a random variable X

2.4.2 Second-order Reliability Method (SORM)

The computations required for the reliability analysis of problems with linear limit state equations are relatively simple. However, the limit state could be nonlinear due to the nonlinear relationship between the random variables in the limit state equation or due to some variables being non-normal. If any of the variables is non-normal, a linear limit state equation in the original space becomes nonlinear when transformed to the standard normal space, which is where the search for the minimum distance point is made. Besides that, the transformation from correlated to uncorrelated variables might induce nonlinearity (Achintya & Sankaran, 2000).

If the joint probability density function (PDF) of the random variables decays rapidly as one moves away from the minimum distance point, then the first-order estimate of failure probability is quite accurate. On the other hand, if the decay of the joint PDF is slow and the limit state is highly nonlinear, then one has to use a higher-order approximation for the failure probability computation (Achintya & Sankaran, 2000).

In FORM approach which uses only a first-order approximation at the minimum distance point, the curvature of the nonlinear limit state is ignored. Hence, the curvature of the limit state around the minimum distance point determines the accuracy of the first-order approximation in FORM. The curvature of any equation is related to the second-order derivatives with respect to the basic variables. Thus, the second-order reliability method (SORM) improves the FORM result by including additional information about the curvature of the limit state.

The Taylor series expansion of a general nonlinear function $g(X_1, X_2, \dots, X_n) = g(x_1{}^*, x_2{}^*, \dots, x_n{}^*)$ at the value $(x_1{}^*, x_2{}^*, \dots, x_n{}^*)$ is as denoted in Equation (2.5) where the derivatives are evaluated at the design point of the X_1's.

$$SI = \frac{(\frac{\partial Z}{\partial X})}{\left(\sqrt{\Sigma(\frac{\partial Z}{\partial X})}^{2}\right)} g(X_1, X_2, \dots, X_n) \tag{2.5}$$

$$= g(x_1{}^*, x_2{}^*, \dots, x_n{}^*) + \sum_{i=1}^{n} (x_i - x_i{}^*) \frac{\partial g}{\partial X_i}$$

$$+ \frac{1}{2} \sum_{i=1}^{n} \sum_{j=1}^{n} (x_i - x_i{}^*)(x_j - x_j{}^*) \frac{\partial^2 g}{\partial X_i \partial X_j} + \cdots$$

The variables $X_1, X_2, \dots, X_n$ are used in Equation (2.5) in a generic sense. One should use the appropriate set of variables and notation depending on the space being considered. In the case of reliability analysis, the second-order approximation to g( ) is being constructed in the space of standard normal variables, at the minimum distance point (Achintya & Sankaran, 2000).

The following notation is used in this section, whereby X_i refers to a random variable in the original space, and Y_i refers to the random variable in the equivalent uncorrelated standard normal space. If all the variables are uncorrelated, Equation (2.6) is to be used (Achintya & Sankaran, 2000).

$$Y_i = \frac{\left(X_i - \mu_{X_i}{}^N\right)}{\sigma_{X_i}{}^N} \tag{2.6}$$

Where:

$\mu_{X_i}{}^N$ = equivalent normal mean of X_i at the design point $x_1{}^*$

$\sigma_{X_i}{}^N$ = equivalent normal standard deviation of X_i at the design point $x_1{}^*$

FORM ignores the terms beyond the first-order term involving first-order derivatives, and SORM ignores the terms beyond the second-order term involving the second-order derivatives (Achintya & Sankaran, 2000).

2.4.2.1 Breitung's Formula

A simple closed-form solution for the probability computation using a second-order approximations, P_{f_2} was given by Breitung using the theory of asymptotic approximation as denoted in Equation (2.7) (Achintya & Sankaran, 2000).

$$P_{f_2} \approx \Phi(-\beta_{FORM}) \prod_{i=1}^{n-1} (1 + \beta k_i)^{-1/2} \tag{2.7}$$

Where:

k_i = principal curvatures of the limit state at the minimum distance point

β_{FORM} = reliability index using FORM

Breitung showed that this second-order probability estimate asymptotically approaches the first-order estimate as β approaches infinity, given that βk_i remains constant. (Achintya & Sankaran, 2000)

Breitung's SORM method uses a parabolic approximation which does not use a general second-order approximation in Equation (2.5). Besides that, is uses the theory of asymptotic approximation to derive the probability estimate. The downside of this method is that the asymptotic formula is only accurate for large values of β, which is the case for practical high-reliability problems. If the value of β is low, the SORM estimate could be inaccurate. Tvedt (1990) developed two alternative SORM formulations to take care of these problems. Tvedt's method uses a parabolic and a general second-order approximation to the limit state and it does not use asymptotic approximations (Achintya & Sankaran, 2000).

2.4.2.2 Tvedt's Formula

Tvedt has derived a three-term approximation for this equation by a power series expansion in term of $\frac{1}{2} = \sum_{i=1}^{n-1} k_i {y_i'}^2$, ignoring terms higher than two, and the resulting approximation for probability of failure is as shown in Equation (2.8d) (Choi et al., 2006).

$$A_1 = \Phi(-\beta) \prod_{i=1}^{n-1} (1 + \beta k_i)^{-1/2} \quad (2.8a)$$

$$A_2 = [\beta\Phi(-\beta) - \emptyset(\beta)]\{\prod_{i=1}^{n-1} (1 + \beta k_i)^{-\frac{1}{2}} - \prod_{i=1}^{n-1} (1 + (\beta + 1)k_i)^{-\frac{1}{2}}\} \quad (2.8b)$$

$$A_3 = (\beta + 1)[\beta\Phi(-\beta) - \emptyset(\beta)]\{\prod_{i=1}^{n-1} (1 + \beta k_i)^{-1/2}\} \quad (2.8c)$$

$$P_f = A_1 + A_2 + A_3 \quad (2.8d)$$

2.4.2.3 Curvature Fitting Method with Computation of the Hessian

In the curvature fitting SORM, the approximated second-order limit state surface is defined by matching its principal curvatures to the principal curvatures of the limit state surface at the design point. The principal curvature of the limit state surface is obtained as the eigenvalues of the rotational transformed second-order derivative matrix which is also known as the Hessian matrix of the performance function in standard normal space (Yan-Gang & Tetsuro, 1999).

If the second-order surface in u-space has been obtained, the failure probability is given as the probability content outside the second-order surface. Various formulas have been derived in closed form for the paraboloid approximation which includes numerical integration method, importance sampling updating method, and more accurate closed form formulas were derived using McLaurin series expansion and Taylor series expansion. In general, these formulas work well in the case of large curvature radius and a small number of random variables (Yan-Gang & Tetsuro, 1999).

However, the computation of the Hessian matrix is required in the application of the curvature fitting method, which can be very costly when the number of random variables is large and performance function involves complicated numerical algorithms. Besides that, rotational transformation and eigenvalue analysis of Hessian matrix for obtaining the principal curvature at the design point are quite complicated and time consuming, whereby the Hessian matrix is used to construct a paraboloid approximation of the limit state surface and compute a second-order estimate of the failure probability (Yan-Gang & Tetsuro, 1999).

2.4.2.4 Point Fitting Method

Since the computation of Hessian matrix is difficult and is time consuming, the problem is solved by deriving an efficient point-fitting algorithm in which the major principal axis of the limit state surface and the corresponding curvature are obtained in the course of obtaining the design point without computing the Hessian matrix and hence, an alternative point-fitting SORM was developed in which the performance function is directly point-fitted using a general form of the second-order polynomial of standard normal random variables in an iterative manner. Once the point-fitted limit state surface is obtained, the failure probability is conveniently obtained using the empirical second-order reliability index without any rotational transformation or eigenvalue analysis (Yan-Gang & Tetsuro, 1999).

2.4.3 Monte Carlo Simulation (MCS)

Monte Carlo Simulation (MCS) is also known as simple random sampling method, or statistical trial method that makes realizations based on randomly generated sampling sets for uncertain variables. Monte Carlo Simulation is also a great mathematical tool for the determination of approximate probability of a specific event which is the outcome of a series of stochastic process (Choi et al, 2006).

Monte Carlo method consists of digital generation of random variables and functions, statistical analysis of trial outputs, and variable reduction techniques. The computation procedure of MCS is somewhat simple whereby in the first step, distribution type for the random variable are to be selected, and in the second step, a sampling set from the distribution are to be generated, and the last step, simulations are being conducted by using the generated sampling set (Choi et al, 2006).

The idea of Monte Carlo method can be extended to structural reliability analysis. Firstly, the sampling set of the corresponding random variables are to be generated according to probability density functions. The subsequent step is to set the mathematical model of $g(\cdot)$ namely the limit state, which can determine the failures for drawing samples of the random variables. After conducting simulations using the generated sampling set, the probabilistic characteristics of the structure response can be obtained. The structure or structural element "failed" if the limit state function g(·) is violated. The trial is repeated a lot of times to guarantee convergence of the statistical results whereby in each trial, sample values can be digitally generated and analyzed (Choi et al, 2006).

If N trials are conducted, the probability of failure is denoted as in Equation (2.9):

$$P_f = \frac{N_f}{N} \tag{2.9}$$

Where:

N_f = number of trials for which g(·) is violated out of the N times the experiment is conducted.

2.5 Comparison of API WSD code with ISO LRFD code

In general, the main difference between the API WSD and ISO LRFD is that WSD follows the equation in which the resistance multiplied with safety factor shall be larger than the load.

$$\emptyset R > L$$

On the other hand, ISO LRFD follows the equation in which the resistance multiplied with safety factor shall be larger than the load which is multiplied with load factor. The value of ϕ is less than 1, while the value of γ is larger than 1 in general.

$$\emptyset R > \gamma L$$

Besides that, the API WSD uses yield stress, while ISO LRFD uses ultimate stress in the design.

2.6 Summary

In this chapter, section 2.1 states some of the types of offshore structures which are commonly used, which includes jack-up rig, submersible rig, semi-submersible rig, drillship, jacket platform, tower platform, and tension leg platform. Generally, different types of offshore structures are designed to be used in different water depth. Section 2.2 is discussion about the general type of uncertainties which include aleatory uncertainty, epistemic uncertainty, model uncertainty and human error, and also uncertainties in reliability analysis which include the load, resistance and stress model uncertainties. Load uncertainty consists of wave, wind and current, while resistance uncertainty consists of material and geometric uncertainties. Section 2.3 is the introduction of the methods of structural analysis, which includes the first-order reliability method (FORM), second-order reliability method (SORM) and Monte Carlo simulation (MCS). This research is conducted due to the requirements of ISO LRFD code which requires that for each geographical region separate load factor should be determined (ISO 19902).

CHAPTER 3

METHODOLOGY

3.1 Design Codes of Practice for Jacket Platforms

Structural design codes provide a set of minimum technical guideline for satisfactory design. Besides that, they also provide a path for research findings to create their way into practice of this field (Mangiavacchi et al, 2005).

In place of WSD, LRFD or limit state design has proved to be more rational due to the reason that it is based on probabilistic models. The jacket platforms reliability is maintained by API RP2A-LRFD by setting the same target safety factor as WSD designs. In other words, structures designed using LRFD code will have the same reliability with WSD, which has already provided safe structures and the best available practice for design (Idrus et al, 2011).

Knowledge of the strength equations in different codes and also the differences and similarities between different codes is useful for calibration. When adopting LRFD methodology, the process of calibration can optimize the appropriate load and resistance. The first step in the process of calibration is to determine the reliability of structural members of the jacket designed according to practice of design codes (Idrus et al, 2011).

3.1.1 API RP2A-WSD

In WSD, design safety factor is provided only on resistance side and the safety factor is based on judgement and experience. API WSD uses the same safety factor for all type of loads. The safety factor of API WSD was found empirically (ISO 19902, 2007). Allowable stresses in WSD are expressed either implicitly as a fraction of yield, or by the application of safety factor on critical buckling stress (Graff et al, 1994). In WSD strength of component or joint can be evaluated using Equation (3.1).

$$\frac{R}{FS} \geq D_l + L_l + E_l \tag{3.1}$$

Where:

R = resistance effect,

FS = factor of safety,

D_l = dead load,

L_l = live load,

E_l = environmental load

WSD method provide safety factor only to the resistance, without providing consideration to the uncertainties related to the loads, which can be shown in Equation (3.2).

$$Q < \emptyset R \tag{3.2}$$

Where:

Q = load,

$\emptyset$ = safety factor of material strength

Material strength safety factor covers the randomness of load and material. The factor of safety takes into consideration the uncertainties as shown in Equation (3. 3).

$$FS = \frac{R}{Q} \tag{3.3}$$

Where:

R = resistance

Q = load

The structure is safe if the resistance is larger than load. However, if resistance is smaller than load, structure failure will occur.

There are some major drawbacks in WSD. In WSD, design resistance is divided by only factor of safety, without taking into consideration regarding the uncertainties due to load action which results WSD being excessive conservative thus do not provide engineers any insight of degree of risk or design safety of jacket platform. Besides that, WSD do not have risk balance capabilities, and there is little justification for safety factors. Other than that, uncertainty using deterministic factor of safety could lead to inconsistent reliability levels and may results in over design. The main disadvantage of using deterministic measure includes structural model uncertainty, uncertainty of external loads, and human error. (Nizamani, 2015) Besides that, deterministic safety factors do not provide adequate information to achieve optimal use of the available resources to maximize safety (Haldar & Mahadevan, 2000).

3.1.2 API RP2A-LRFD / ISO 19902

API RP2A-LRFD was published in 1993 and ISO LRFD was published in 2007. Compared to API WSD which uses the same safety factor for all type of loads, API LRFD and ISO use different safety factor based on each type of stresses (ISO 19902, 2007). In LRFD, load and resistance are factored using uncertainty. LRFD is defined as balanced design as it provides a balanced allocation of resources. (Pradnyana et al, 2000) Besides that, LRFD provides a safe and economically efficient way of designing jackets to different environmental conditions. Other than that, it also incorporates regional and geographical conditions in the design (Nizamani, 2015). Equation (3.4) shows the load combination equation.

$$\emptyset R_n \geq \gamma_D D_{l_n} + \gamma_L L_{l_n} + \gamma_w E_{l_n} \tag{3.4}$$

Where:

R_n = nominal resistance,

γ_D = dead load factor,

D_{l_n} = nominal dead load,

γ_L = live load factor,

L_{l_n} = nominal live load,

γ_w = environmental load factor,

E_{l_n} = nominal environmental load (100-year extreme)

LRFD format can be denoted in more general way as shown in Equation (3.5).

$$\emptyset R = \sum_{i=1}^{n} \gamma_i Q_i \tag{3.5}$$

Where:

$\emptyset$ = resistance factor (for uncertainty in stress)

R = nominal/ characteristic value of resistance

γ_i = load factor (for uncertainty in load)

Q_i = nominal/ characteristic value of load

n = number/ type of load components (gravity load and environmental load)

Compared to WSD, in which design resistance is divided by factor of safety, LRFD takes into consideration the inherent natural uncertainties in resistance in component and applied action. Due to this discrepancy, LRFD design method has been introduced to replace WSD. (Theophanatos & Wickham, 1993)

3.2 Types of Stresses in Offshore Structures

3.2.1 Axial Tension

Table 3.1 shows the comparison of equation between API RP2A-WSD, API RP2A-LRFD and ISO 19902. In WSD, the allowable axial tension, $F_t = 0.6 \times F_y$ this equation is based on American Institute of Steel Construction (AISC) and has remained unchanged since 1969. On the other hand, the equation for axial tension is the same for both API RP2A-LRFD and ISO 19902. The safety factor in API RP2A-LRFD and ISO 19902 is larger than API RP2A-WSD due to low consequences of tension yielding. Axial tension acts independently as a governing stress and occurs very rarely for offshore structures. The safety factors have to be removed from the equations for comparison of equations so that they will be on par with each other. Table 3.2 shows the comparison of equations after removing safety factors. (Idrus et al, 2011)

Table 3.1 Comparison of axial tension equations

(Source: adapted from MSL Engineering Limited, 2001)

API RP2A-WSD	API RP2A-LRFD	ISO 19902
$F_t = 0.6 \times F_y$ Where: F_t = tensile stress Safety factor = 0.6 F_y = yield strength	$F_t = \emptyset_t \times F_y$ Where: F_t = tensile stress $\emptyset_t$ = 0.95 Safety factor = 0.95 F_y = yield strength	$F_t = \frac{f_t}{\gamma_t}$ Where: F_t = tensile stress f_t = tensile strength = f_y γ_t = 1.05

Table 3.2 Comparison of axial tension equations without safety factors

(Source: adapted from MSL Engineering Limited, 2001)

API RP2A-WSD	API RP2A-LRFD	ISO 19902
$F_t = F_y$	$F_t = F_y$	$F_t = f_y$

3.2.2 Axial Compression

3.2.2.1 Overall Column Buckling

Table 3.3 shows the comparison of equations for axial compression between API WSD, API LRFD and ISO. The WSD formula is based on American Institute of Steel Construction (AISC). On the other hand, the equations in LRFD and ISO are similar, with some differences which are the constant, limiting value and column slenderness parameter, λ. The value of constant is 0.25 in LRFD and 0.28 in ISO, while the limiting value for λ is $\sqrt{2}$ in LRFD and 1.34 in ISO. There is also a variation in the expressions for $\lambda > \sqrt{2}$ or 1.34 in which the expression in ISO is factored by 0.9. Although ISO takes 1.18 as safety factor whereas LRFD takes 0.85 as safety factor, however both become equal when safety factors are put in respective equations. Members with low diameter to thickness ratio are not subjected to local buckling under axial compression. The axial compressive stress of each section is obtained by dividing force or pressure by the respective cross-sectional area. (Idrus et al, 2011)

Table 3.3 Comparison of axial compression equations (overall column buckling)

(Source: adapted from MSL Engineering Limited, 2001)

API WSD	API LRFD	ISO
$F_a = \frac{\left[1-\frac{(Kl/r)^2}{2{C_c}^2}\right]F_y}{\frac{5}{3}+\frac{3(\frac{Kl}{r})}{8C_c}-\frac{(\frac{Kl}{r})^3}{8{C_c}^3}}$, Kl/r < C_c $F_a = \frac{12\pi^3 E}{23(\frac{Kl}{r})^2}$, Kl/r ≥ C_c Where: $C_c = \left(\frac{2\pi^2 E}{F_y}\right)^{1/2}$ E = Young's Modulus of elasticity K = effective length factor l = unbraced length r = radius of gyration	$f_{cn} = (1.0 - 0.25\lambda^2)f_y$, $\lambda < \sqrt{2}$ $f_{cn} = \frac{f_y}{\lambda^2}$, $\lambda > \sqrt{2}$ $\lambda = \frac{KL}{\pi r}\sqrt{\frac{f_{yc}}{E}}$ Where: f_{cn} = representative axial compressive strength f_y = representative local buckling strength λ = column slenderness parameter E = Young's modulus of elasticity K = effective length factor in the y- or z-direction selected L = unbraced length in y- or z- direction r = radius of gyration, $r = \sqrt{\frac{l}{A}}$	$f_c = (1.0 - 0.278\lambda^2)f_{yc}$, $\lambda \leq 1.34$ $f_c = \frac{0.9}{\lambda^2}f_{yc}$, $\lambda > 1.34$ $\lambda = \frac{KL}{\pi r}\sqrt{\frac{f_{yc}}{E}}$ Where: f_c = representative axial compressive strength f_{yc} = representative local buckling strength λ = column slenderness parameter E = Young's modulus of elasticity K = effective length factor in the y- or z-direction selected L = unbraced length in y- or z- direction r = radius of gyration, $r = \sqrt{\frac{l}{A}}$

Table 3.4 Comparison of axial compression equations (local buckling)

(Source: adapted from MSL Engineering Limited, 2001)

API WSD	API LRFD	ISO
$F_{xe} = 2C_x\ Et/D$ $F_{xc} = F_y \times \left[1.64 - 0.23(D/t)^{1/4}\right]$ D/t > 60 $F_{xc} = F_y$ D/t ≤ 60 Where: F_y = representative yield strength F_{xe} = representative elastic local buckling strength F_{xc} = representative inelastic local buckling strength C_x = elastic critical buckling coefficient E = Young's modulus of elasticity D = outside diameter of the member t = wall thickness of the member	$F_{xe} = 2C_xEt/D$ $F_{xc} = F_y \times \left[1.64 - 0.23(D/t)^{1/4}\right]$ D/t > 60 $F_{xc} = F_y$ D/t ≤ 60 Where: F_y = representative yield strength F_{xe} = representative elastic local buckling strength F_{xc} = representative inelastic local buckling strength C_x = elastic critical buckling coefficient E = Young's modulus of elasticity D = outside diameter of the member t = wall thickness of the member	$F_{yc} = F_y$ $\frac{F_y}{F_{xe}} \leq 0.170$ $F_{yc} = \left(1.047 - 0.274\frac{F_y}{F_{xe}}\right)$ $0.170 < \frac{F_y}{F_{xe}} < 1.911$ $F_{xe} = 2C_xEt/D$ Where: F_y = representative yield strength F_{xe} = representative elastic local buckling stength f_{yc} = representative local buckling strength strength C_x = elastic critical buckling coefficient E = Young's modulus of elasticity D = outside diameter of the member t = wall thickness of the member

32
32

3.2.2.2 Local buckling

Local buckling stress is taken equal to yield stress. Circular members with low diameter to thickness, D/t ratio are not subjected to local buckling under axial compression and are designed with respect to material failure. However, as D/t ratio increases, elastic buckling strength decreases. Hence, member should be checked for local buckling when D/t ratio increases. (Idrus et al, 2011)

3.2.3 Bending

The bending strength equation for WSD is $0.75F_y$ for $D/t \leq 10340/F_y$. The equations for ISO and LRFD are basically the same. In comparison of the design resistance formula of partial safety factor, ISO design resistance is $\frac{1}{1.05}$ while LRFD is 0.95. By dividing the partial safety factor of FRFD to ISO's, 100% is obtained. (Idrus et al, 2011)

$\frac{0.95}{\frac{1}{1.05}} = 100\%$ of LRFD resistance

The comparison of bending equations in WSD, LRFD and ISO codes are shown in Table 3.5.

Table 3.5 Comparison of bending equations

(Source: adapted from MSL Engineering Limited, 2001)

API WSD	API LRFD	ISO
$F_b = 0.75F_y$ D/t < 10340/F_y $F_b = (0.84 - \frac{1.74F_yD}{Et})F_y$ 10340/F_y < D/t < 20680/F_y $F_b = (0.72 - \frac{0.58F_yD}{Et})F_y$ 20680/F_y < D/t < 300 Where: F_y = representative yield strength F_b = allowable bending strength D = outside diameter of the member E = Young's modulus of elasticity t = wall thickness of the member member	$f_b \leq \emptyset_b F_b$ ($\emptyset_b$ = 0.95) $F_b = (\frac{Z}{S})F_y$ D/t<10340/F_y $F_b = (1.13 - \frac{2.58F_yD}{Et})(\frac{Z}{S})F_y$ 10340/F_y < D/t < 20680/F_y $F_b = (0.94 - \frac{0.76F_yD}{Et})(\frac{Z}{S})F_y$ 20680/F_y < D/t < 300 Where: Z = Plastic modulus S = Elastic modulus F_y = representative yield strength F_b = allowable bending strength D = outside diameter of the member t = wall thickness of the member member $\emptyset_b$ = partial resistance safety factor for bending strength	$f_b \leq F_b/\gamma_{Rb}$ (γ_{Rb}= 1.05) $F_b = (\frac{Z}{S})F_y$ F_yD/E/t <0.0517 $F_b = (1.13 - \frac{2.58F_yD}{Et})(\frac{Z}{S})F_y$ 0.0517<F_yD/E/t<0.1034 $F_b = (0.94 - \frac{0.76F_yD}{Et})(\frac{Z}{S})F_y$ 0.1034 < F_yD/E/t < 120F_y/E Where: Z = Plastic section modulus S = Elastic section modulus F_y = representative yield strength F_b = allowable bending strength f_b = representative bending strength D = outside diameter of the member γ_{Rb} = partial resistance factor for bending strength

3.2.4 Shear

3.2.4.1 Beam Shear

The equations in WSD, LRFD and ISO are similar when the factors are removed. In WSD, the allowable beam shear is taken as 0.4 times the yield strength, while the representative shear strength, f_v is:

$$\tau_b = \frac{2V}{A} \leq \frac{f_v}{\gamma_{R,v}} \tag{3.6}$$

Where:

τ_b = maximum beam shear stress due to forces from factored actions

f_v = representative shear strength, in stress units, $f_v = \frac{f_y}{\sqrt{3}}$

$\gamma_{R,v}$ = partial resistance factor for shear strength, $\gamma_{R,v}$=1.05 in ISO, 0.95 in LRFD

V = beam shear due to factored actions, in force units

A = cross-sectional area

The partial resistance factor in ISO is 1.05 while the partial resistance factor in LRFD is 0.95, which is the same in ISO, whereby:

$\frac{1}{1.05} \approx 0.95.$

3.2.4.2 Torsional Shear

Similar to beam shear, the equations in WSD, LRFD and ISO are similar when the partial factors are removed. In WSD, the allowable beam shear is taken as 0.4 times the yield strength. The partial resistance factor in ISO is 1.05 while the partial resistance factor in LRFD is 0.95, which is the same in ISO. (Idrus et al, 2011)

$$\tau_t = \frac{M_{v,t}D}{2I_p} \leq \frac{f_v}{\gamma_{R,v}} \tag{3.7}$$

Where:

τ_t = torsional shear stress due to forces in factored actions

$M_{v,t}$ = torsional moment due to factored actions

I_p = polar moment of inertia, $I_p = \frac{\pi}{32}[D^4 - (D - 2t)^4]$

$\gamma_{R,v}$ = partial resistance factor for shear strength, $\gamma_{R,v}$=1.05 in ISO, 0.95 in LRFD

3.2.5 Hydrostatic Pressure

For F_{hc} , equations are given for elastic stress ranges. By comparing the design resistance formula of LRFD and ISO with respect to partial factor of safety, the ISO design resistance is 100% of LRFD design resistance in which:

$\frac{0.8}{\frac{1}{1.25}} = 100\%$

The expressions in LRFD and ISO are the same. However, LRFD provides only one equation for critical hoop buckling while ISO provides formula for 3 ranges of elastic hoop buckling strength. (Idrus et al, 2011) The design formula given in WSD is as denoted in Table 3.6.

Table 3.6 Comparison of hydrostatic pressure equations

(Source: adapted from MSL Engineering Limited, 2001)

API RP2A-WSD	API RP2A-LRFD	ISO 19902
$f_h \leq \frac{F_{hc}}{SF_{hc}}$	$p = \gamma_{f,G1}\rho_w g H_z$	$p = \gamma_{f,G1}\rho_w g H_z$
Where: f_h = hoop stress due to hydrostatic pressure p = hydrostatic pressure SF_{hc} = safety factor against hydrostatic collapse	Where: $\gamma_{f,G1}$ = partial action factor for permanent actions ρ_w = density of sea water, $1025 kg/m^3$ G = acceleration due to gravity H_z = effective hydrostatic head	

3.2.5.1 Design Hydrostatic Head

Equations for design hydrostatic head in WSD and LFRD are identical. In ISO, the equations are similar, but uses depth below still water surface including tide,z with positive measured upwards. Equation of design hydrostatic head for API WSD, API LRFD and ISO are denoted in Table 3.7.

Table 3.7 Comparison of design hydrostatic head equations

(Source: adapted from MSL Engineering Limited, 2001)

API WSD	API LRFD	ISO
$H_z = z + \frac{H_w}{2}\left(\frac{cosh[k(d-z)]}{\cosh(kd)}\right)$ Where: z = depth below still water including tide d = still water depth H_w = wave height k = wave number, $k = \frac{2\pi}{\lambda}$ Where: λ = wave length		$H_z = -z + \frac{H_w}{2}\left(\frac{cosh[k(d+z)]}{\cosh(kd)}\right)$ Where: z = depth of the member relative to still water level d = still water depth to the sea floor H_w = wave height k = wave number, $k = \frac{2\pi}{\lambda}$ Where: λ = wave length

3.2.5.2 Hoop Buckling Stress

The equations of elastic hoop buckling stress for WSD, LRFD and ISO are identical. However, API and ISO has different critical hoop buckling coefficient. The equation of elastic critical hoop buckling stress is denoted in Equation (3.8).

$$F_{he} = \frac{2C_h Et}{D} \tag{3.8}$$

Where:

F_{he} = representative elastic critical hop buckling strength

C_h = critical hoop buckling coefficient

E = Young's Modulus of elasticity

t = wall thickness of the member

Table 3.8 Values of elastic critical hoop buckling strength

(Source: adapted from MSL Engineering Limited, 2001)

<table>
<tr><th>API WSD</th><th>API LRFD</th><th>ISO</th></tr>
<tr><td colspan="2">$C_h = 0.44\, t/D$
$\mu \geq 1.6D/t$

$C_h = 0.44\left(\frac{t}{D}\right) + \frac{0.21(D/t)^3}{M^4}$
0.825D/t≤ μ <1.6D/t

$C_h = 0.736/(M - 0.636)$
3.5 ≤ μ < 0.825 D/t

$C_h = 0.755/(M - 0.559)$
1.5 ≤ μ < 3.5

$C_h = 0.8$
μ <1.5

Where:
Geometric parameter, $\mu = \frac{L_r}{D}(2D/t)^{1/2}$
Where:
L_r = length of cylinder between cylinder rings, diaphragms, or end connections
D = diameter for external rings
t = thickness of member</td><td>$C_h = 0.44\, t/D$
$\mu \geq 1.6\, D/t$

$C_h = \frac{0.44t}{D} + 0.21(D/t)^3\mu^4$
$0.825D/t \leq \mu < 1.6\, D/t$

$C_h = 0.737/(\mu - 0.579)$
$1.5 \leq \mu < 0.825\, D/t$

$C_h = 0.80$
$\mu < 1.5$

Where:
Geometric parameter, $\mu = \frac{L_r}{D}(2D/t)^{1/2}$
L_r= length of cylinder between cylinder rings, diaphragms, or end connections
D = diameter for external rings
t = thickness of member</td></tr>
</table>

3.2.5.3 Ring Stiffener Design

The equations of ring stiffener design for WSD, LRFD and ISO are identical. Circumferential stiffening ring size may be calculated using Equation (3.9) for internal rings and Equation (3.10) for external rings.

$$I_c = F_{he}\frac{tL_sD^2}{8E} \tag{3.9}$$

$$I_c = F_{he}\frac{tL_s{D_r}^2}{8E} \tag{3.10}$$

Where:

I_c = required moment of inertia for the composite ring section

L_s = ring spacing

D = outside diameter of the member

D_r = diameter of the centroid of the composite ring section

E = Young's modulus of elasticity

3.3 Environmental load factors using SORM

Component and joint reliability is used to find environmental load and resistance factors for jacket platform. At the moment, the environmental load and resistance factors used in ISO and API are calibrated for extreme environments, for example, in Gulf of Mexico Nova Scotia, which are the areas of hurricanes such as typhoons in Pacific Ocean, and severe winter storms (Nizamani, 2015).

The load and resistance factor in LRFD needs to be checked for site-specific conditions due to change of geographical and material fabrications. Hence, LRFD method brings out regional differences in variation to design for extreme and operating conditions. This results in variability of loads and affects the structural reliability which is measured by reliability index, β (Nizamani, 2015).

The environmental load factors can be decided by using target reliability, for example, in Figure 3.1 in which the target reliability is shown is by using target reliability. In this figure, the target reliability is shown by using API LRFD and ISO gives the reliability of new code, whereby the new code's reliability index at We/G ratio of 1.0 gives higher reliability compared to API WSD. This new code's higher reliability will then give the required load factor (Nizamani, 2015).

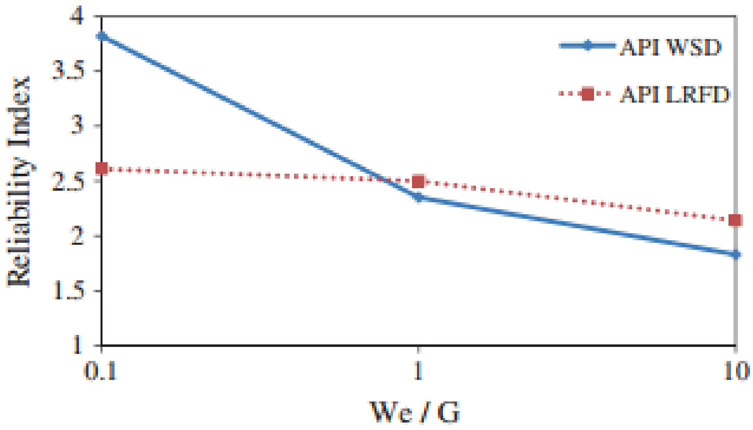

Figure 3.1 Variation of We/G ratio with reliability index for axial tension

(Source: adapted from Ferguson, 1990)

3.4 Target reliability

Target reliability levels are required for the utilization of LRFD method. Target reliability can be used to find the probability of failure of the structure in order to ensure that certain safety levels are achieved. After probability of failure is found, the value of load and resistance factors can then be determined. Reliability analysis is then used to check whether the structure or structural element has achieved the target reliability. The target reliability levels are different for each levels in currently used design practices, consequence and nature of failure, design life for the structure, and other political, economic and societal factors (Yusuke, et al., 2002).

3.4.1 Methods to find target reliability

In general, two approaches are used to find target reliability levels, first method is calibrated reliability levels which are implied in currently used codes, and the second method is cost benefit analysis (Yusuke, et al., 2002).

For the first approach, the target reliability level is based on the implied probability of failure or reliability level of structure in given codes or guidelines. The advantage of using code is that it can be applied in the determination of the minimum acceptable reliability level. The reliability level can be obtained through reliability analysis using probabilistic model by satisfying a specified code. The minimum value of target reliability depends on the nature and consequence of failure in which consequence is evaluated according to human injury, environmental impact and economical loss, while nature of failure is related to the type of structural failure. Besides that, in order to achieve target reliability, several cases of structural geometries, material properties and load conditions are to be considered and hence, the implied probability of failure or reliability level of structure may vary from one industry application to another (Gudfinnur , et al., 1996).

On the other hand, the second method is based on cost-benefit analysis. This method is effectively used in dealing with designs for which there is only economic losses and consequences due to failure, which include repair or replacement of facility, delay in operation, pollution damage, and fatalities and injury (Gudfinnur , et al., 1996).

3.4.2 Selection of target reliability

The annual target reliability and probability of failure of structure can be selected based on ISO code. The value of lifetime target reliability index in accordance with ISO coding is shown in Table 3.9.

Table 3.9 Values of lifetime target reliability index in accordance with ISO 2394, 1998

Relative costs of safety measures	Consequences of failure			
	Small	Some	Moderate	Great
High	0	1.5	2.3	3.1
Moderate	1.3	2.3	3.1	3.8
Low	2.3	3.1	3.8	4.3

3.5 Environmental to gravity load ratio (We/G)

Environmental to gravity load ratio (W_e/G) is the ratio of environmental load to gravity load. Gravity load is the addition of live load and dead load. When W_e/G ratio is high, it means that environmental load governs and if the W_e/G ratio is low, it means that gravity load governs. In this study, W_e/G ratio are varied to obtain reliability indices. The variation of W_e/G ratio is to find out the effects on reliability due to increasing in environmental load and decreasing in gravity load. In other words, it is to find out the effect on reliability when environmental load governs or gravity load governs. We/G ratio of 1.0 is chosen in this study as was determined by BOMEL (BOMEL Ltd, 2003).

CHAPTER 4

RESULTS AND DISCUSSION

4.1 Reliability index Vs Environmental to gravity load ratio

The variations of reliability index with respect to increasing in environmental to gravity load ratio using FORM and SORM are shown in Figure 4.1.1.1 to 4.1.1.14 for vertical diagonal member, Figure 4.1.2.1 to 4.1.2.14 for horizontal diagonal member, Figure 4.1.3.1 to 4.1.3.14 for horizontal periphery member, and Figure 4.1.4.1 to 4.1.4.14 for leg member. It can be seen that as environmental to gravity load ratio, W_e/G ratio increases, the steepness of the curve decreases. Besides that, reliability decreases as W_e/G ratio increases. The value of reliability indices are higher when gravity load governs compared to when environmental load governs.

4.1.1 Vertical Diagonal

4.1.1.1 Axial Tension

According to Figure 4.1.1.1, by using FORM, the value of reliability index when environmental load to gravity load ratio is equal to 1.0 using ISO code with load factor of 1.35 is 4.0424, while reliability index of ISO Malaysia with load factor of 1.23 is 3.8126. On the other hand, value of reliability index of WSD is 3.8684.

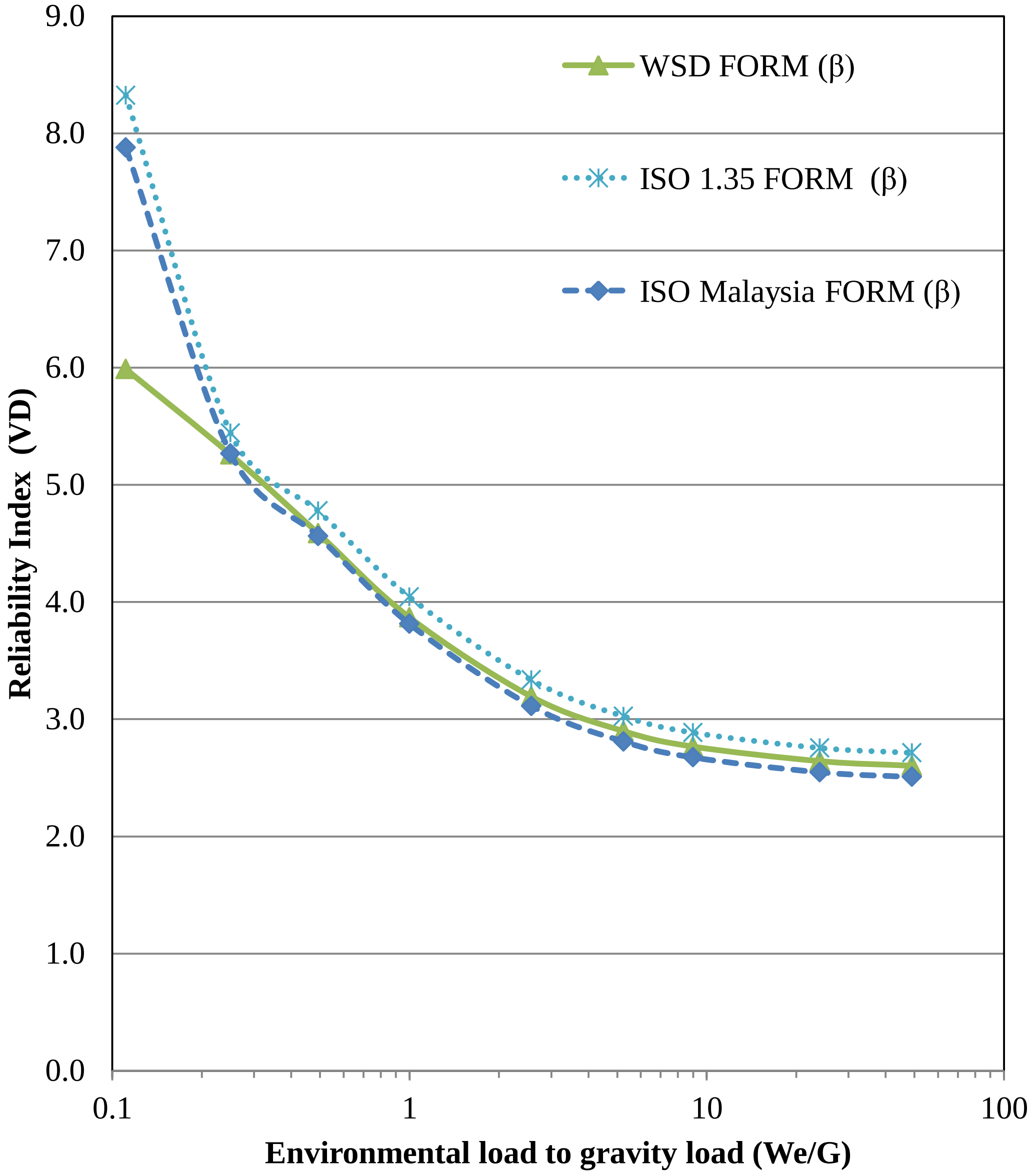

Figure 4.1.1.1 Graph of reliability index Vs environmental load to gravity load ratio for component under axial tension for vertical diagonal member using FORM

According to Figure 4.1.1.2, by using SORM, the value of reliability index when environmental load to gravity load ratio is equal to 1.0 using ISO code with load factor of 1.35 is 3.8911, while reliability index of ISO Malaysia with load factor of 1.23 is 3.6504. On the other hand, value of reliability index of WSD is 3.7112.

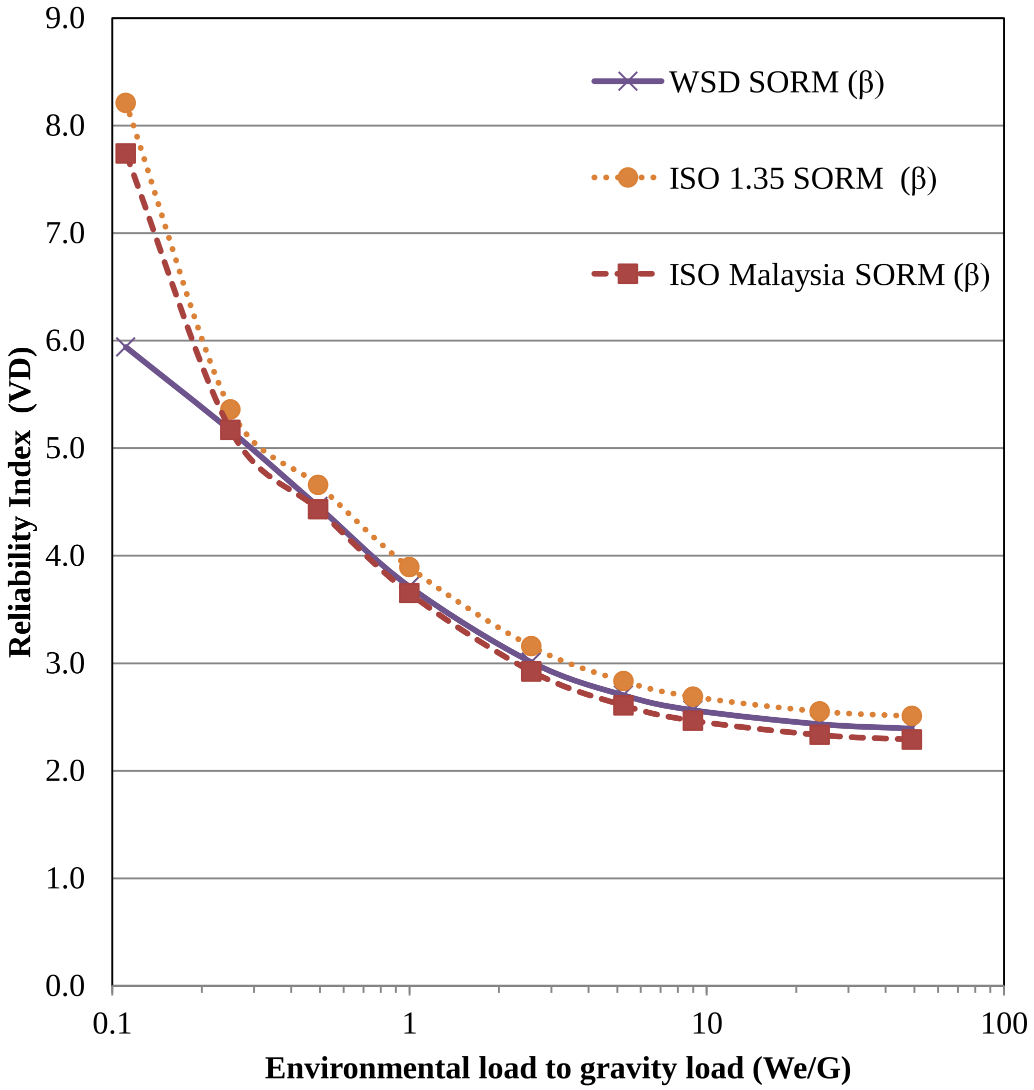

Figure 4.1.1.2 Graph of reliability index Vs environmental load to gravity load ratio for component under axial tension for vertical diagonal member using SORM

4.1.1.2 Axial Compression

According to Figure 4.1.1.3, by using FORM, the value of reliability index when environmental load to gravity load ratio is equal to 1.0 using ISO code with load factor of 1.35 is 4.3521, while reliability index of ISO Malaysia with load factor of 1.23 is 4.1455. On the other hand, value of reliability index of WSD is 4.0471.

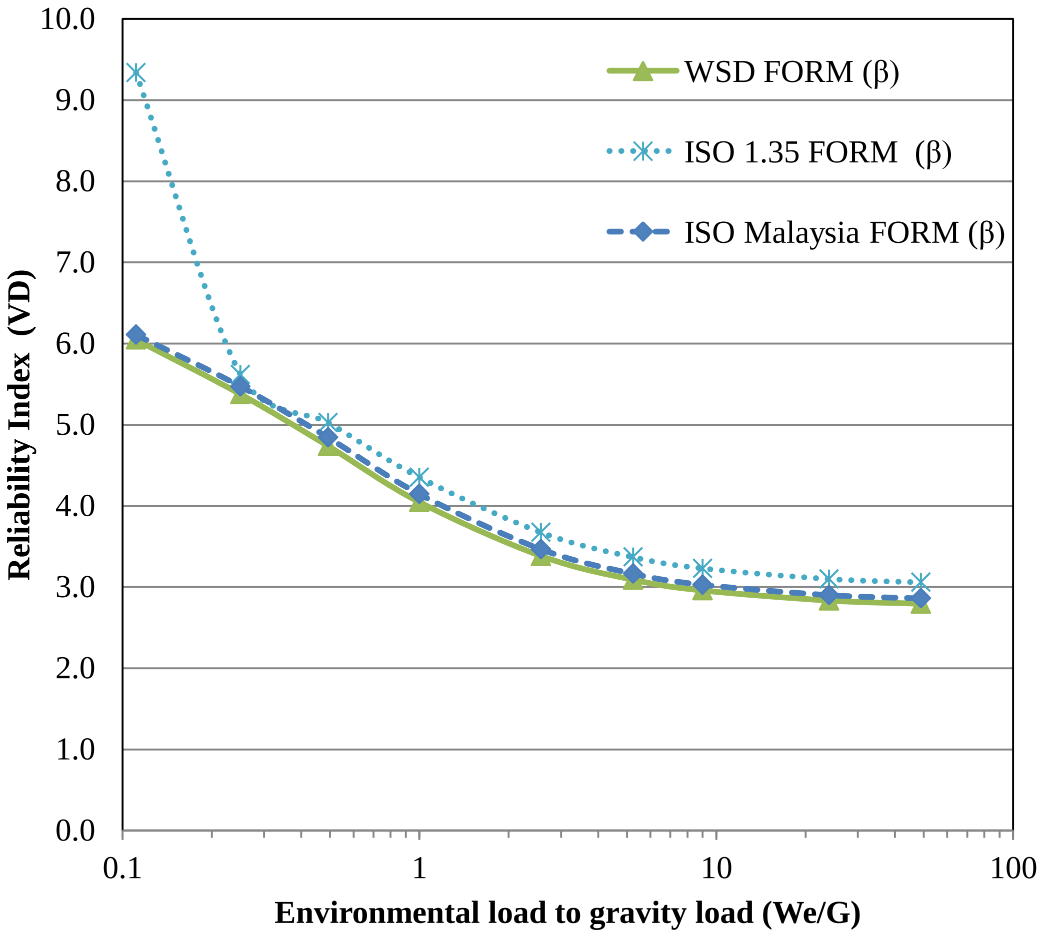

Figure 4.1.1.3 Graph of reliability index Vs environmental load to gravity load ratio for component under axial compression for vertical diagonal member using FORM

According to Figure 4.1.1.4, by using SORM, the value of reliability index when environmental load to gravity load ratio is equal to 1.0 using ISO code with load factor of 1.35 is 4.2121, while reliability index of ISO Malaysia with load factor of 1.23 is 3.995. On the other hand, value of reliability index of WSD is 3.8917.

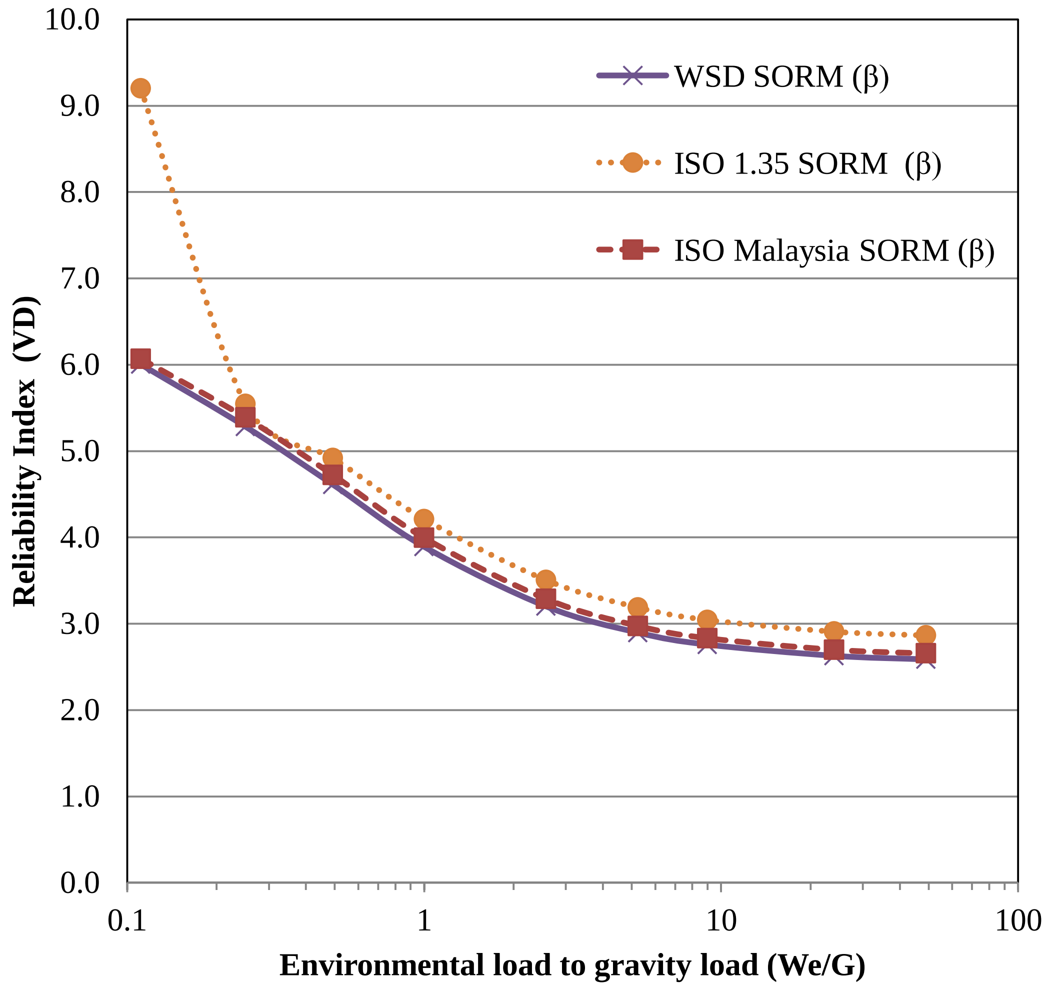

Figure 4.1.1.4 Graph of reliability index Vs environmental load to gravity load ratio for component under axial compression for vertical diagonal member using SORM

4.1.1.3 Bending

According to Figure 4.1.1.5, by using FORM, the value of reliability index when environmental load to gravity load ratio is equal to 1.0 using ISO code with load factor of 1.35 is 3.0663, while reliability index of ISO Malaysia with load factor of 1.23 is 2.7691. On the other hand, value of reliability index of WSD is 2.6576.

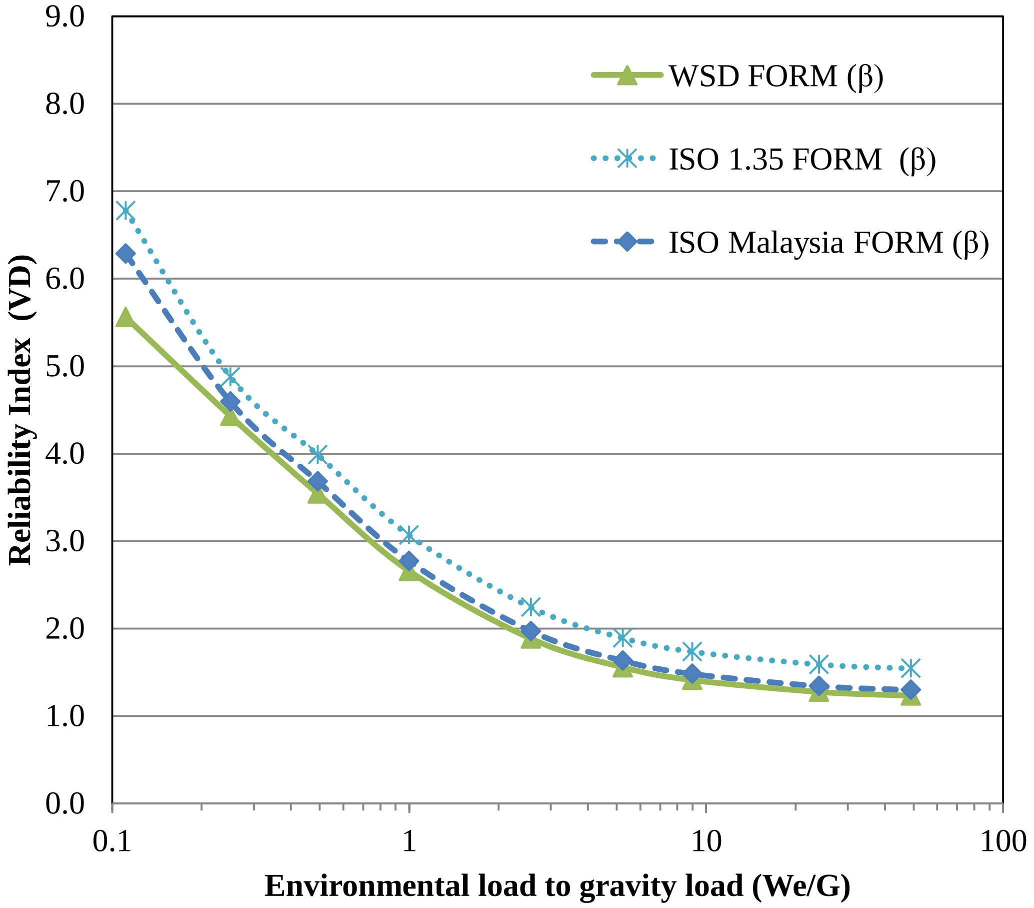

Figure 4.1.1.5 Graph of reliability index Vs environmental load to gravity load ratio for component under bending for vertical diagonal member using FORM

According to Figure 4.1.1.6, by using SORM, the value of reliability index when environmental load to gravity load ratio is equal to 1.0 using ISO code with load factor of 1.35 is 2.8219, while reliability index of ISO Malaysia with load factor of 1.23 is 2.5111. On the other hand, value of reliability index of WSD is 2.3962.

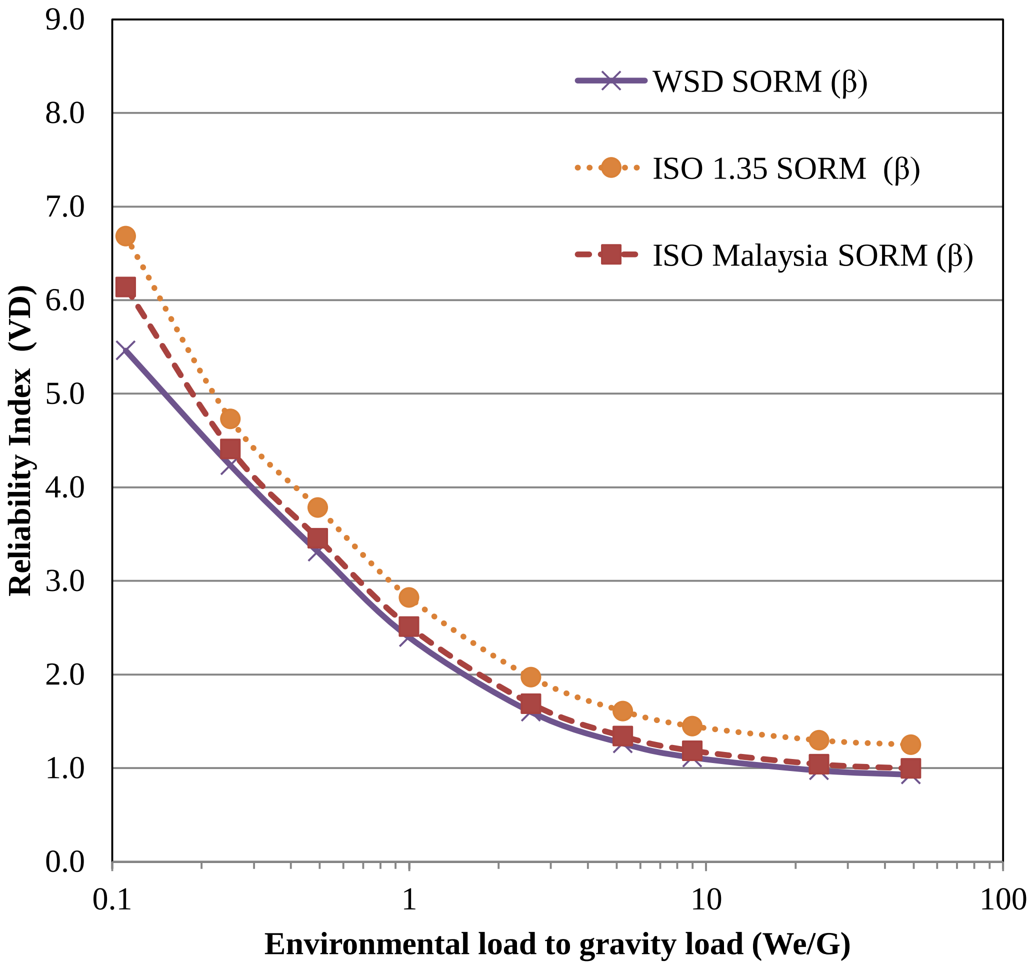

Figure 4.1.1.6 Graph of reliability index Vs environmental load to gravity load ratio for component under bending for vertical diagonal member using SORM

4.1.1.4 Tension and Bending

According to Figure 4.1.1.7, by using FORM, the value of reliability index when environmental load to gravity load ratio is equal to 1.0 using ISO code with load factor of 1.35 is 3.7422, while reliability index of ISO Malaysia with load factor of 1.23 is 3.4872. On the other hand, value of reliability index of WSD is 3.3369.

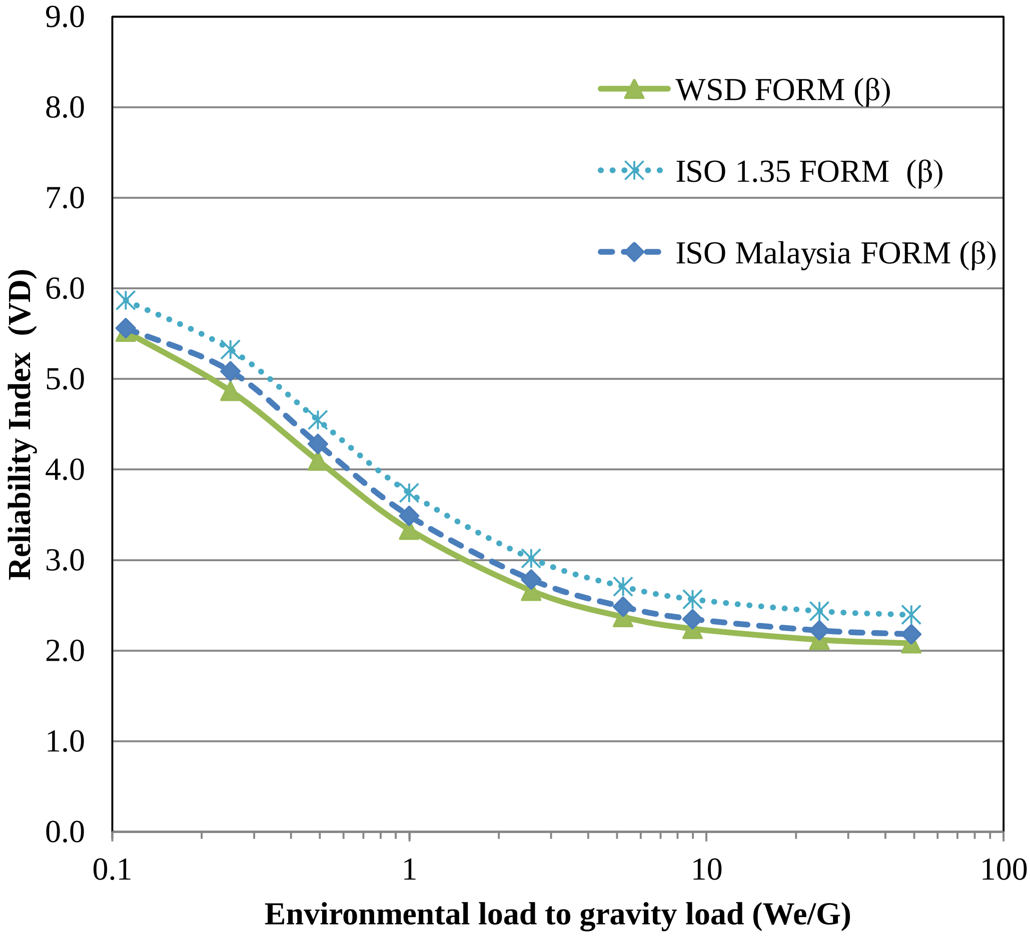

Figure 4.1.1.7 Graph of reliability index Vs environmental load to gravity load ratio for component under tension and bending for vertical diagonal member using FORM

According to Figure 4.1.1.8, by using SORM, the value of reliability index when environmental load to gravity load ratio is equal to 1.0 using ISO code with load factor of 1.35 is 3.5349, while reliability index of ISO Malaysia with load factor of 1.23 is 3.2697. On the other hand, value of reliability index of WSD is 3.1012.

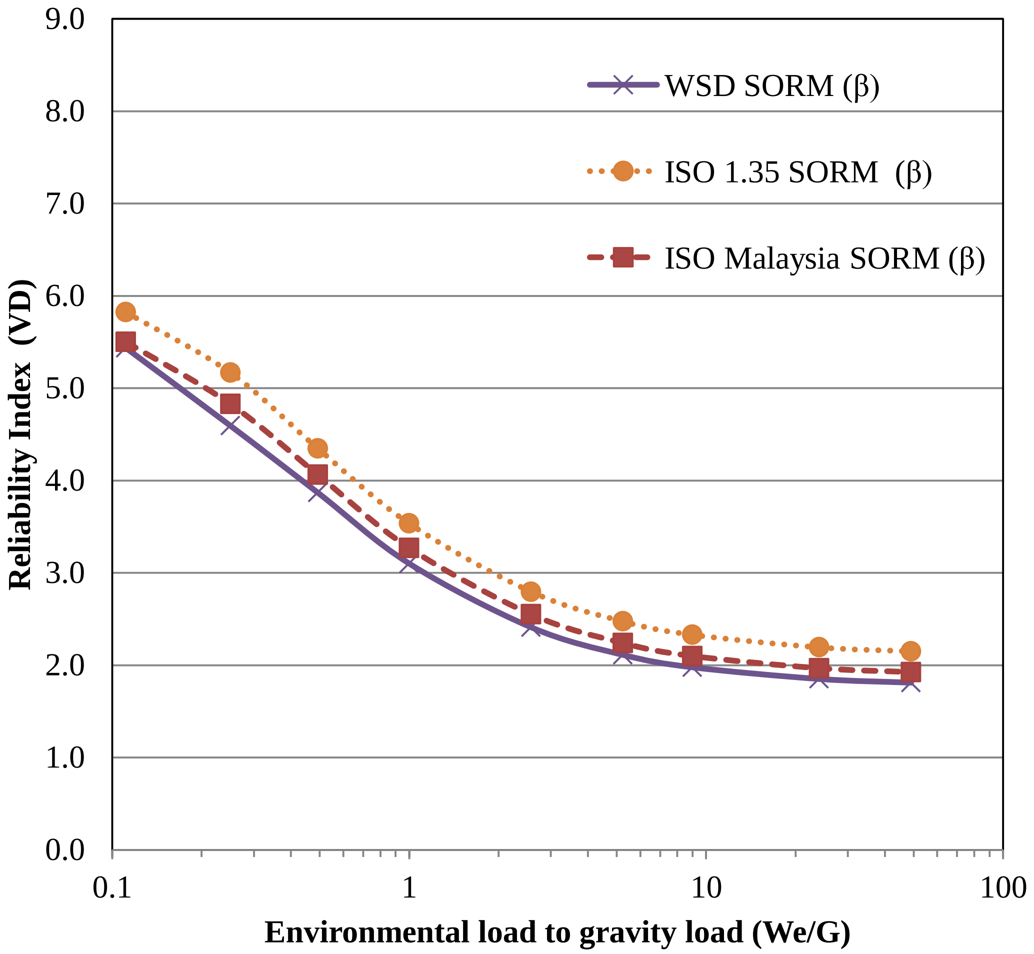

Figure 4.1.1.8 Graph of reliability index Vs environmental load to gravity load ratio for component under tension and bending for vertical diagonal member using SORM

4.1.1.5 Compression and Bending

According to Figure 4.1.1.9, by using SORM, the value of reliability index when environmental load to gravity load ratio is equal to 1.0 using ISO code with load factor of 1.35 is 3.8482, while reliability index of ISO Malaysia with load factor of 1.23 is 3.595. On the other hand, value of reliability index of WSD is 3.4501.

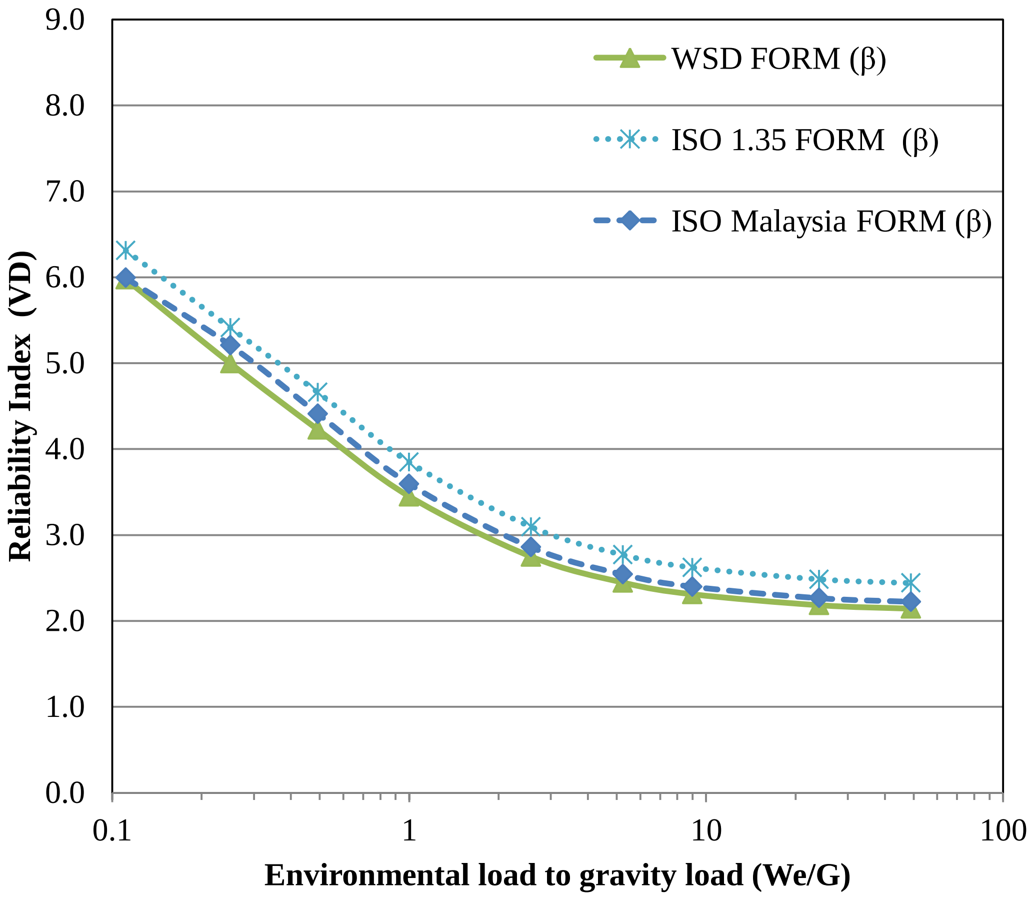

Figure 4.1.1.9 Graph of reliability index Vs environmental load to gravity load ratio for component under compression and bending for vertical diagonal member using FORM

According to Figure 4.1.1.10, by using SORM, the value of reliability index when environmental load to gravity load ratio is equal to 1.0 using ISO code with load factor of 1.35 is 3.6456, while reliability index of ISO Malaysia with load factor of 1.23 is 3.3802. On the other hand, value of reliability index of WSD is 3.213.

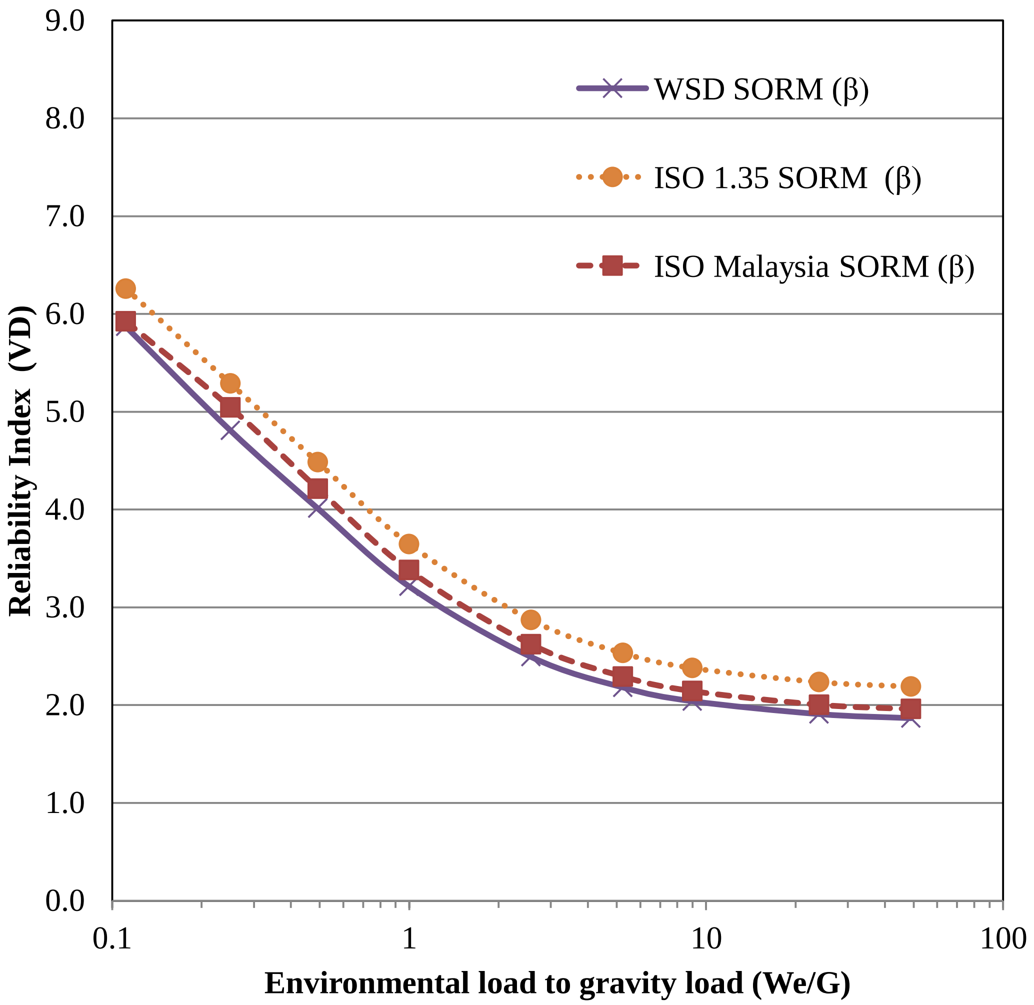

Figure 4.1.1.10 Graph of reliability index Vs environmental load to gravity load ratio for component under compression and bending for vertical diagonal member using SORM

4.1.1.6 Tension, Bending and Hydrostatic Pressure

According to Figure 4.1.1.11, by using FORM, the value of reliability index when environmental load to gravity load ratio is equal to 1.0 using ISO code with load factor of 1.35 is 4.0564, while reliability index of ISO Malaysia with load factor of 1.23 is 3.817. On the other hand, value of reliability index of WSD is 3.5653.

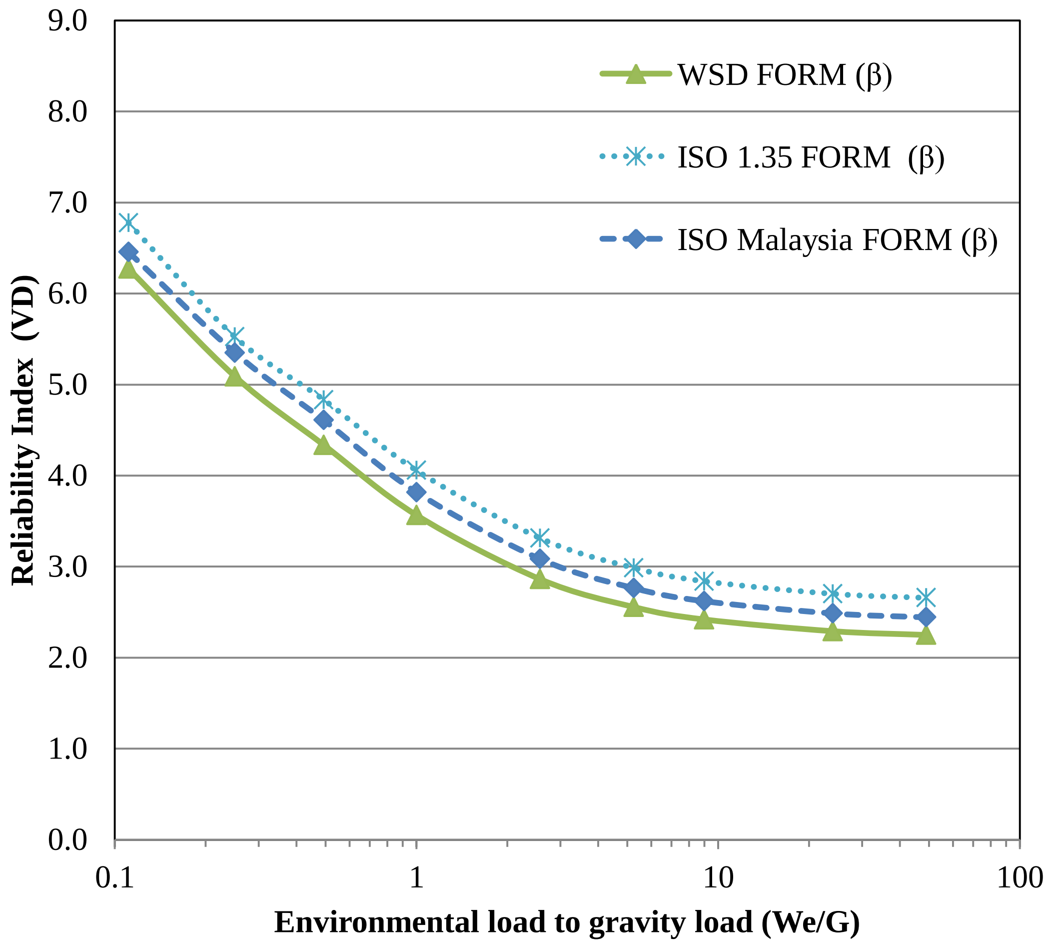

Figure 4.1.1.11 Graph of reliability index Vs environmental load to gravity load ratio for component under tension, bending and hydrostatic pressure for vertical diagonal member using FORM

According to Figure 4.1.1.12, by using SORM, the value of reliability index when environmental load to gravity load ratio is equal to 1.0 using ISO code with load factor of 1.35 is 3.8749, while reliability index of ISO Malaysia with load factor of 1.23 is 3.6234. On the other hand, value of reliability index of WSD is 3.3427.

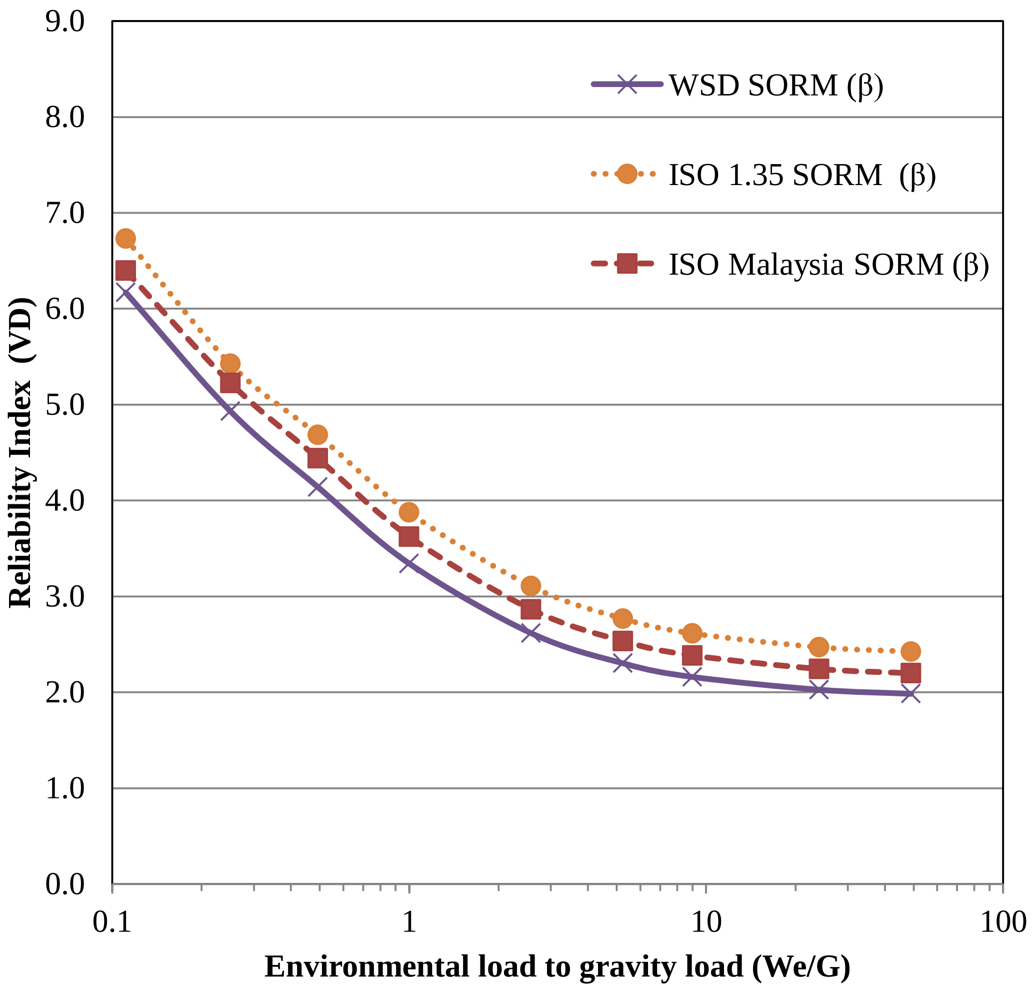

Figure 4.1.1.12 Graph of reliability index Vs environmental load to gravity load ratio for component under tension, bending and hydrostatic pressure for vertical diagonal member using SORM

4.1.1.7 Compression, Bending and Hydrostatic Pressure

According to Figure 4.1.1.13, by using FORM, the value of reliability index when environmental load to gravity load ratio is equal to 1.0 using ISO code with load factor of 1.35 is 4.5658, while reliability index of ISO Malaysia with load factor of 1.23 is 4.3652. On the other hand, value of reliability index of WSD is 4.2052.

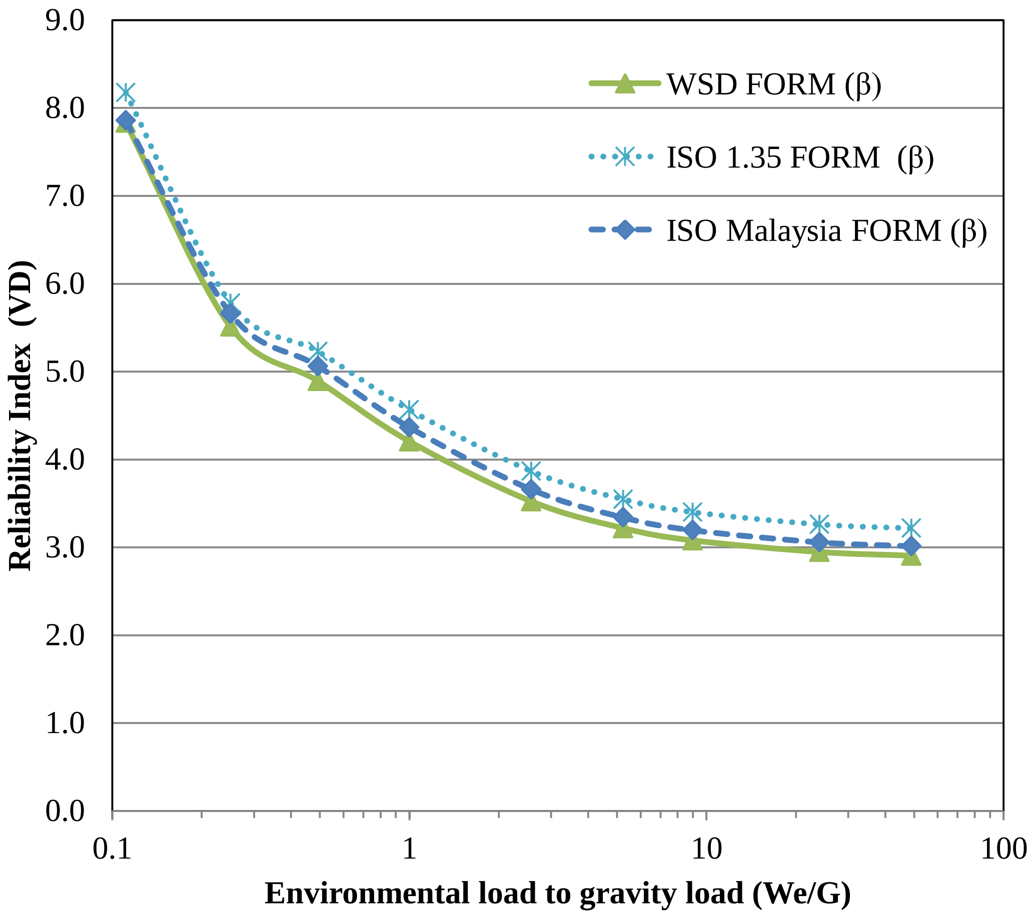

Figure 4.1.1.13 Graph of reliability index Vs environmental load to gravity load ratio for component under compression, bending and hydrostatic pressure for vertical diagonal member using FORM

According to Figure 4.1.1.14, by using SORM, the value of reliability index when environmental load to gravity load ratio is equal to 1.0 using ISO code with load factor of 1.35 is 4.4203, while reliability index of ISO Malaysia with load factor of 1.23 is 4.2075. On the other hand, value of reliability index of WSD is 4.0268.

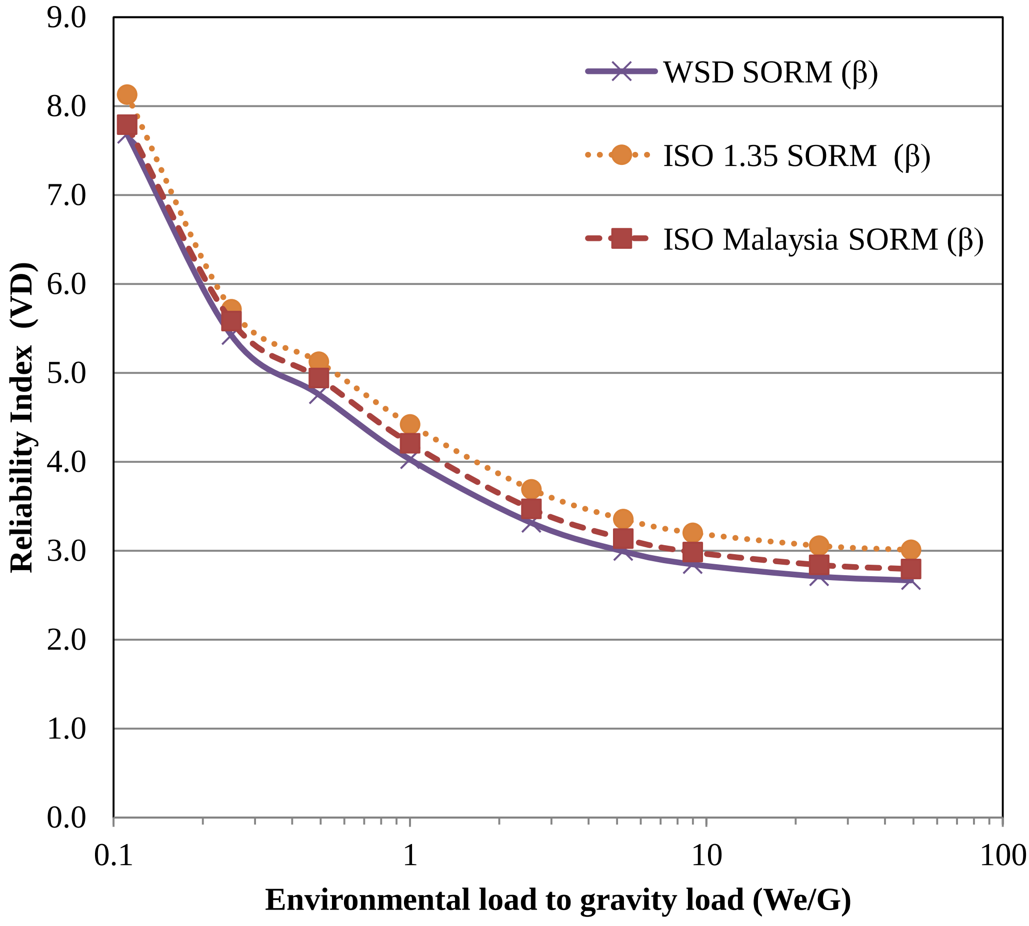

Figure 4.1.1.14 Graph of reliability index Vs environmental load to gravity load ratio for component under compression, bending and hydrostatic pressure for vertical diagonal member using SORM

4.1.2 Horizontal Diagonal

4.1.2.1 Axial Tension

According to Figure 4.1.2.1, by using FORM, the value of reliability index when environmental load to gravity load ratio is equal to 1.0 using ISO code with load factor of 1.35 is 3.0693, while reliability index of ISO Malaysia with load factor of 1.23 is 2.7673. On the other hand, value of reliability index of WSD is 2.8397.

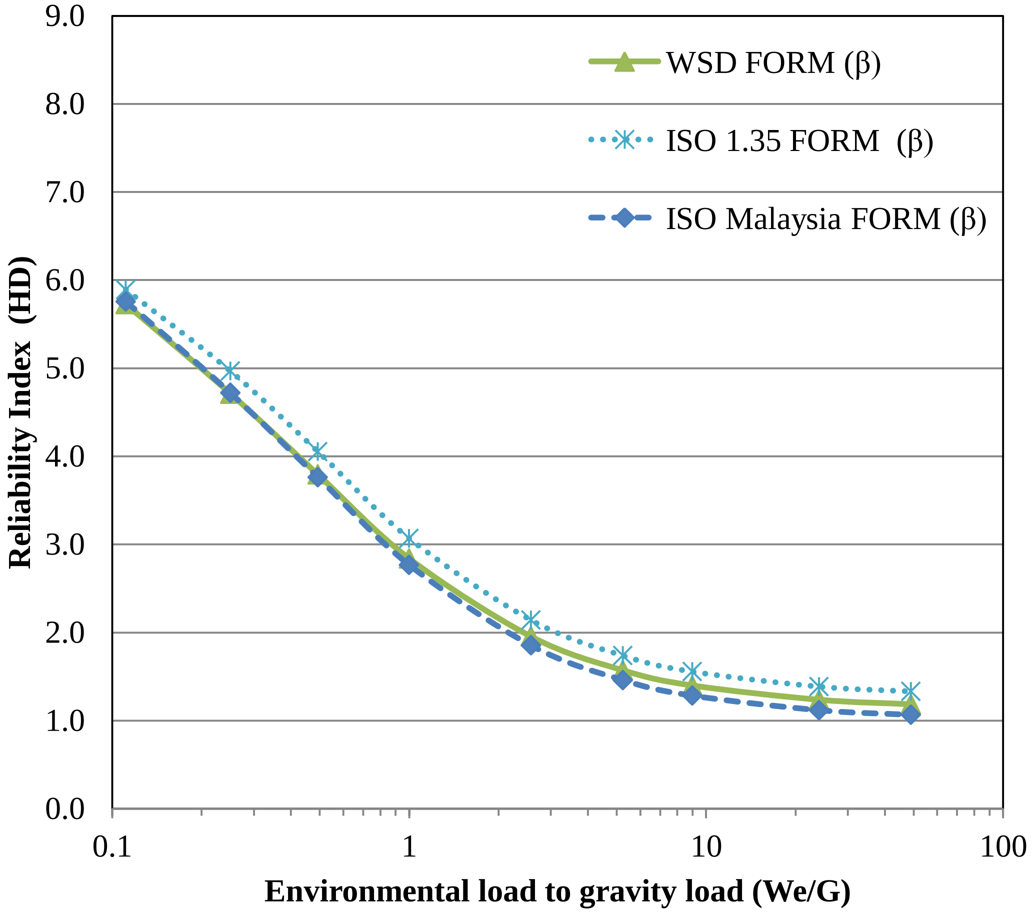

Figure 4.1.2.1 Graph of reliability index Vs environmental load to gravity load ratio for component under axial tension for horizontal diagonal member using FORM

According to Figure 4.1.2.2, by using SORM, the value of reliability index when environmental load to gravity load ratio is equal to 1.0 using ISO code with load factor of 1.35 is 2.9097, while reliability index of ISO Malaysia with load factor of 1.23 is 2.5978. On the other hand, value of reliability index of WSD is 2.6741.

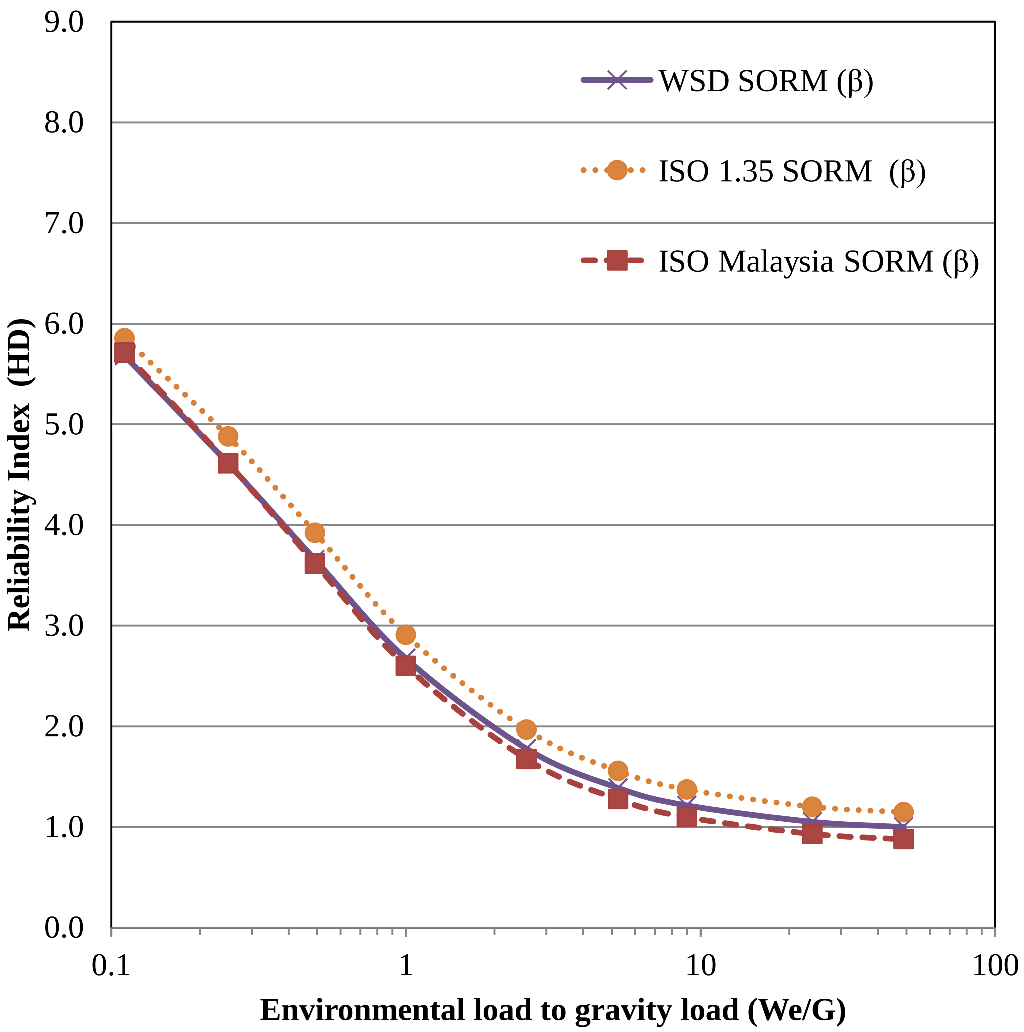

Figure 4.1.2.2 Graph of reliability index Vs environmental load to gravity load ratio for component under axial tension for horizontal diagonal member using SORM

4.1.2.2 Axial Compression

According to Figure 4.1.2.3, by using FORM, the value of reliability index when environmental load to gravity load ratio is equal to 1.0 using ISO code with load factor of 1.35 is 2.2379, while reliability index of ISO Malaysia with load factor of 1.23 is 2.0062. On the other hand, value of reliability index of WSD is 2.2763.

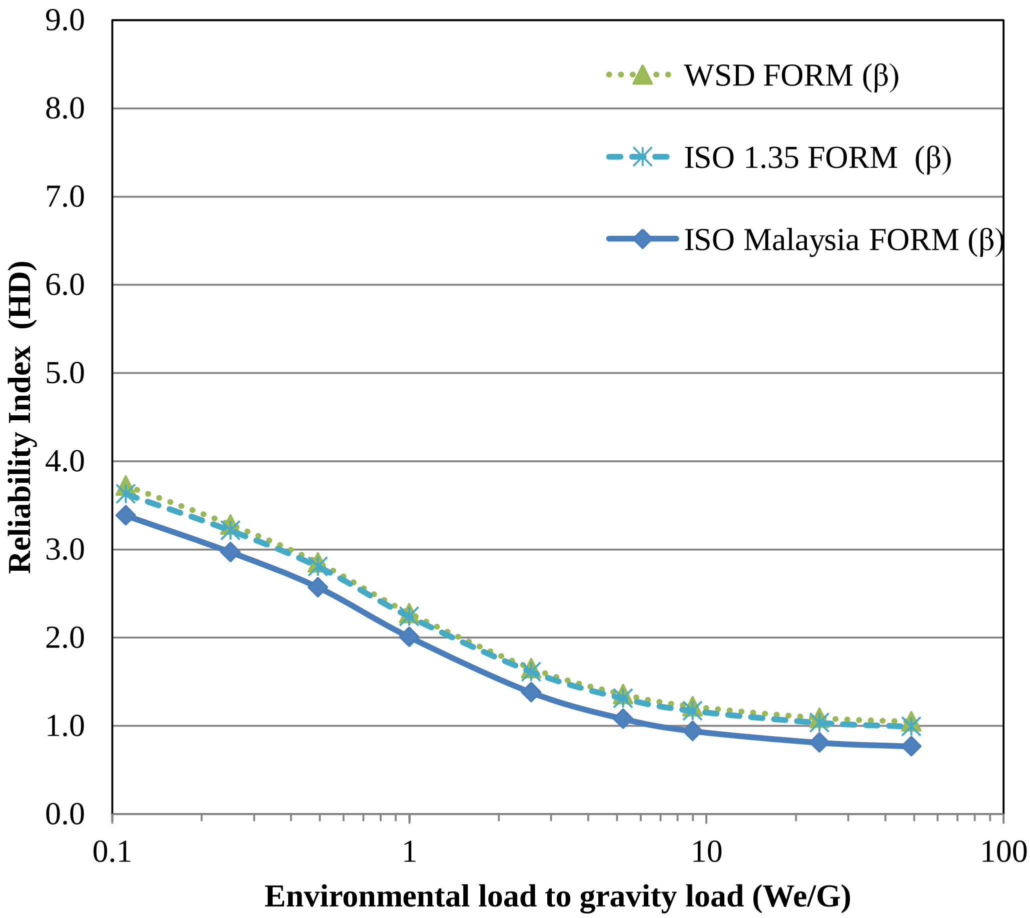

Figure 4.1.2.3 Graph of reliability index Vs environmental load to gravity load ratio for component under axial compression for horizontal diagonal member using FORM

According to Figure 4.1.2.4, by using SORM, the value of reliability index when environmental load to gravity load ratio is equal to 1.0 using ISO code with load factor of 1.35 is 2.0177, while reliability index of ISO Malaysia with load factor of 1.23 is 1.7785. On the other hand, value of reliability index of WSD is 2.0339.

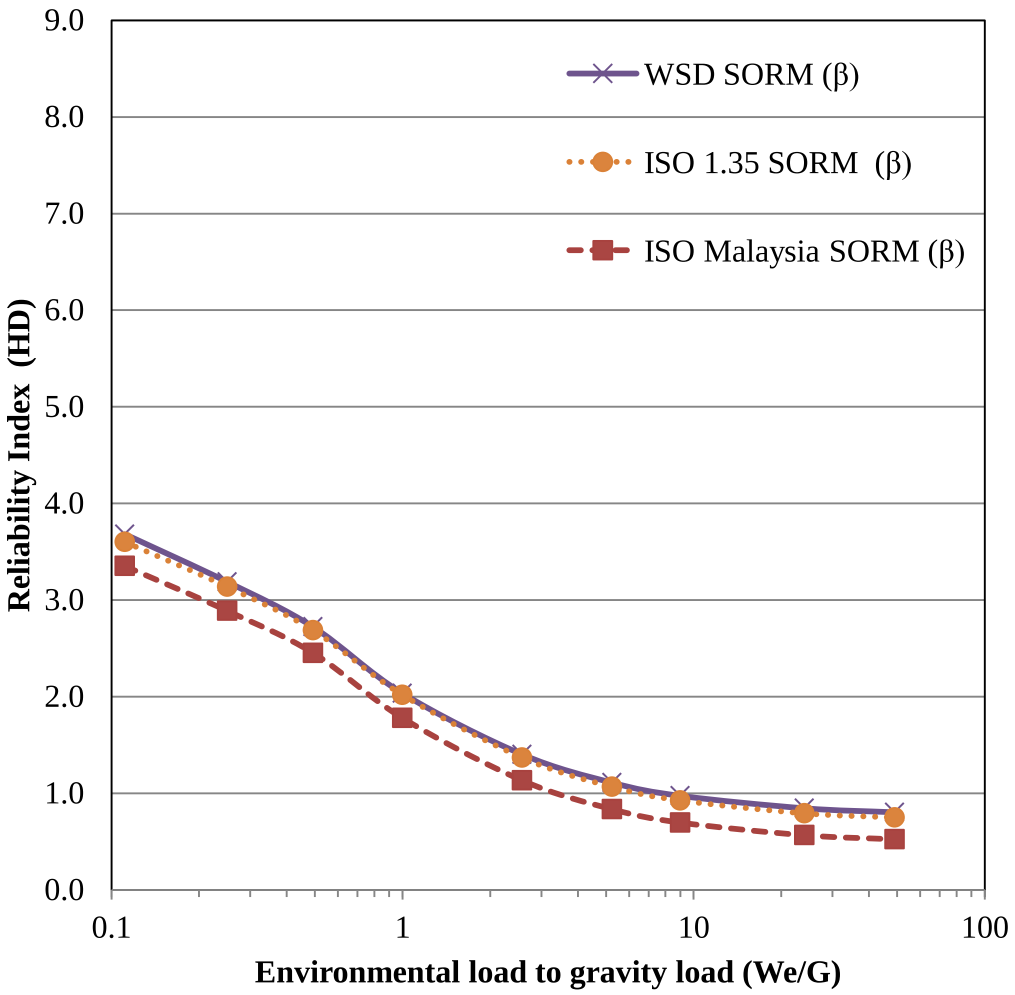

Figure 4.1.2.4 Graph of reliability index Vs environmental load to gravity load ratio for component under axial compression for horizontal diagonal member using SORM

4.1.2.3 Bending

According to Figure 4.1.2.5, by using FORM, the value of reliability index when environmental load to gravity load ratio is equal to 1.0 using ISO code with load factor of 1.35 is 2.4444, while reliability index of ISO Malaysia with load factor of 1.23 is 2.1102. On the other hand, value of reliability index of WSD is 2.0693.

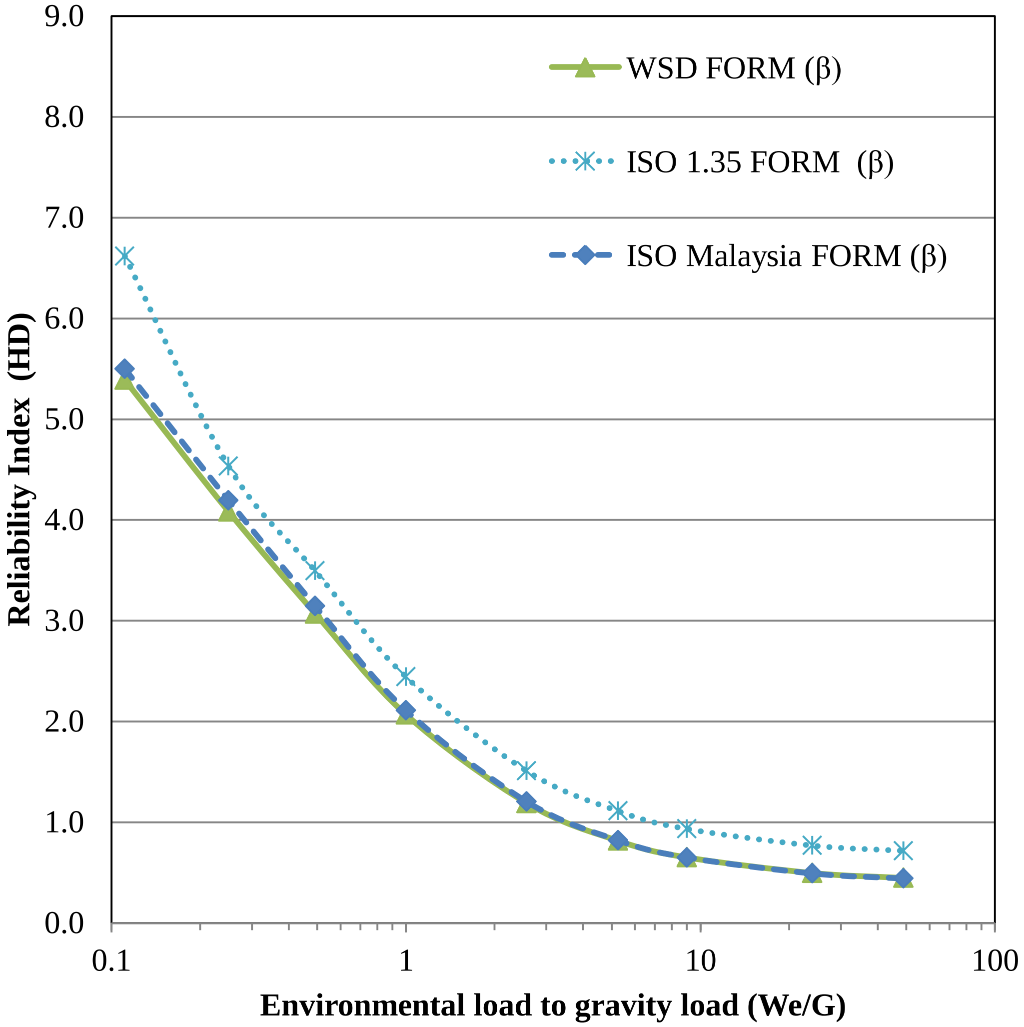

Figure 4.1.2.5 Graph of reliability index Vs environmental load to gravity load ratio for component under bending for horizontal diagonal member using FORM

According to Figure 4.1.2.6, by using SORM, the value of reliability index when environmental load to gravity load ratio is equal to 1.0 using ISO code with load factor of 1.35 is 2.2611, while reliability index of ISO Malaysia with load factor of 1.23 is 1.9212. On the other hand, value of reliability index of WSD is 1.8812.

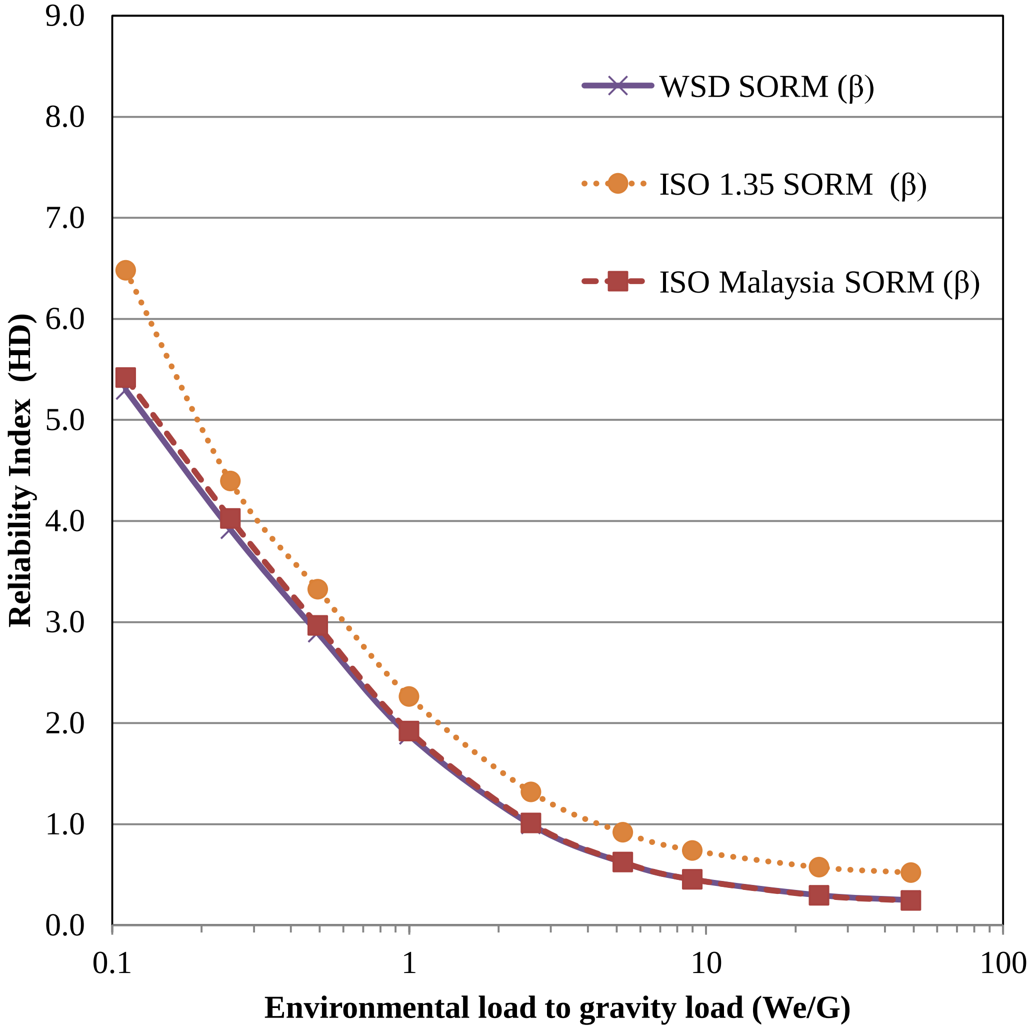

Figure 4.1.2.6 Graph of reliability index Vs environmental load to gravity load ratio for component under bending for horizontal diagonal member using SORM

4.1.2.4 Tension and Bending

According to Figure 4.1.2.7, by using FORM, the value of reliability index when environmental load to gravity load ratio is equal to 1.0 using ISO code with load factor of 1.35 is 2.739, while reliability index of ISO Malaysia with load factor of 1.23 is 2.4393. On the other hand, value of reliability index of WSD is 2.4846.

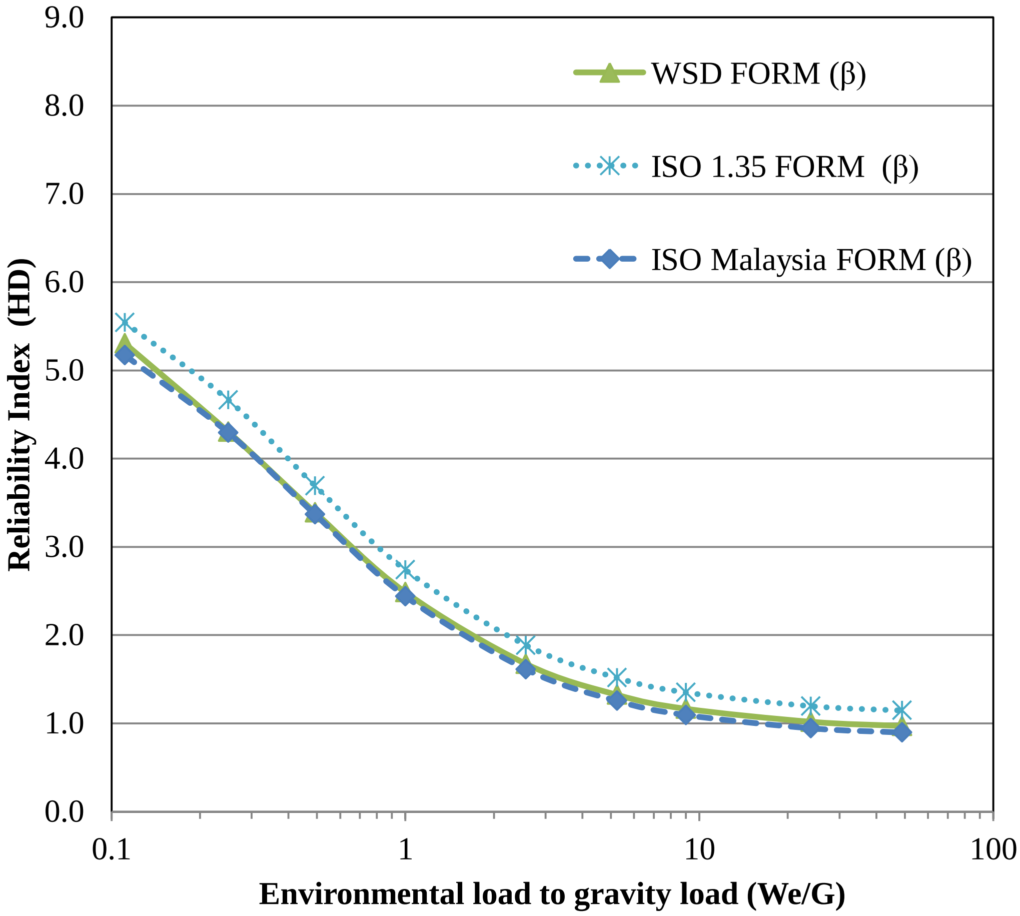

Figure 4.1.2.7 Graph of reliability index Vs environmental load to gravity load ratio for component under tension and bending for horizontal diagonal member using FORM

According to Figure 4.1.2.8, by using SORM, the value of reliability index when environmental load to gravity load ratio is equal to 1.0 using ISO code with load factor of 1.35 is 2.5481, while reliability index of ISO Malaysia with load factor of 1.23 is 2.2468. On the other hand, value of reliability index of WSD is 2.2943.

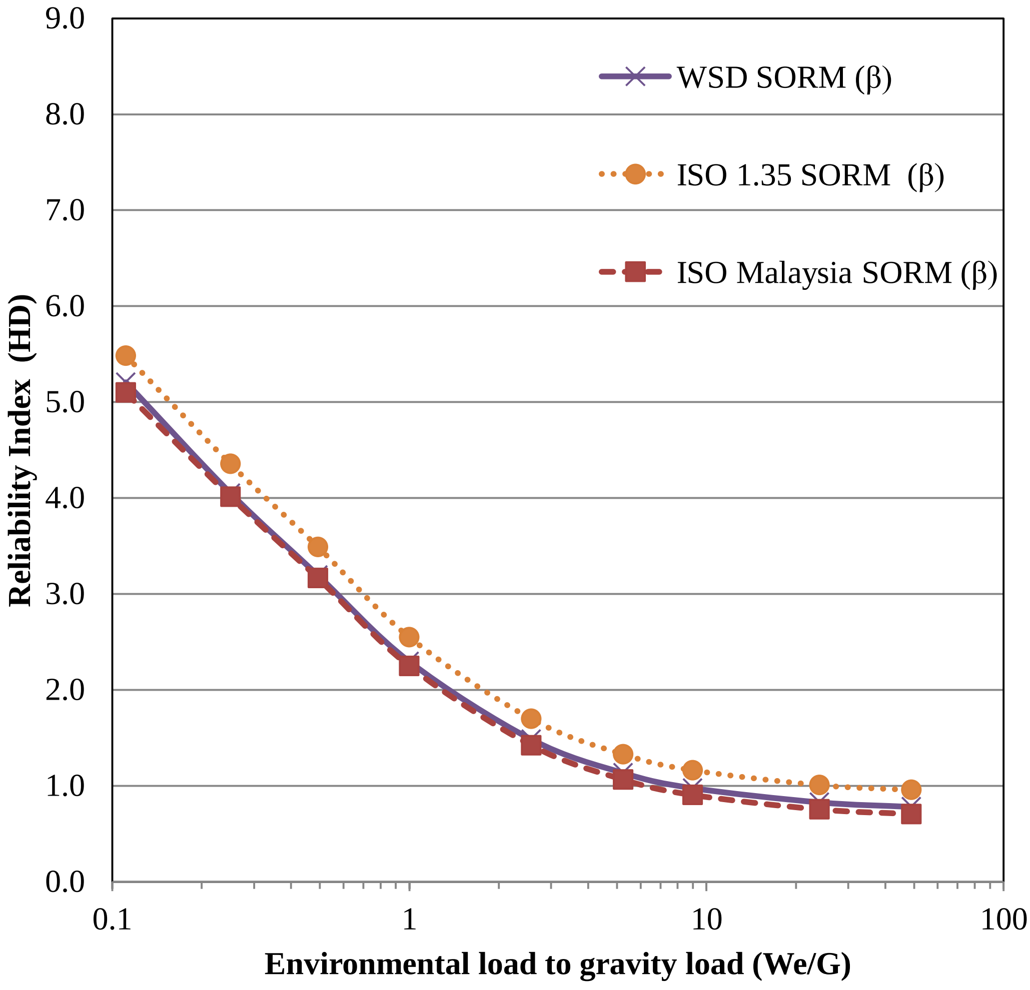

Figure 4.1.2.8 Graph of reliability index Vs environmental load to gravity load ratio for component under tension and bending for horizontal diagonal member using SORM

4.1.2.5 Compression and Bending

According to Figure 4.1.2.9, by using FORM, the value of reliability index when environmental load to gravity load ratio is equal to 1.0 using ISO code with load factor of 1.35 is 2.4846, while reliability index of ISO Malaysia with load factor of 1.23 is 2.1855. On the other hand, value of reliability index of WSD is 2.4375.

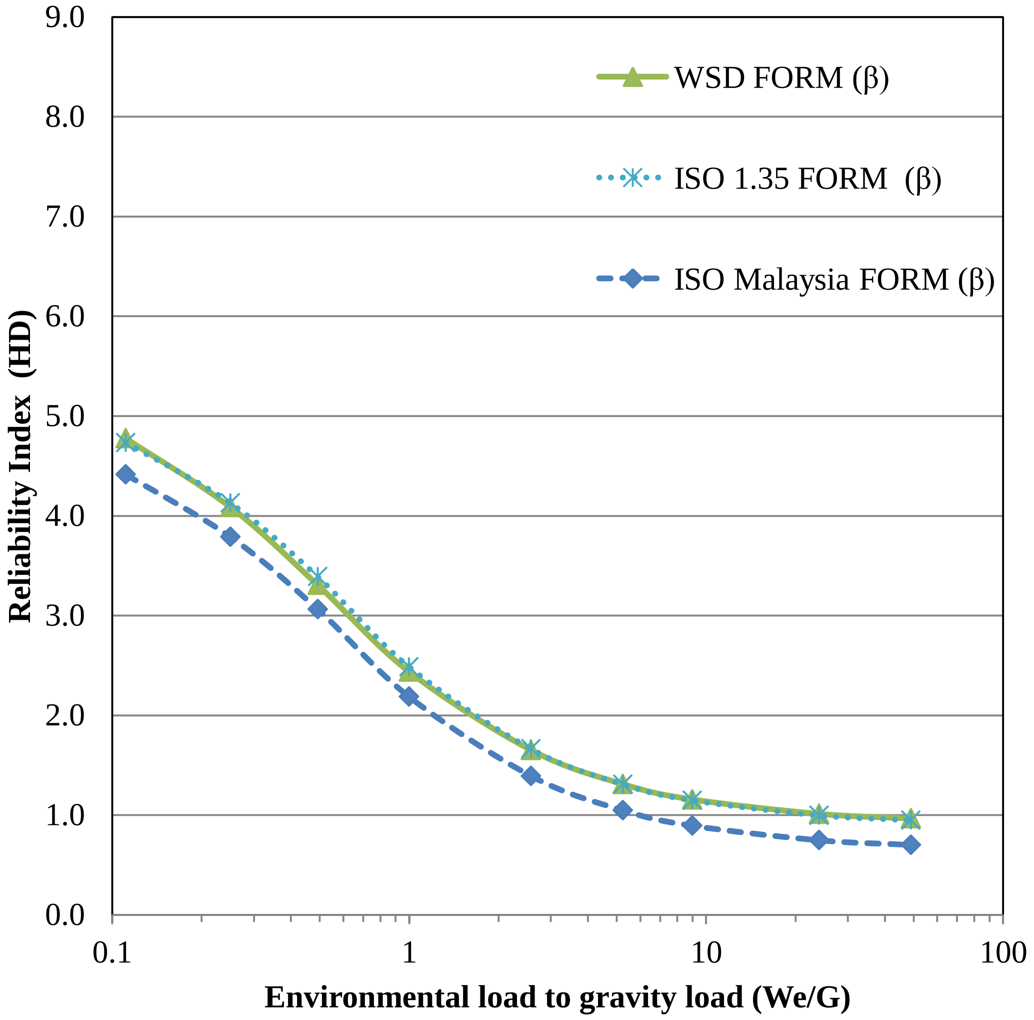

Figure 4.1.2.9 Graph of reliability index Vs environmental load to gravity load ratio for component under compression and bending for horizontal diagonal member using FORM

According to Figure 4.1.2.10, by using FORM, the value of reliability index when environmental load to gravity load ratio is equal to 1.0 using ISO code with load factor of 1.35 is 2.2257, while reliability index of ISO Malaysia with load factor of 1.23 is 1.9295. On the other hand, value of reliability index of WSD is 2.1883.

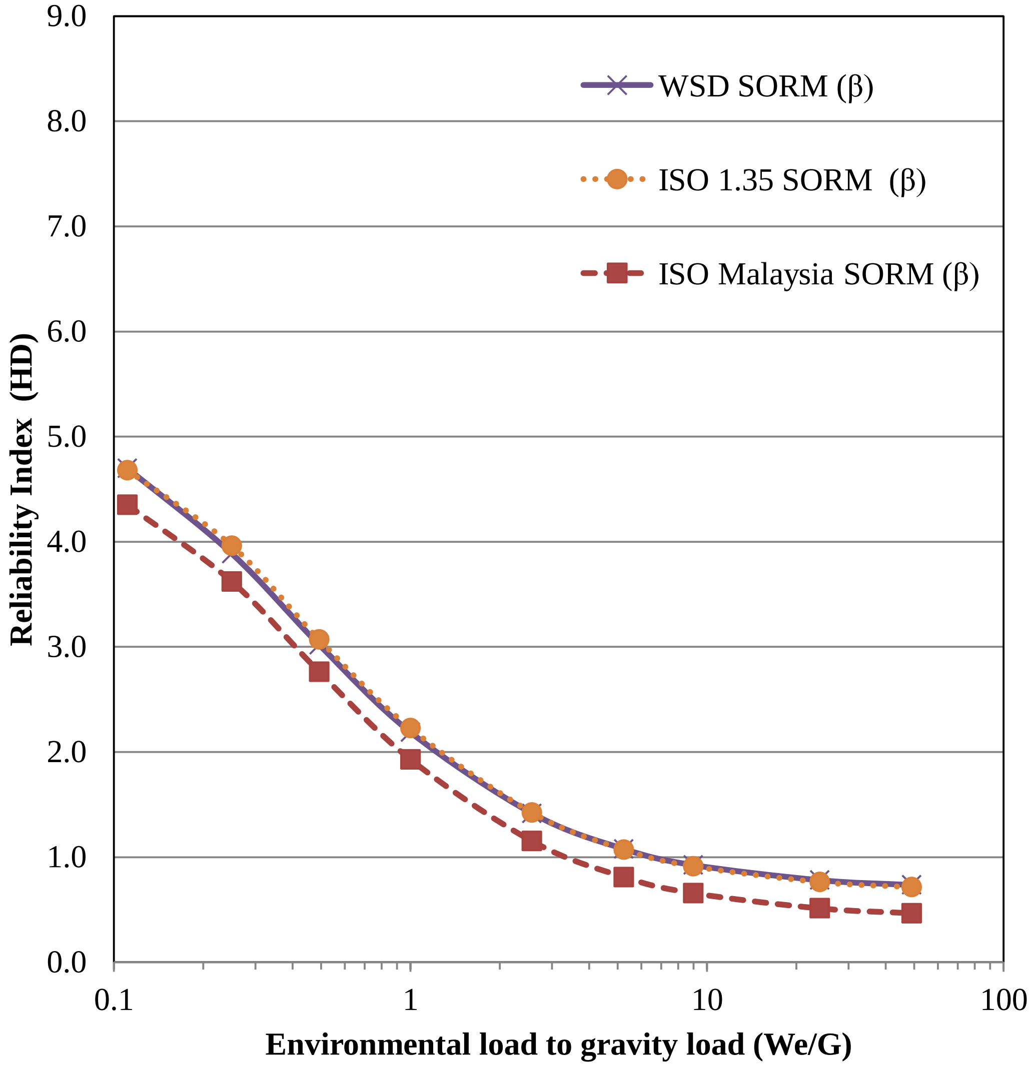

Figure 4.1.2.10 Graph of reliability index Vs environmental load to gravity load ratio for component under compression and bending for horizontal diagonal member using SORM

4.1.2.6 Tension, Bending and Hydrostatic Pressure

According to Figure 4.1.2.11, by using FORM, the value of reliability index when environmental load to gravity load ratio is equal to 1.0 using ISO code with load factor of 1.35 is 3.1298, while reliability index of ISO Malaysia with load factor of 1.23 is 2.8412. On the other hand, value of reliability index of WSD is 2.849.

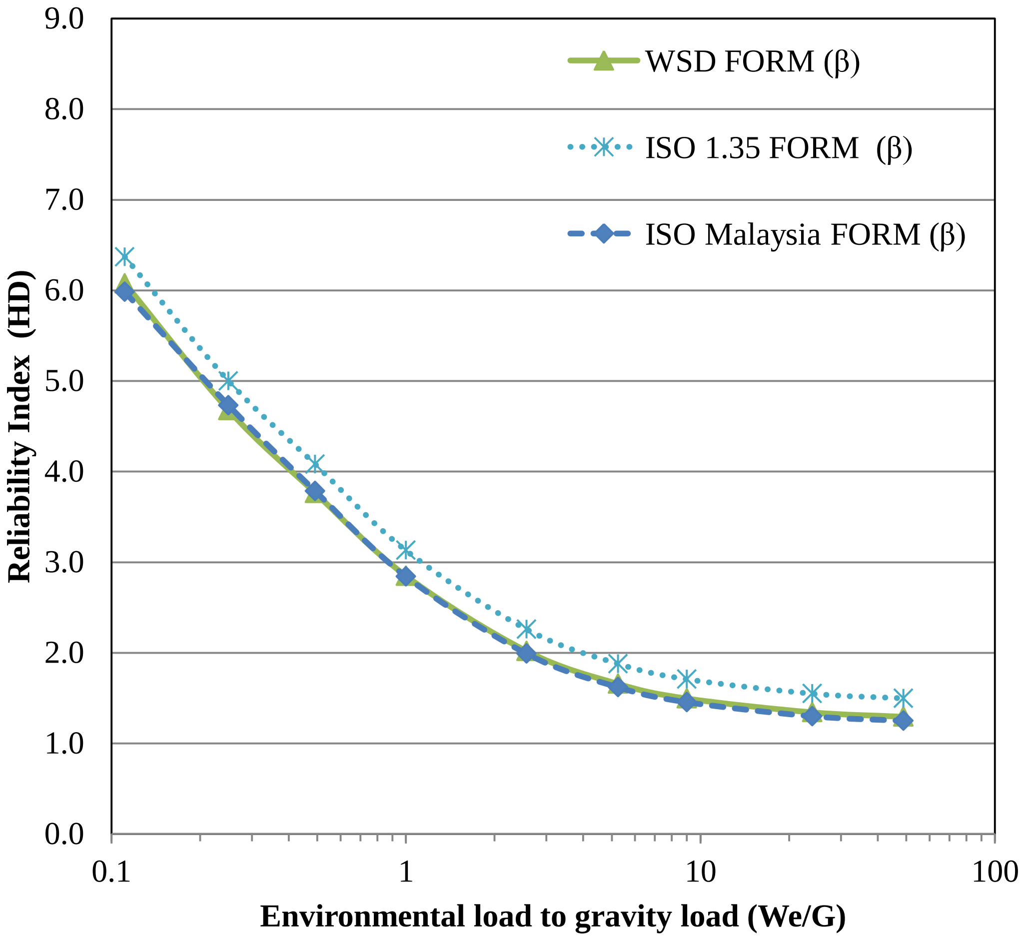

Figure 4.1.2.11 Graph of reliability index Vs environmental load to gravity load ratio for component under tension, bending and hydrostatic pressure for horizontal diagonal member using FORM

According to Figure 4.1.2.12, by using SORM, the value of reliability index when environmental load to gravity load ratio is equal to 1.0 using ISO code with load factor of 1.35 is 2.9499, while reliability index of ISO Malaysia with load factor of 1.23 is 2.6568. On the other hand, value of reliability index of WSD is 2.6673.

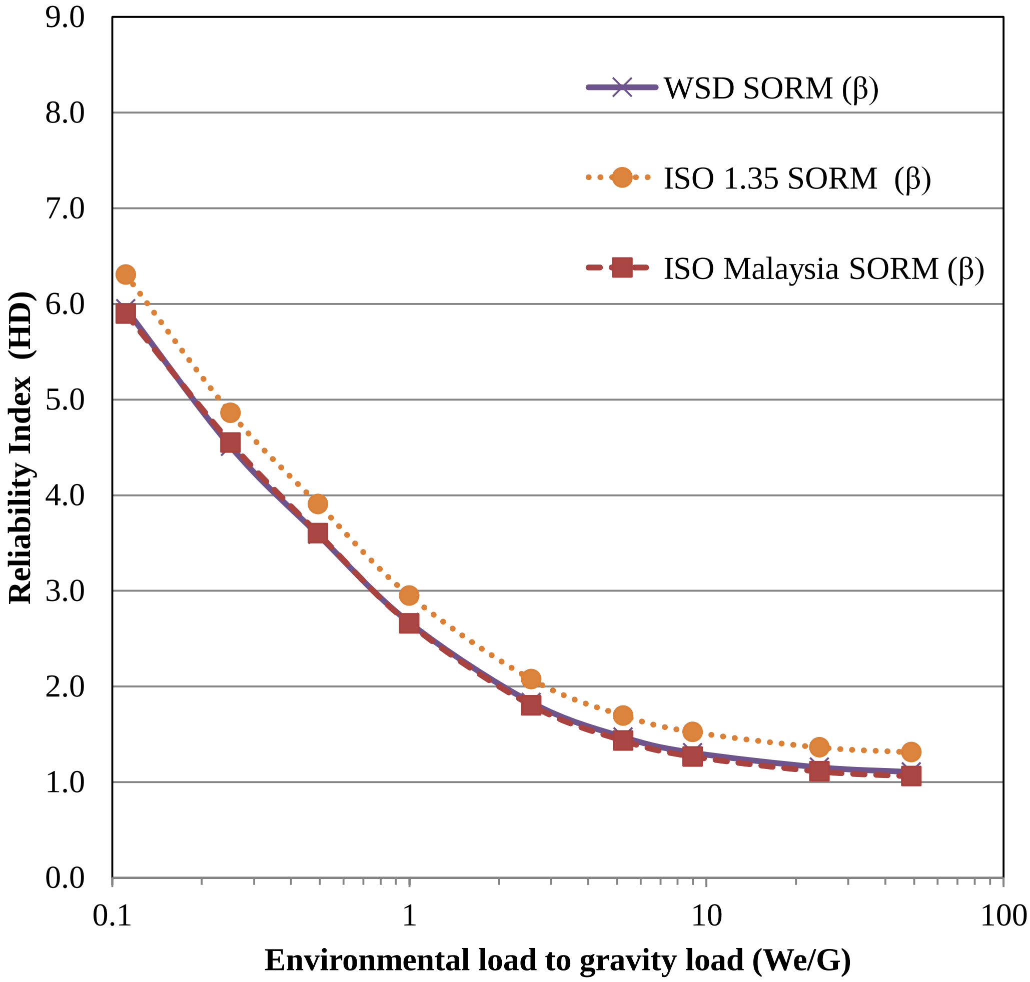

Figure 4.1.2.12 Graph of reliability index Vs environmental load to gravity load ratio for component under tension, bending and hydrostatic pressure for horizontal diagonal member using SORM

4.1.2.7 Compression, Bending and Hydrostatic Pressure

According to Figure 4.1.2.13, by using FORM, the value of reliability index when environmental load to gravity load ratio is equal to 1.0 using ISO code with load factor of 1.35 is 3.5252, while reliability index of ISO Malaysia with load factor of 1.23 is 3.2572. On the other hand, value of reliability index of WSD is 3.4241.

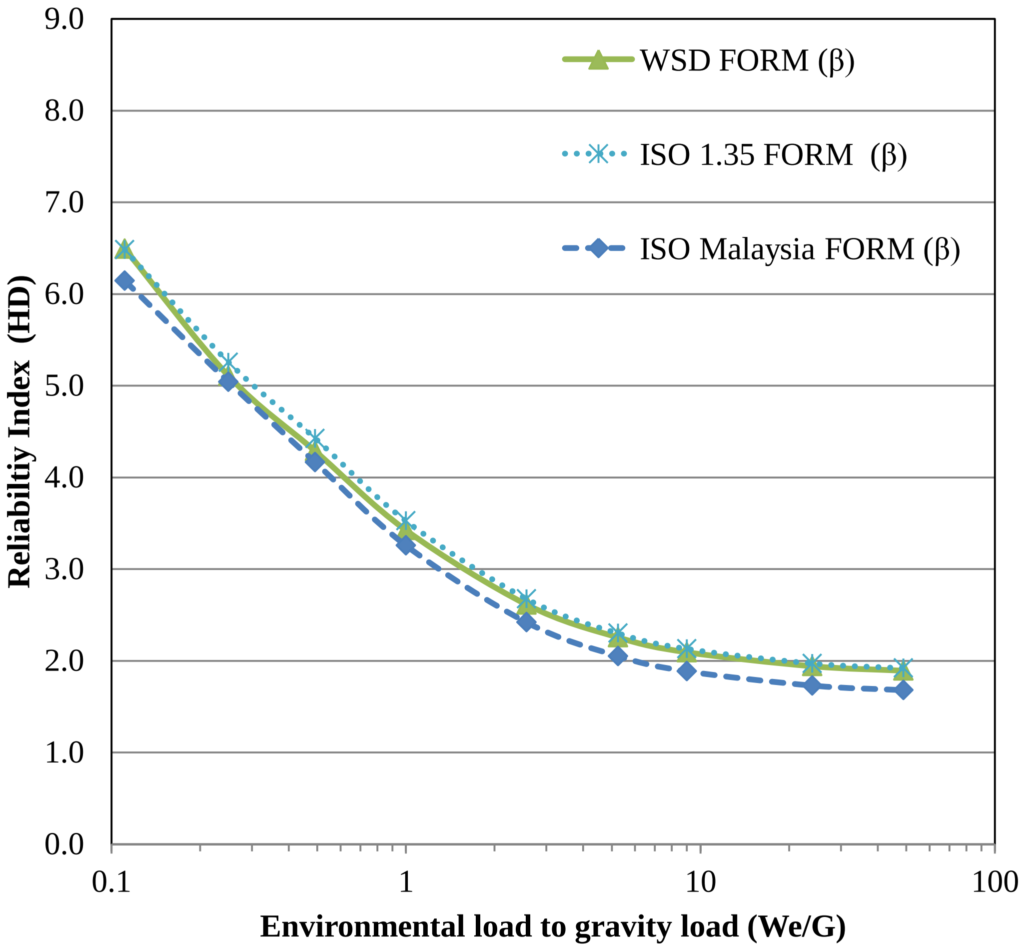

Figure 4.1.2.13 Graph of reliability index Vs environmental load to gravity load ratio for component under compression, bending and hydrostatic pressure for horizontal diagonal member using FORM

According to Figure 4.1.2.14, by using SORM, the value of reliability index when environmental load to gravity load ratio is equal to 1.0 using ISO code with load factor of 1.35 is 3.3084, while reliability index of ISO Malaysia with load factor of 1.23 is 3.0333. On the other hand, value of reliability index of WSD is 3.2144.

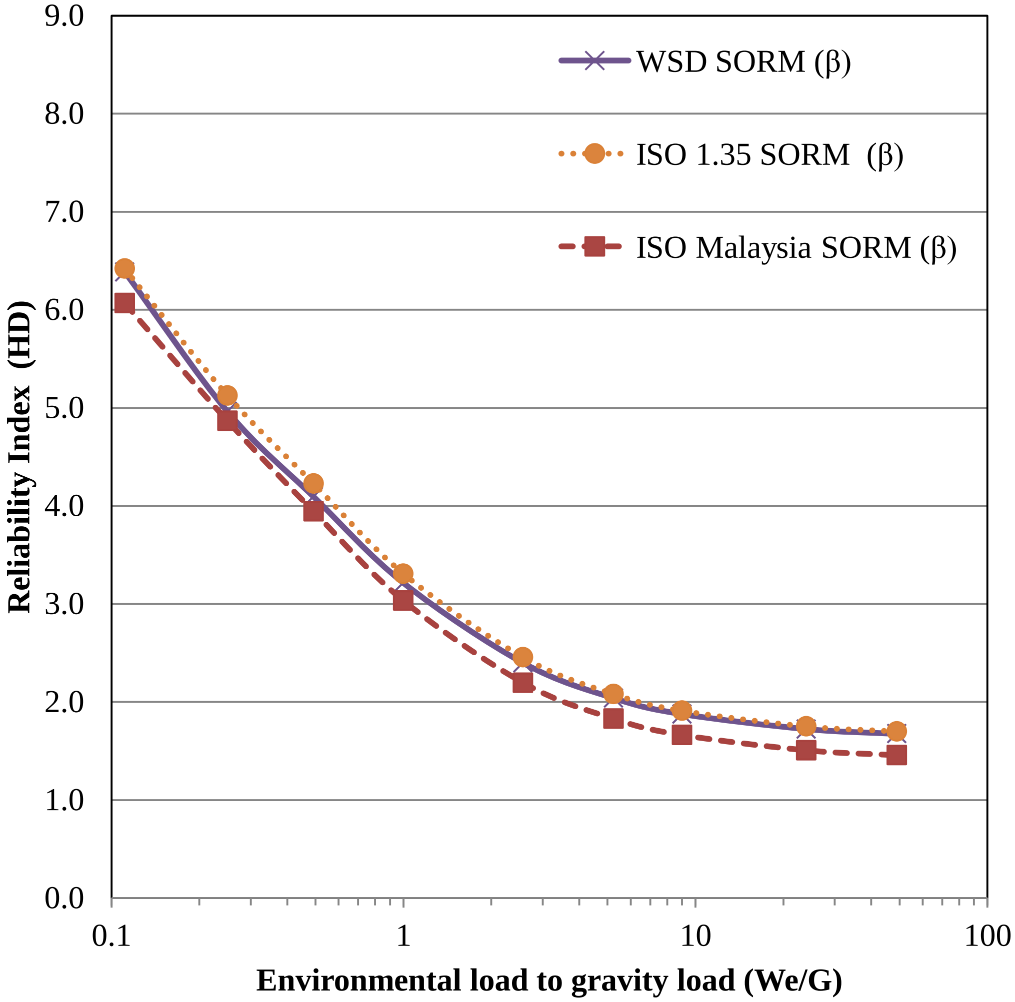

Figure 4.1.2.14 Graph of reliability index Vs environmental load to gravity load ratio for component under compression, bending and hydrostatic pressure for horizontal diagonal member using SORM

4.1.3 Horizontal Periphery

4.1.3.1 Axial Tension

According to Figure 4.1.3.1, by using FORM, the value of reliability index when environmental load to gravity load ratio is equal to 1.0 using ISO code with load factor of 1.35 is 4.1438, while reliability index of ISO Malaysia with load factor of 1.23 is 3.9213. On the other hand, value of reliability index of WSD is 3.9753.

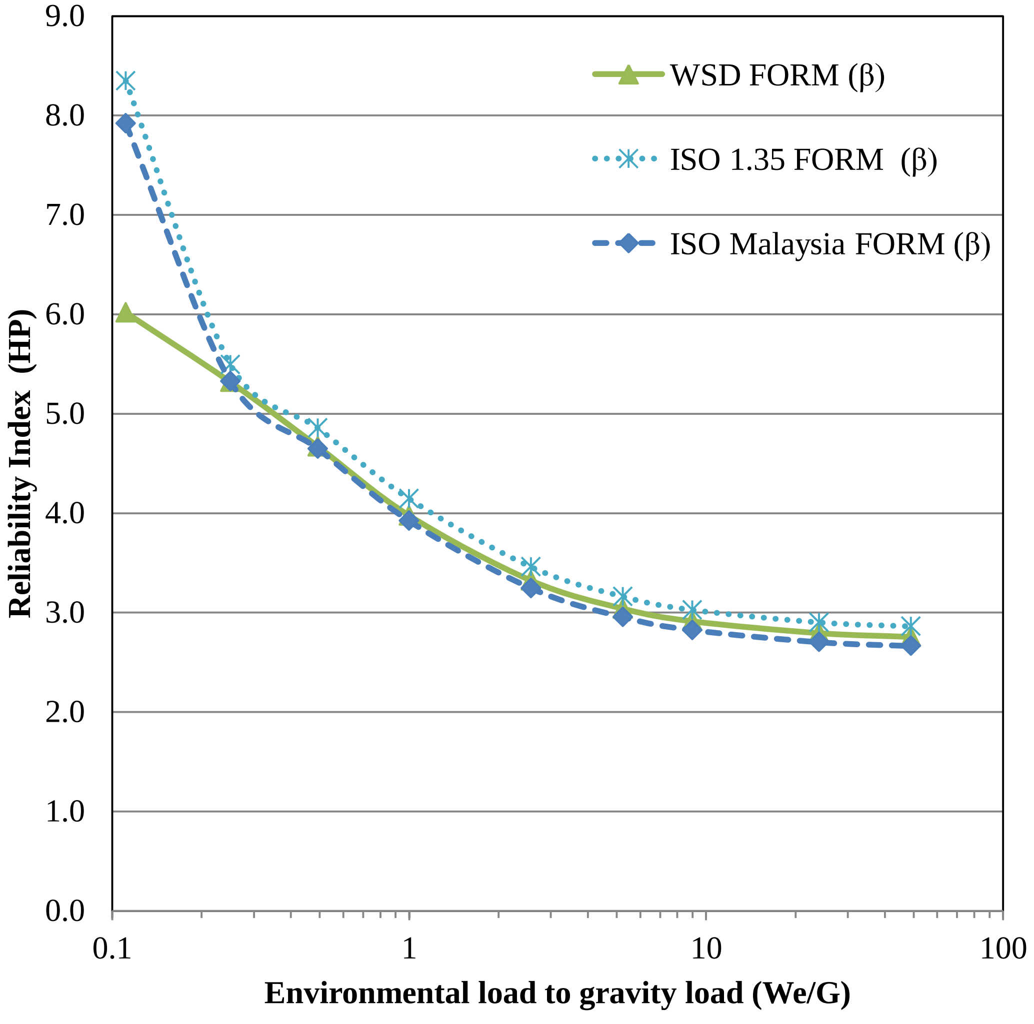

Figure 4.1.3.1 Graph of reliability index Vs environmental load to gravity load ratio for component under axial tension for horizontal periphery member using FORM

According to Figure 4.1.3.2, by using SORM, the value of reliability index when environmental load to gravity load ratio is equal to 1.0 using ISO code with load factor of 1.35 is 3.9918, while reliability index of ISO Malaysia with load factor of 1.23 is 3.7592. On the other hand, value of reliability index of WSD is 3.818.

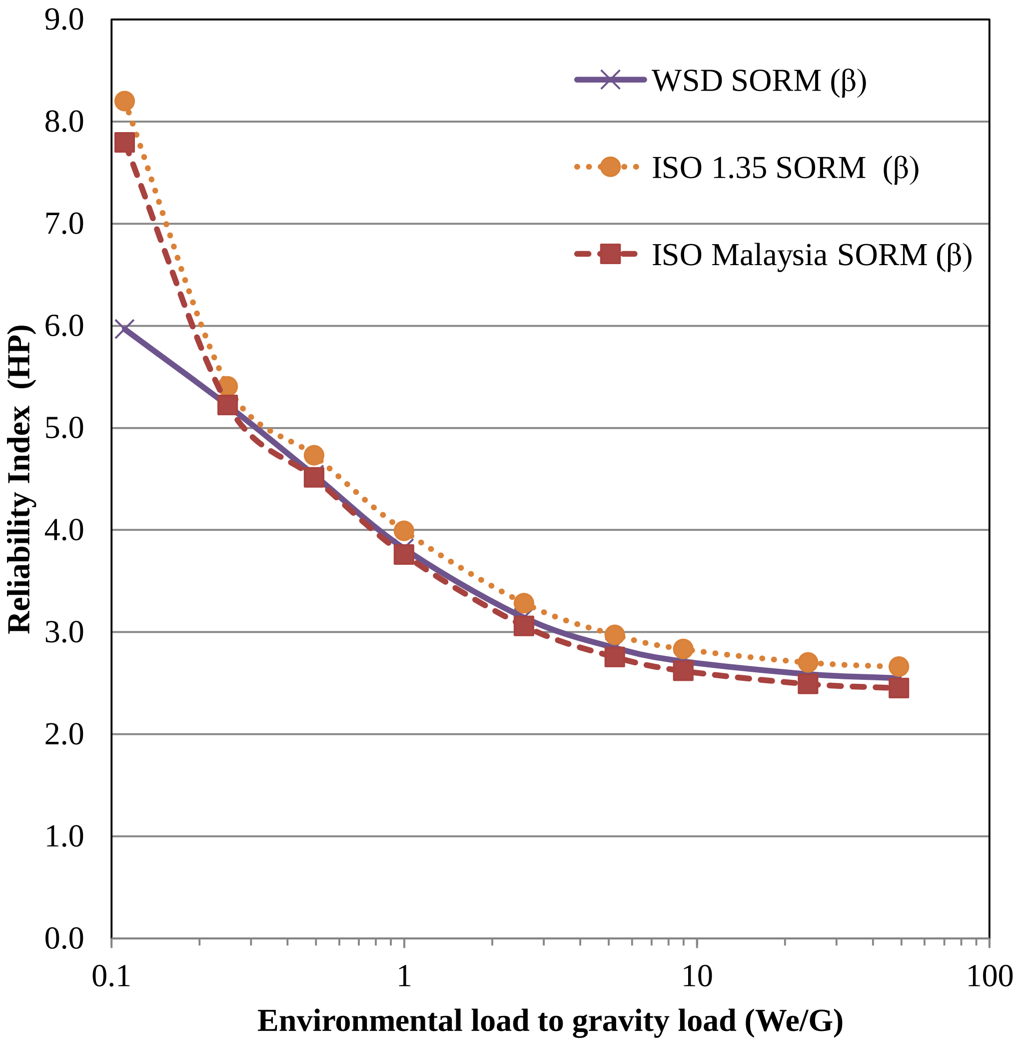

Figure 4.1.3.2 Graph of reliability index Vs environmental load to gravity load ratio for component under axial tension for horizontal periphery member using SORM

4.1.3.2 Axial Compression

According to Figure 4.1.3.3, by using FORM, the value of reliability index when environmental load to gravity load ratio is equal to 1.0 using ISO code with load factor of 1.35 is 4.385, while reliability index of ISO Malaysia with load factor of 1.23 is 4.1802. On the other hand, value of reliability index of WSD is 4.1381.

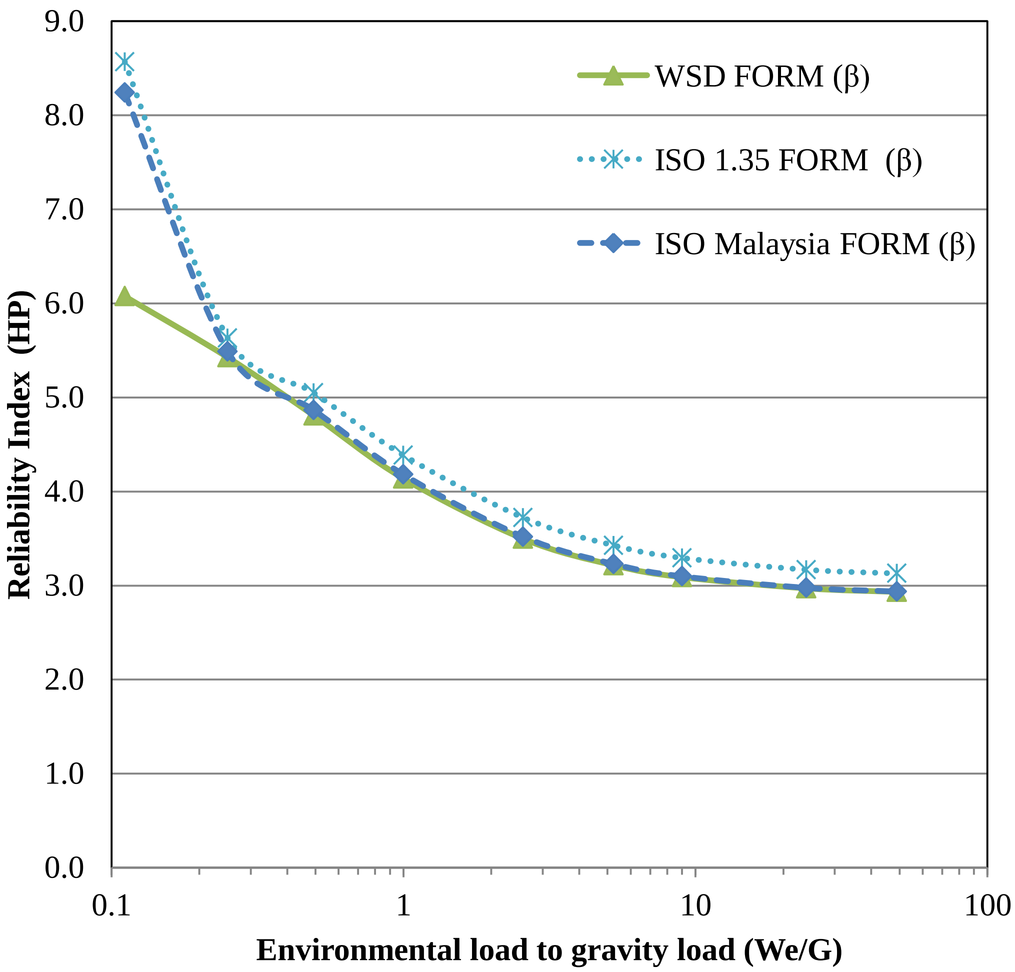

Figure 4.1.3.3 Graph of reliability index Vs environmental load to gravity load ratio for component under axial compression for horizontal periphery member using FORM

According to Figure 4.1.3.4, by using SORM, the value of reliability index when environmental load to gravity load ratio is equal to 1.0 using ISO code with load factor of 1.35 is 4.2339, while reliability index of ISO Malaysia with load factor of 1.23 is 4.0188. On the other hand, value of reliability index of WSD is 3.9752.

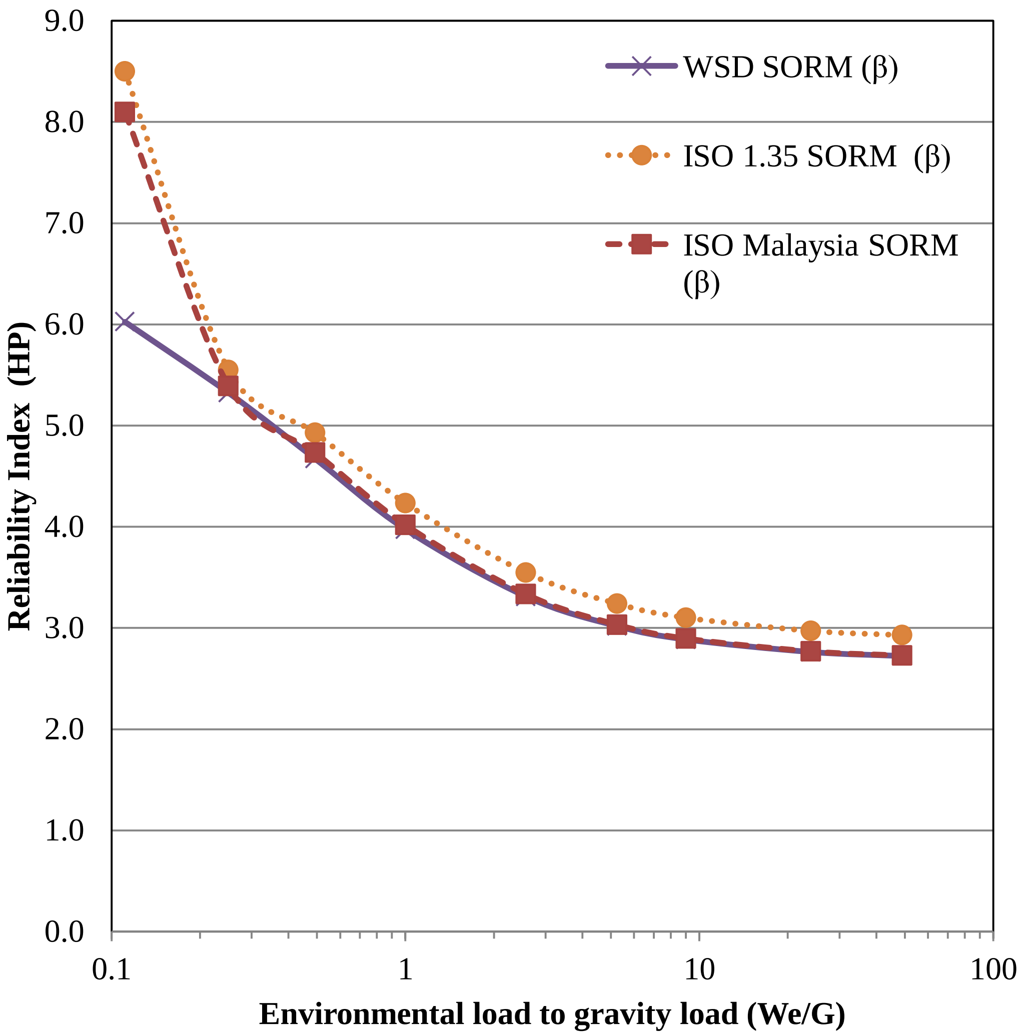

Figure 4.1.3.4 Graph of reliability index Vs environmental load to gravity load ratio for component under axial compression for horizontal periphery member using SORM

4.1.3.3 Bending

According to Figure 4.1.3.5, by using FORM, the value of reliability index when environmental load to gravity load ratio is equal to 1.0 using ISO code with load factor of 1.35 is 4.9745, while reliability index of ISO Malaysia with load factor of 1.23 is 4.8187. On the other hand, value of reliability index of WSD is 4.1835.

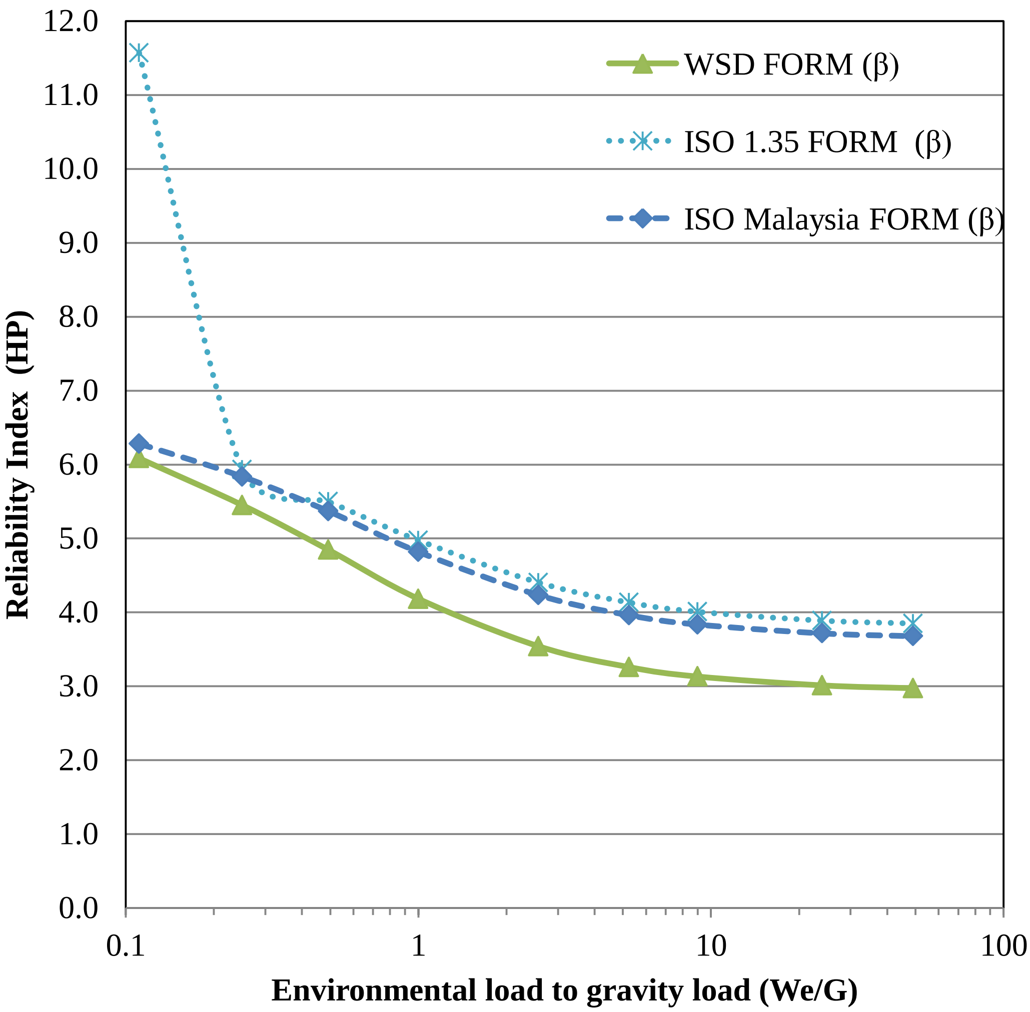

Figure 4.1.3.5 Graph of reliability index Vs environmental load to gravity load ratio for component under bending for horizontal periphery member using FORM

According to Figure 4.1.3.6, by using SORM, the value of reliability index when environmental load to gravity load ratio is equal to 1.0 using ISO code with load factor of 1.35 is 4.8673, while reliability index of ISO Malaysia with load factor of 1.23 is 4.7037. On the other hand, value of reliability index of WSD is 4.0369.

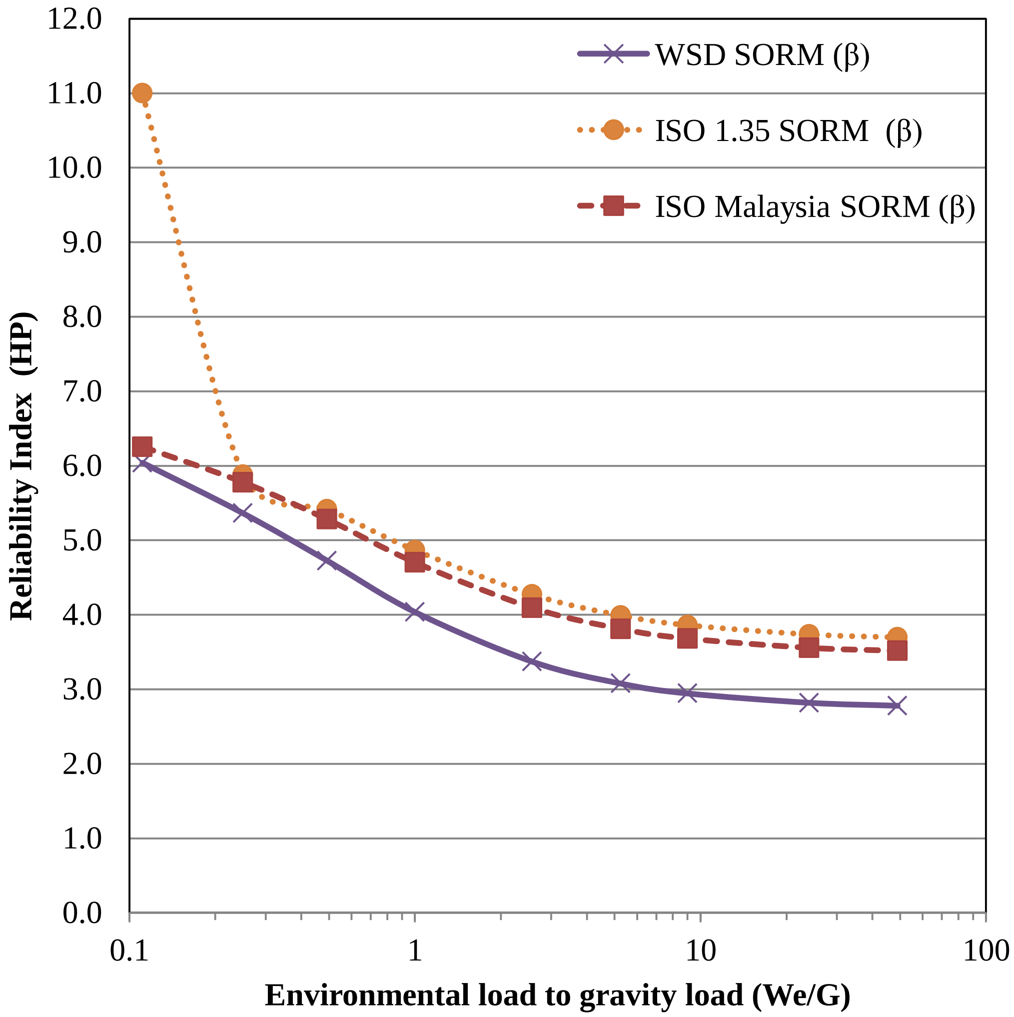

Figure 4.1.3.6 Graph of reliability index Vs environmental load to gravity load ratio for component under bending for horizontal periphery member using SORM

4.1.3.4 Tension and Bending

According to Figure 4.1.3.7, by using FORM, the value of reliability index when environmental load to gravity load ratio is equal to 1.0 using ISO code with load factor of 1.35 is 4.5342, while reliability index of ISO Malaysia with load factor of 1.23 is 4.3409. On the other hand, value of reliability index of WSD is 4.0851.

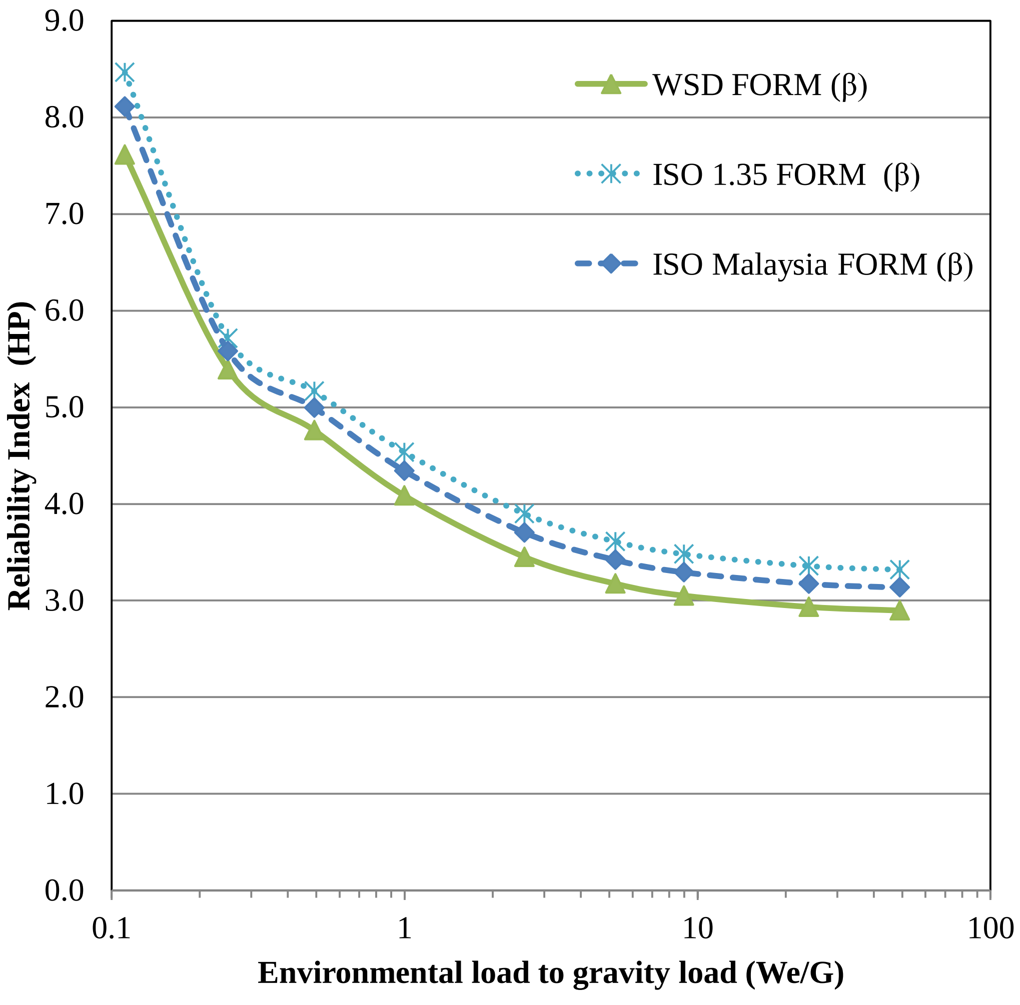

Figure 4.1.3.7 Graph of reliability index Vs environmental load to gravity load ratio for component under tension and bending for horizontal periphery member using FORM

According to Figure 4.1.3.8, by using SORM, the value of reliability index when environmental load to gravity load ratio is equal to 1.0 using ISO code with load factor of 1.35 is 4.3911, while reliability index of ISO Malaysia with load factor of 1.23 is 4.1895. On the other hand, value of reliability index of WSD is 3.9547.

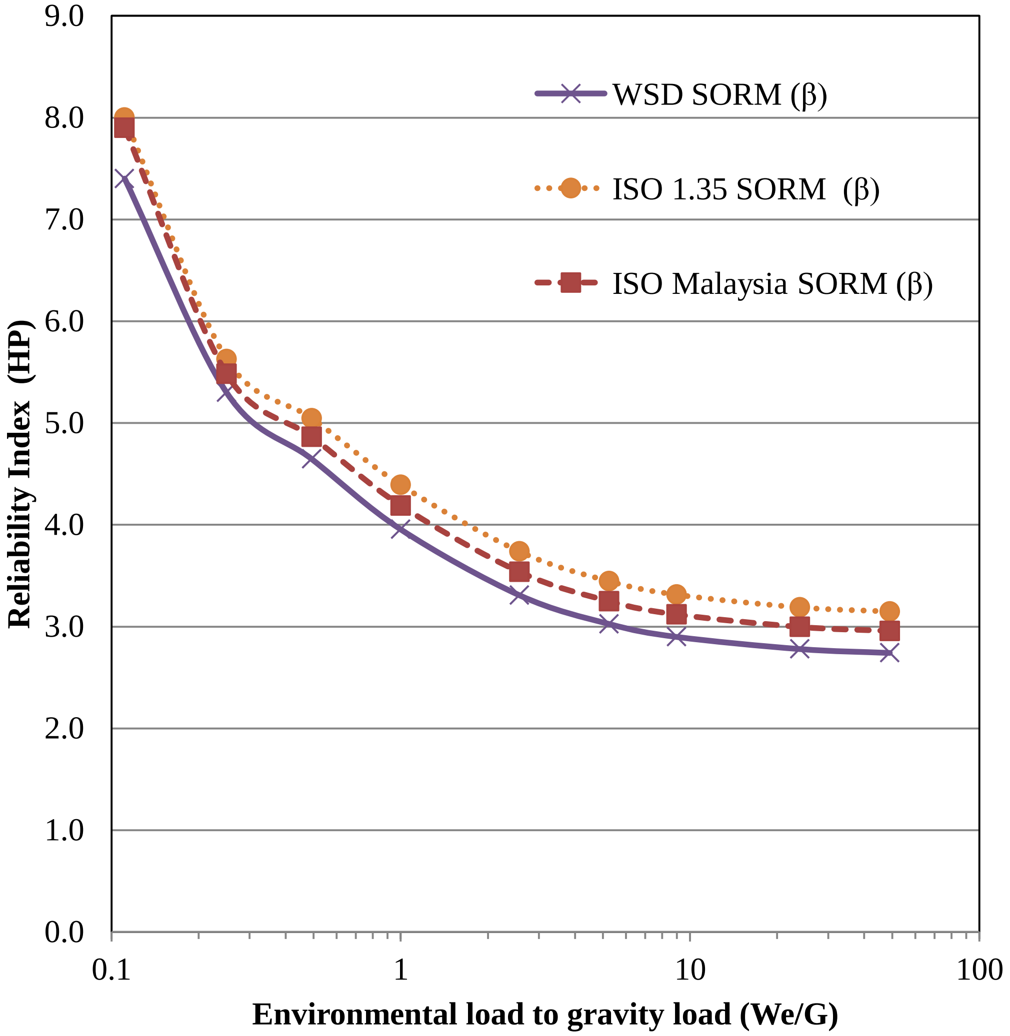

Figure 4.1.3.8 Graph of reliability index Vs environmental load to gravity load ratio for component under tension and bending for horizontal periphery member using SORM

4.1.3.5 Compression and Bending

According to Figure 4.1.3.9, by using FORM, the value of reliability index when environmental load to gravity load ratio is equal to 1.0 using ISO code with load factor of 1.35 is 3.6475, while reliability index of ISO Malaysia with load factor of 1.23 is 3.3952. On the other hand, value of reliability index of WSD is 3.8156.

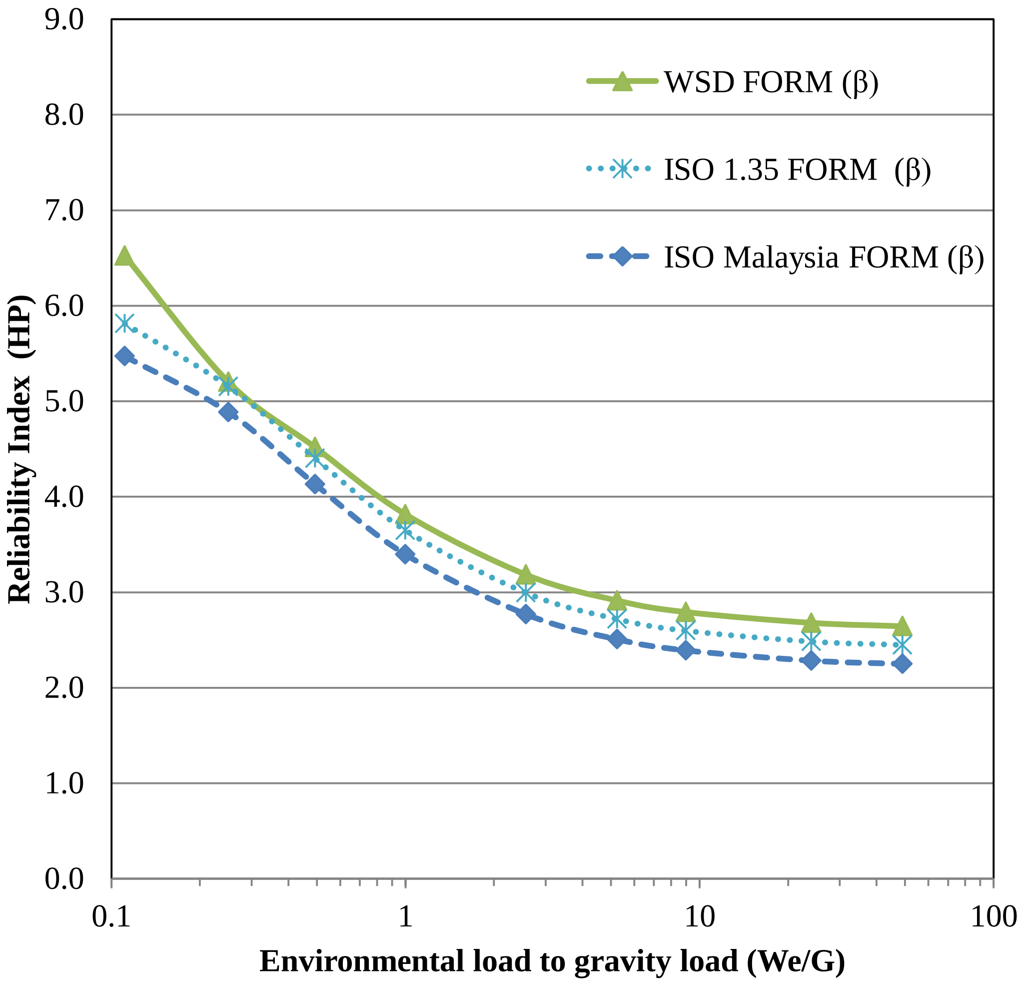

Figure 4.1.3.9 Graph of reliability index Vs environmental load to gravity load ratio for component under compression and bending for horizontal periphery member using FORM

According to Figure 4.1.3.10, by using SORM, the value of reliability index when environmental load to gravity load ratio is equal to 1.0 using ISO code with load factor of 1.35 is 3.4865, while reliability index of ISO Malaysia with load factor of 1.23 is 3.2273. On the other hand, value of reliability index of WSD is 3.6823.

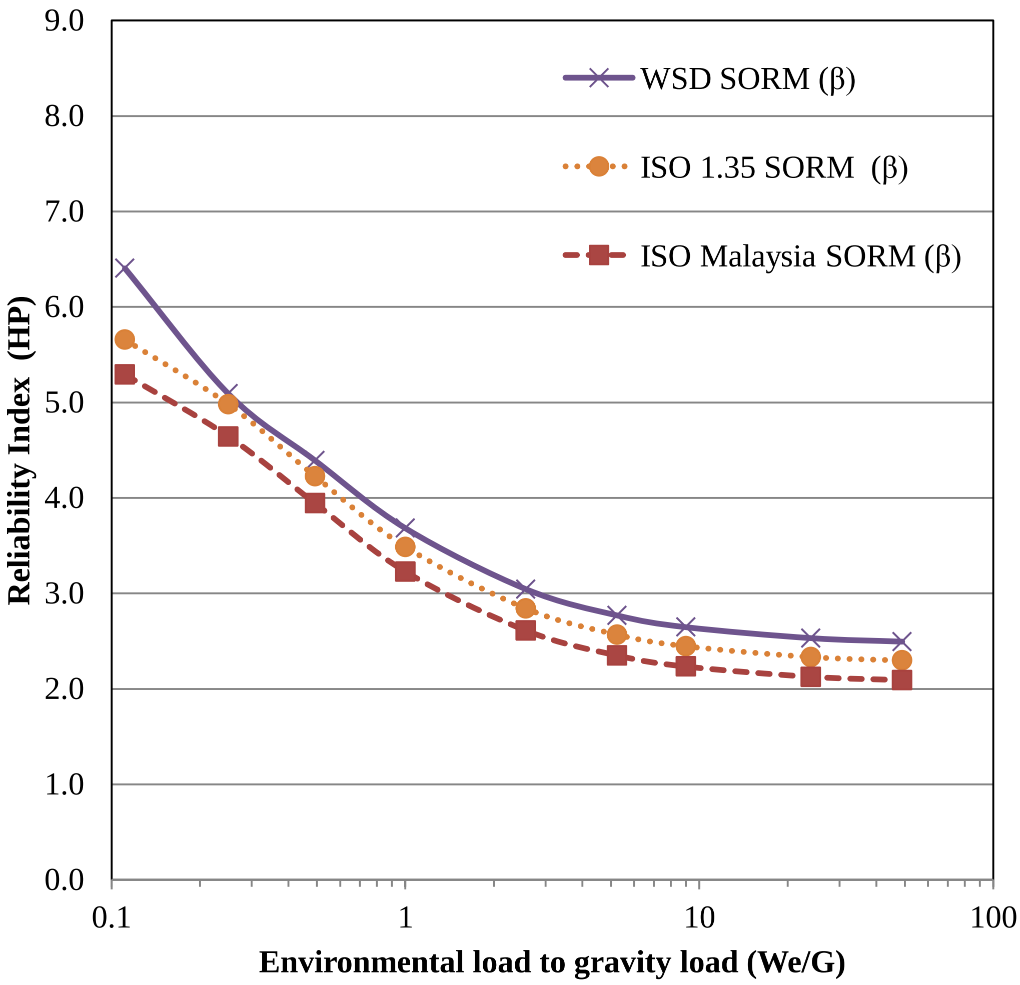

Figure 4.1.3.10 Graph of reliability index Vs environmental load to gravity load ratio for component under compression and bending for horizontal periphery member using SORM

4.1.3.6 Tension, Bending and Hydrostatic Pressure

According to Figure 4.1.3.11, by using FORM, the value of reliability index when environmental load to gravity load ratio is equal to 1.0 using ISO code with load factor of 1.35 is 4.3733, while reliability index of ISO Malaysia with load factor of 1.23 is 4.1681. On the other hand, value of reliability index of WSD is 3.7401.

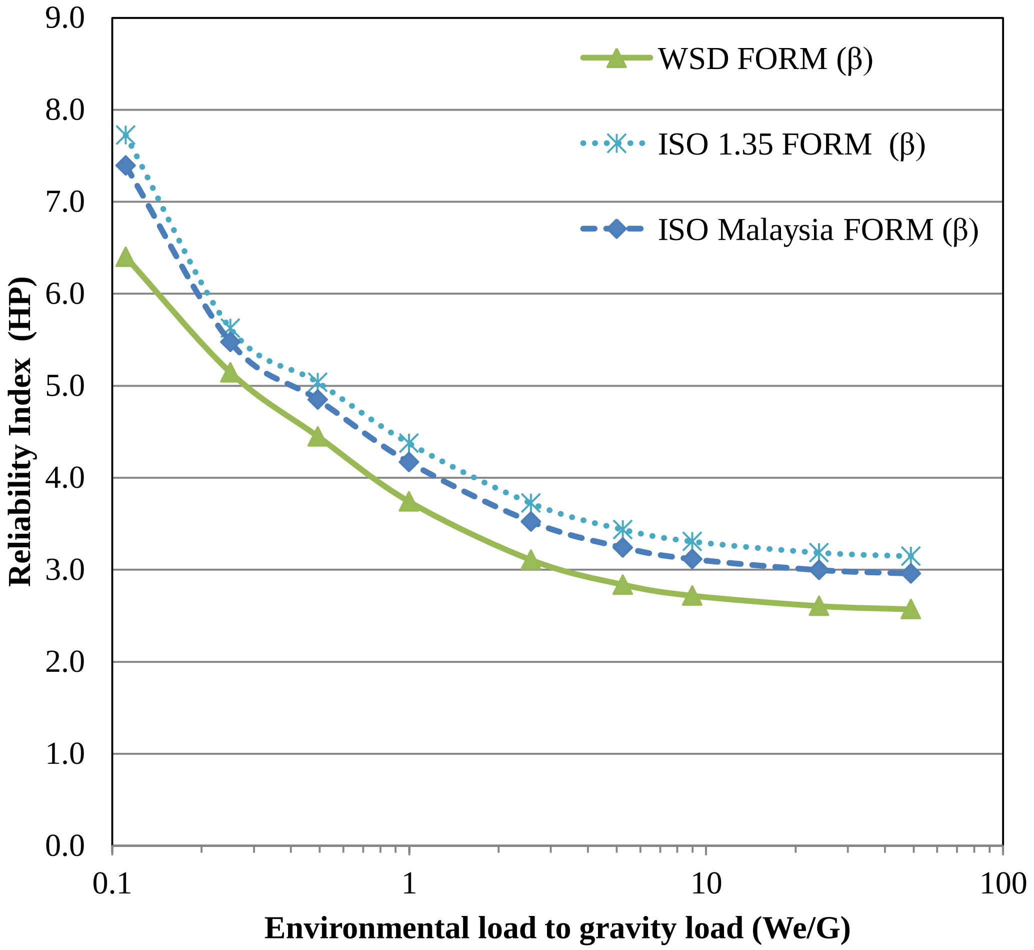

Figure 4.1.3.11 Graph of reliability index Vs environmental load to gravity load ratio for component under tension, bending and hydrostatic pressure for horizontal periphery member using FORM

According to Figure 4.1.3.12, by using SORM, the value of reliability index when environmental load to gravity load ratio is equal to 1.0 using ISO code with load factor of 1.35 is 4.2213, while reliability index of ISO Malaysia with load factor of 1.23 is 4.0083. On the other hand, value of reliability index of WSD is 3.6079.

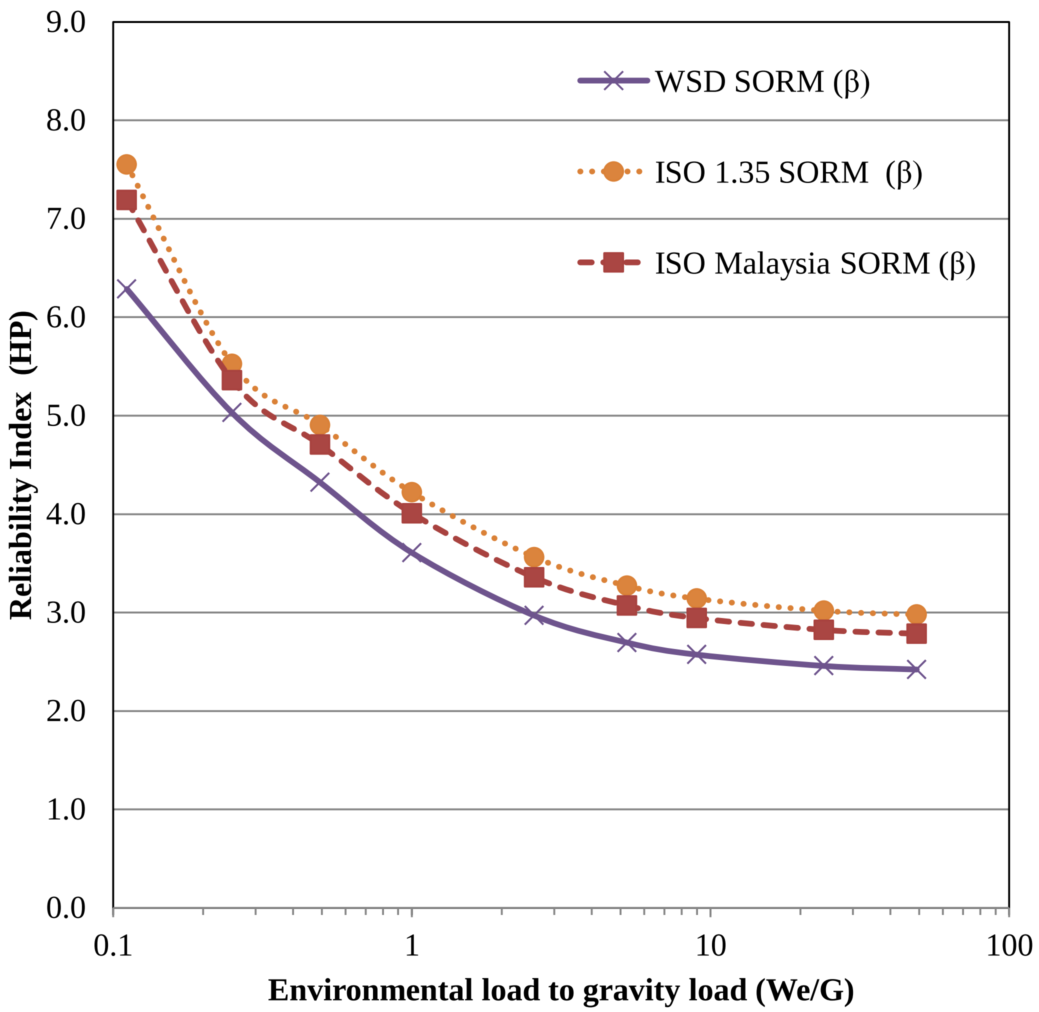

Figure 4.1.3.12 Graph of reliability index Vs environmental load to gravity load ratio for component under tension, bending and hydrostatic pressure for horizontal periphery member using SORM

4.1.3.7 Compression, Bending and Hydrostatic Pressure

According to Figure 4.1.3.13, by using FORM, the value of reliability index when environmental load to gravity load ratio is equal to 1.0 using ISO code with load factor of 1.35 is 4.2475, while reliability index of ISO Malaysia with load factor of 1.23 is 4.0334. On the other hand, value of reliability index of WSD is 3.9338.

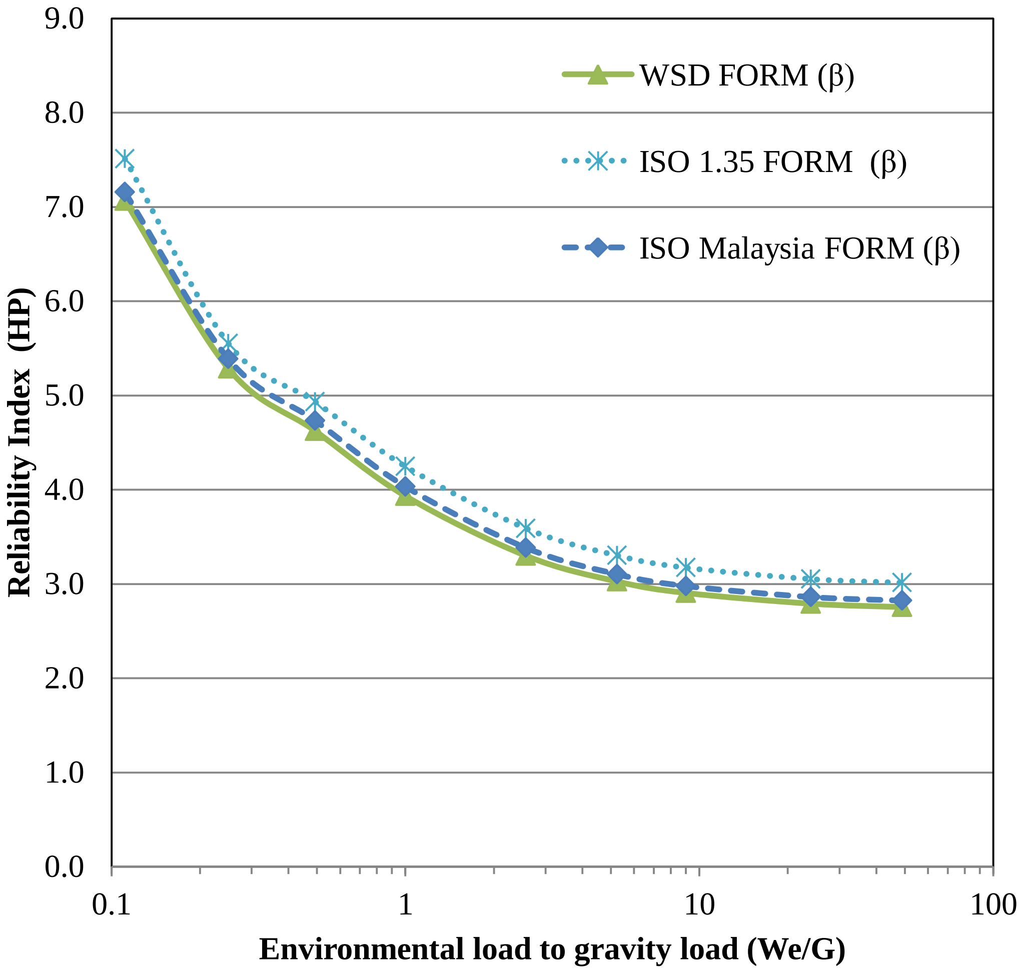

Figure 4.1.3.13 Graph of reliability index Vs environmental load to gravity load ratio for component under compression, bending and hydrostatic pressure for horizontal periphery member using FORM

According to Figure 4.1.3.14, by using FORM, the value of reliability index when environmental load to gravity load ratio is equal to 1.0 using ISO code with load factor of 1.35 is 4.0918, while reliability index of ISO Malaysia with load factor of 1.23 is 3.8702. On the other hand, value of reliability index of WSD is 3.8189.

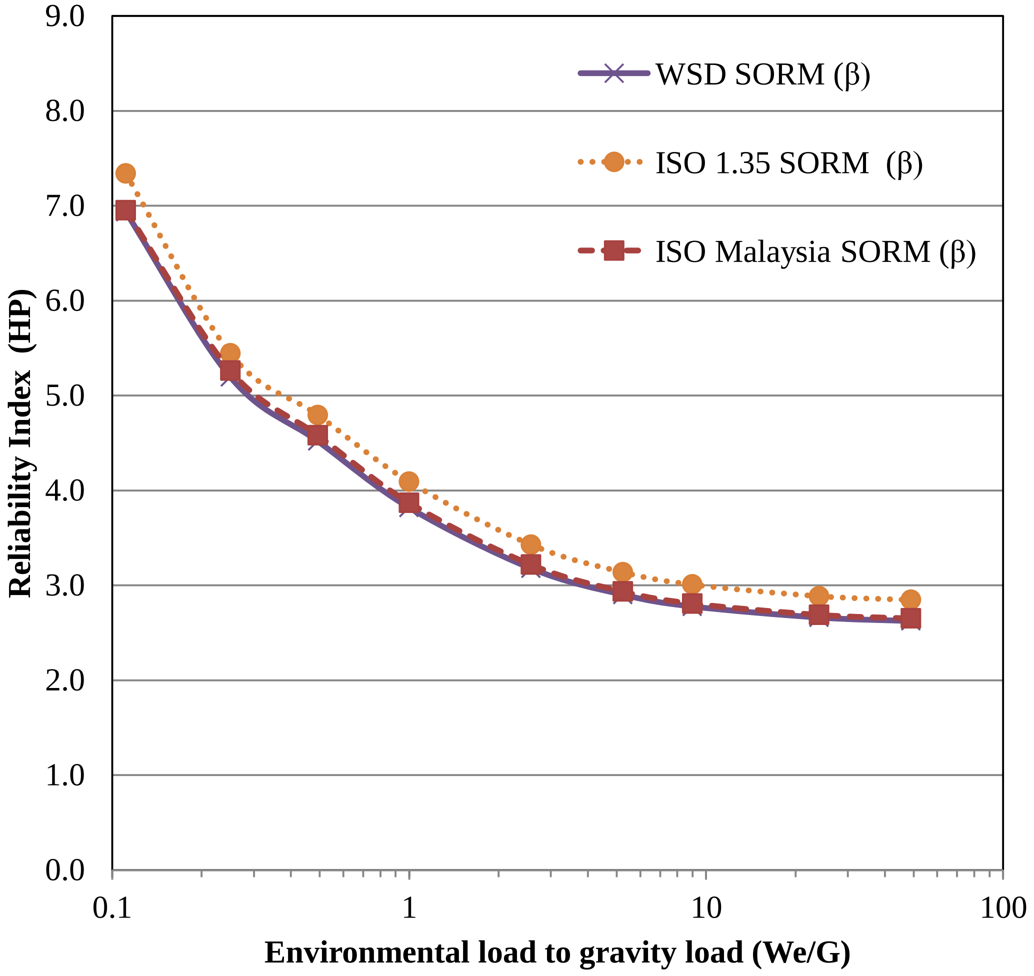

Figure 4.1.3.14 Graph of reliability index Vs environmental load to gravity load ratio for component under compression, bending and hydrostatic pressure for horizontal periphery member using SORM

4.1.4 Leg

4.1.4.1 Axial Tension

According to Figure 4.1.4.1, by using FORM, the value of reliability index when environmental load to gravity load ratio is equal to 1.0 using ISO code with load factor of 1.35 is 4.0409, while reliability index of ISO Malaysia with load factor of 1.23 is 3.81. On the other hand, value of reliability index of WSD is 3.8658.

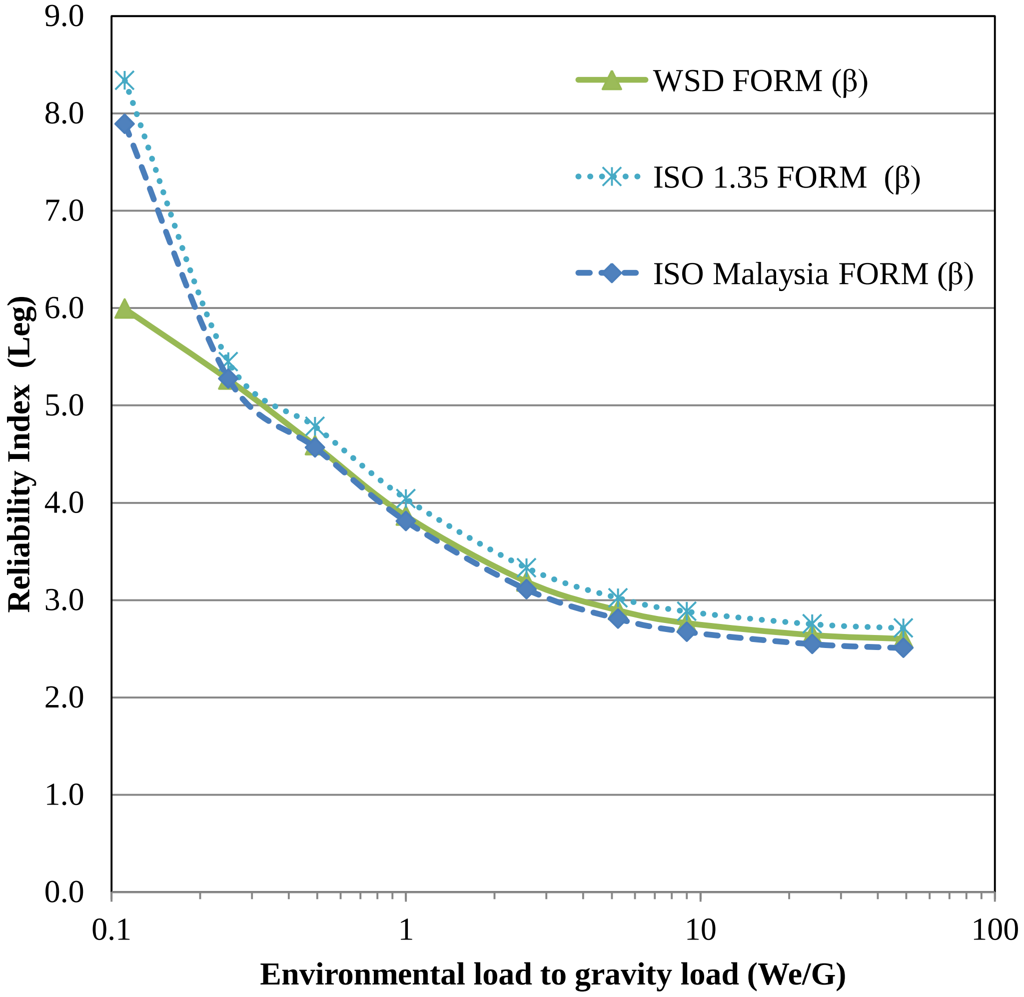

Figure 4.1.4.1 Graph of reliability index Vs environmental load to gravity load ratio for component under axial tension for leg member using FORM

According to Figure 4.1.4.2, by using SORM, the value of reliability index when environmental load to gravity load ratio is equal to 1.0 using ISO code with load factor of 1.35 is 3.8913, while reliability index of ISO Malaysia with load factor of 1.23 is 3.6509. On the other hand, value of reliability index of WSD is 3.7113.

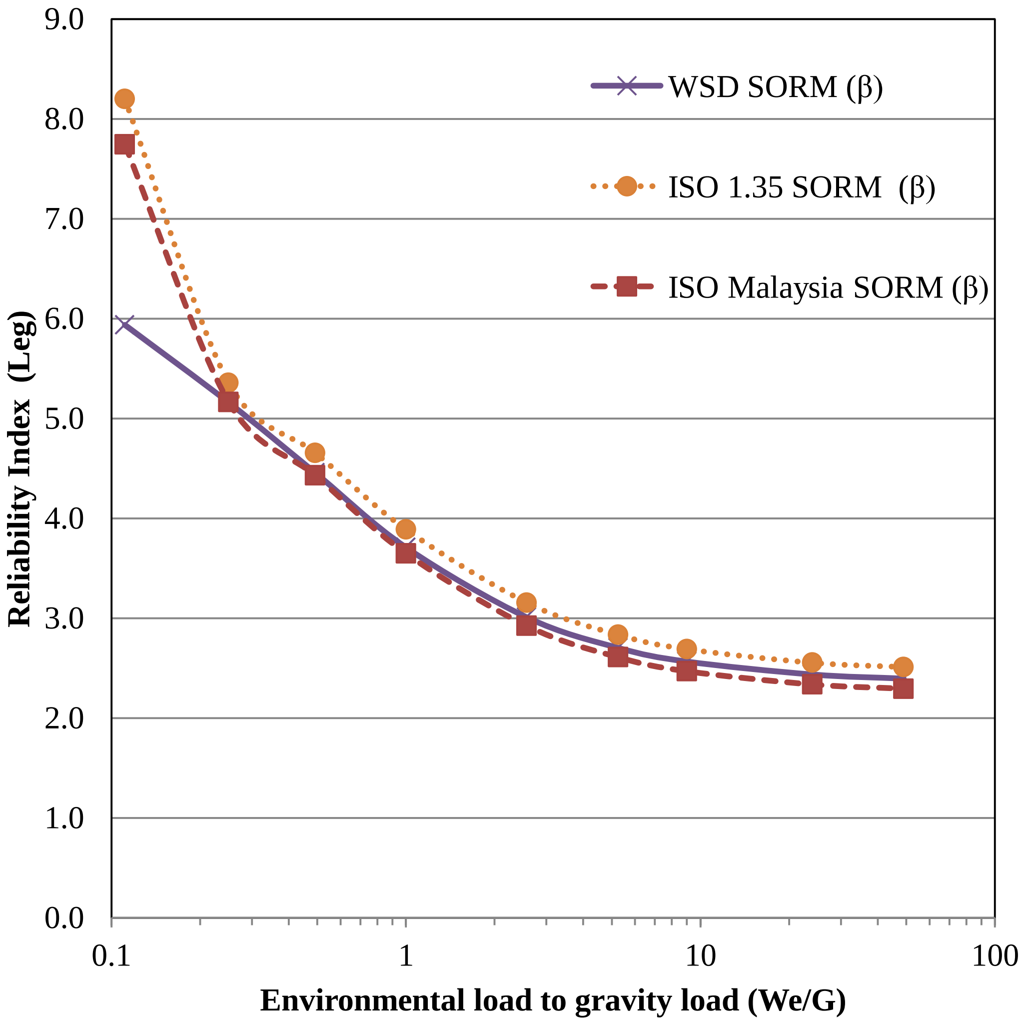

Figure 4.1.4.2 Graph of reliability index Vs environmental load to gravity load ratio for component under axial tension for leg member using SORM

4.1.4.2 Axial Compression

According to Figure 4.1.4.3, by using FORM, the value of reliability index when environmental load to gravity load ratio is equal to 1.0 using ISO code with load factor of 1.35 is 4.5367, while reliability index of ISO Malaysia with load factor of 1.23 is 4.3434. On the other hand, value of reliability index of WSD is 4.336.

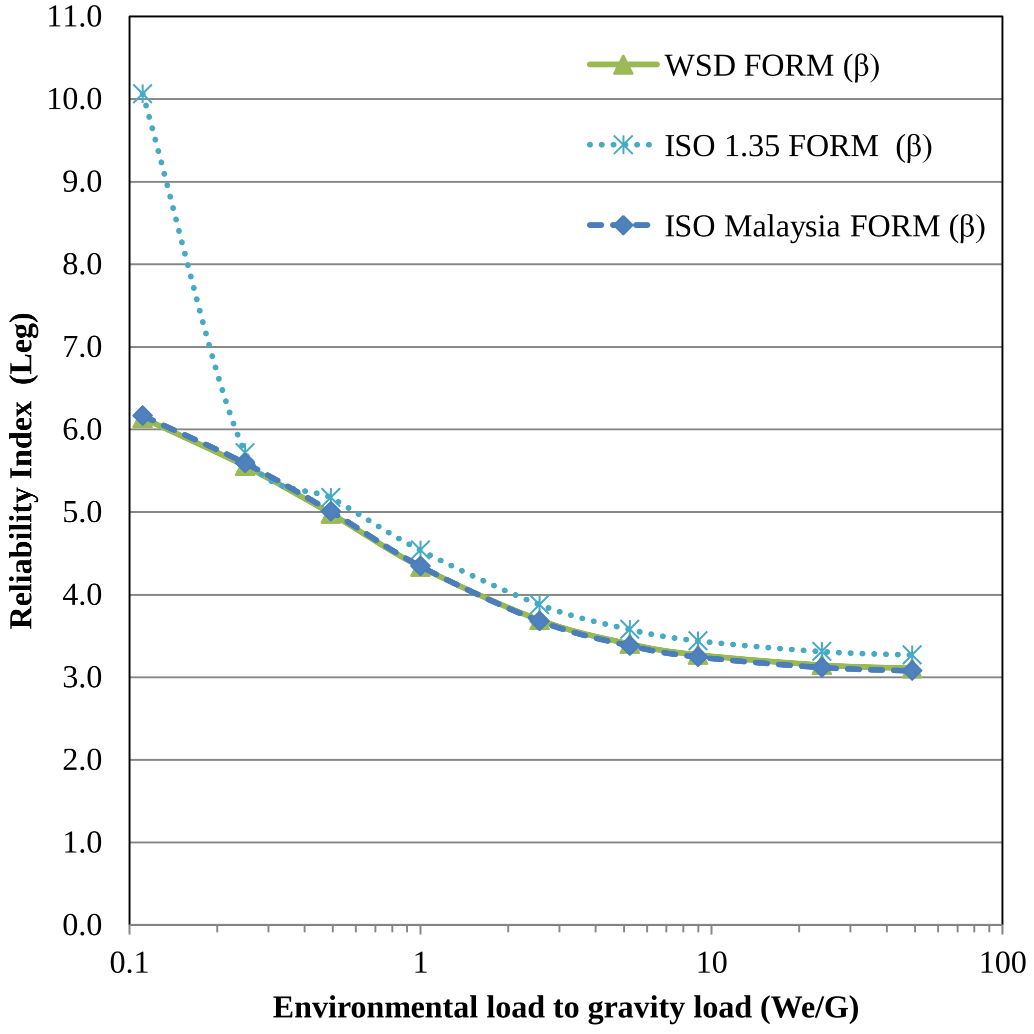

Figure 4.1.4.3 Graph of reliability index Vs environmental load to gravity load ratio for component under axial compression for leg member using FORM

According to Figure 4.1.4.4, by using SORM, the value of reliability index when environmental load to gravity load ratio is equal to 1.0 using ISO code with load factor of 1.35 is 4.4107, while reliability index of ISO Malaysia with load factor of 1.23 is 4.2094. On the other hand, value of reliability index of WSD is 4.203.

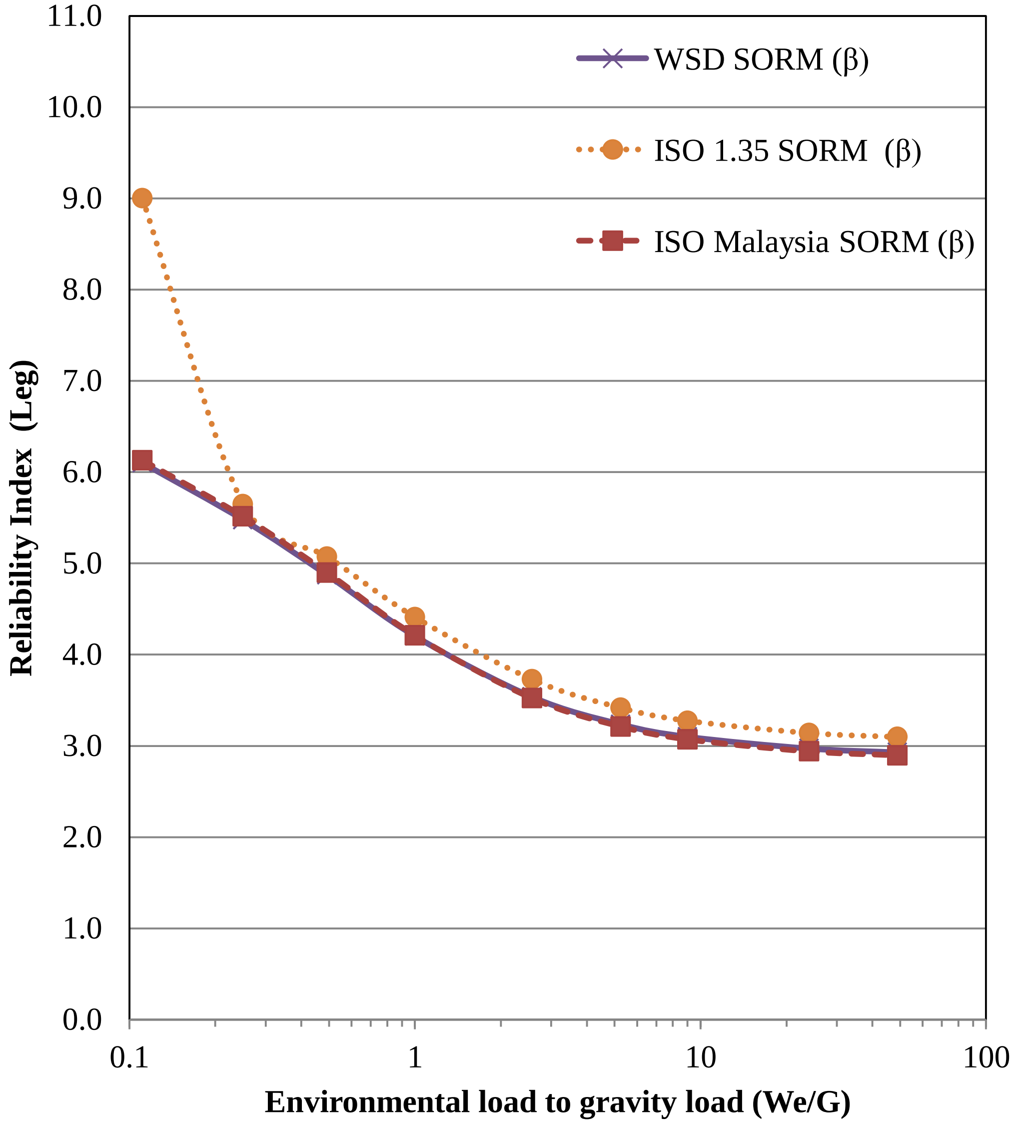

Figure 4.1.4.4 Graph of reliability index Vs environmental load to gravity load ratio for component under axial compression for leg member using SORM

4.1.4.3 Bending

According to Figure 4.1.4.5, by using FORM, the value of reliability index when environmental load to gravity load ratio is equal to 1.0 using ISO code with load factor of 1.35 is 3.5632, while reliability index of ISO Malaysia with load factor of 1.23 is 3.3023. On the other hand, value of reliability index of WSD is 3.9964.

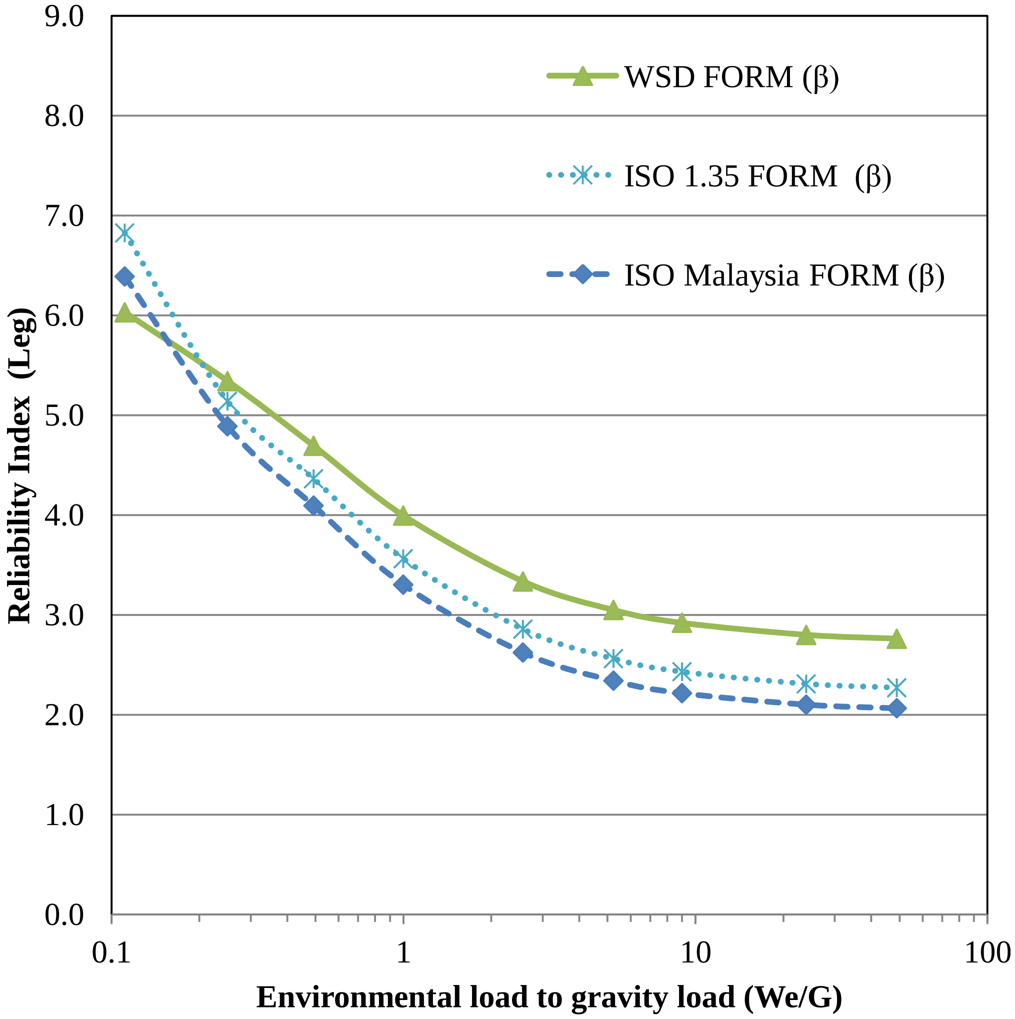

Figure 4.1.4.5 Graph of reliability index Vs environmental load to gravity load ratio for component under bending for horizontal leg using FORM

According to Figure 4.1.4.6, by using SORM, the value of reliability index when environmental load to gravity load ratio is equal to 1.0 using ISO code with load factor of 1.35 is 3.3943, while reliability index of ISO Malaysia with load factor of 1.23 is 3.123. On the other hand, value of reliability index of WSD is 3.8519.

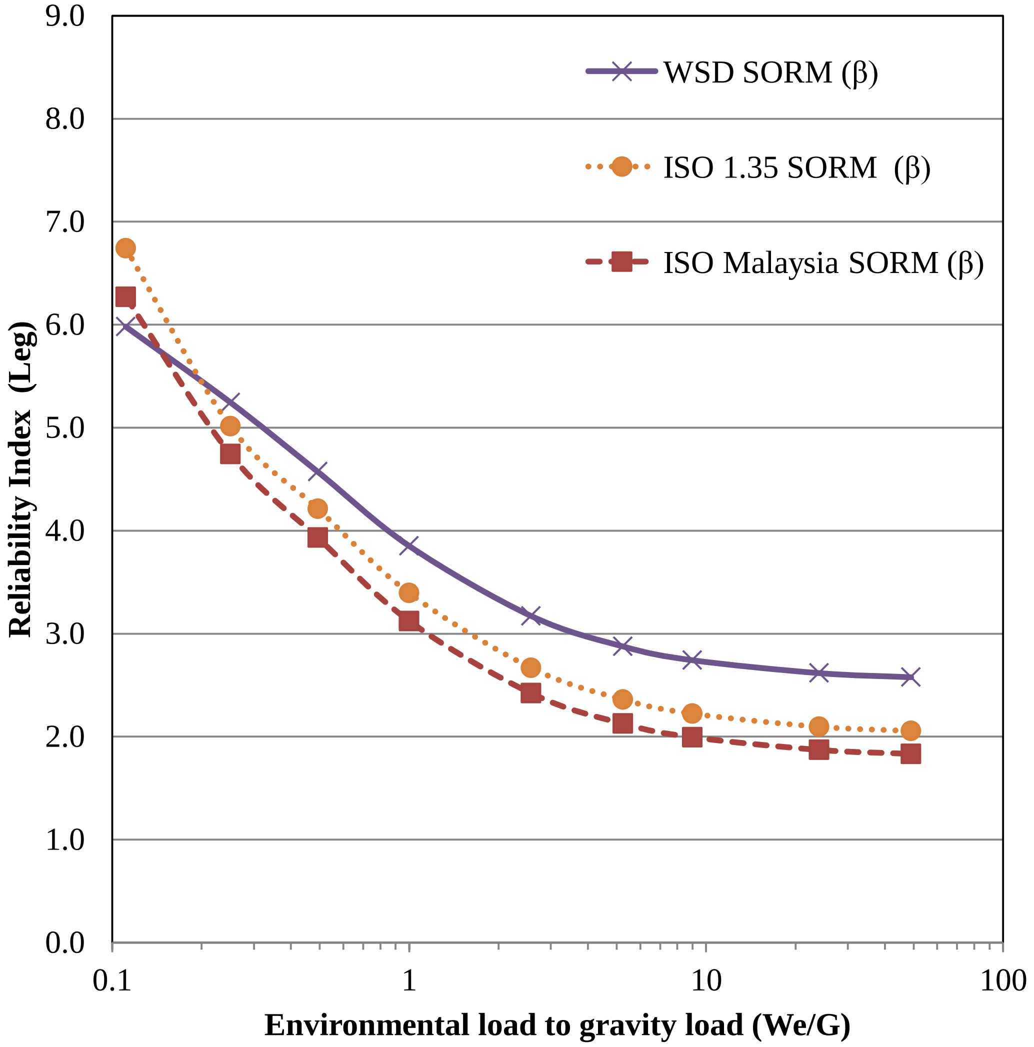

Figure 4.1.4.6 Graph of reliability index Vs environmental load to gravity load ratio for component under bending for leg member using SORM

4.1.4.4 Tension and Bending

According to Figure 4.1.4.7, by using FORM, the value of reliability index when environmental load to gravity load ratio is equal to 1.0 using ISO code with load factor of 1.35 is 3.7416, while reliability index of ISO Malaysia with load factor of 1.23 is 3.4956. On the other hand, value of reliability index of WSD is 3.8525.

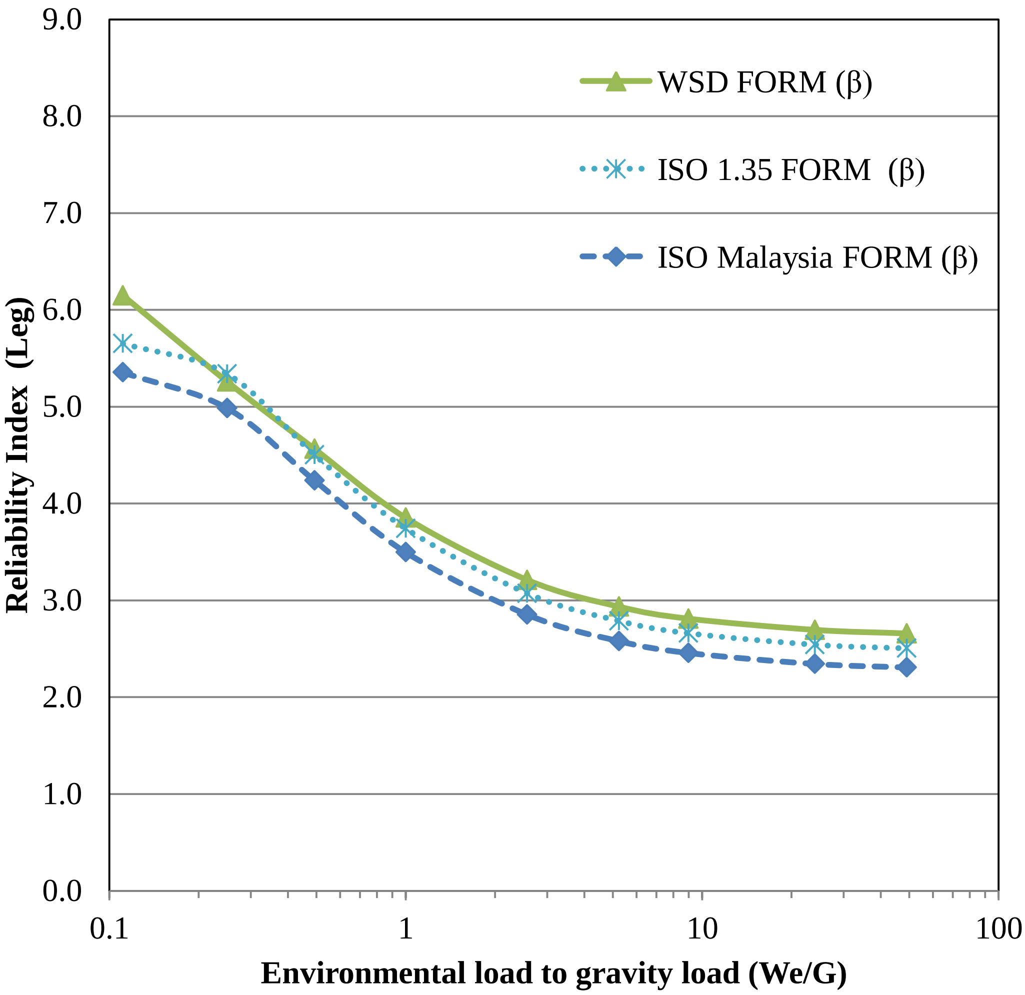

Figure 4.1.4.7 Graph of reliability index Vs environmental load to gravity load ratio for component under tension and bending for leg member using FORM

According to Figure 4.1.4.8, by using SORM, the value of reliability index when environmental load to gravity load ratio is equal to 1.0 using ISO code with load factor of 1.35 is 3.5439, while reliability index of ISO Malaysia with load factor of 1.23 is 3.2904. On the other hand, value of reliability index of WSD is 3.6722.

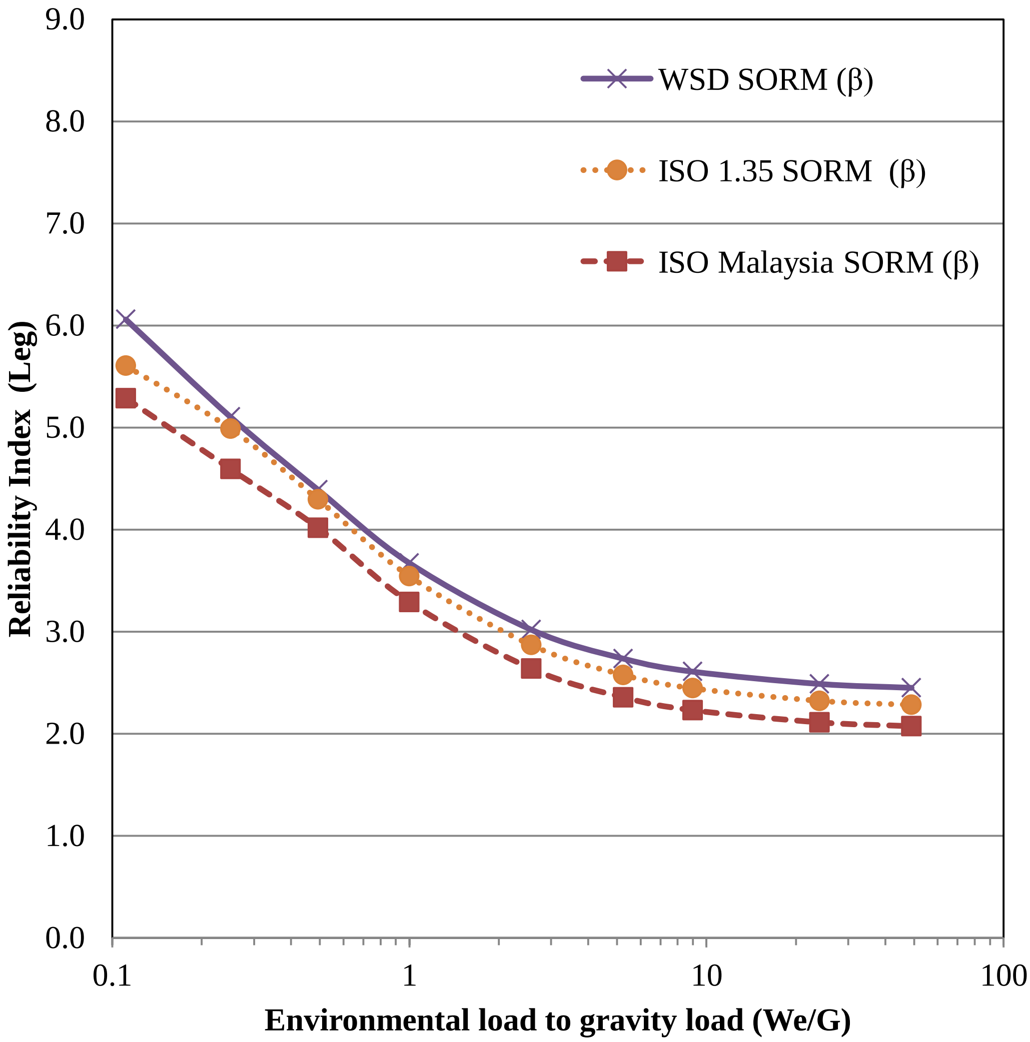

Figure 4.1.4.8 Graph of reliability index Vs environmental load to gravity load ratio for component under tension and bending for leg member using SORM

4.1.4.5 Compression and Bending

According to Figure 4.1.4.9, by using FORM, the value of reliability index when environmental load to gravity load ratio is equal to 1.0 using ISO code with load factor of 1.35 is 3.9663, while reliability index of ISO Malaysia with load factor of 1.23 is 3.732. On the other hand, value of reliability index of WSD is 3.8337.

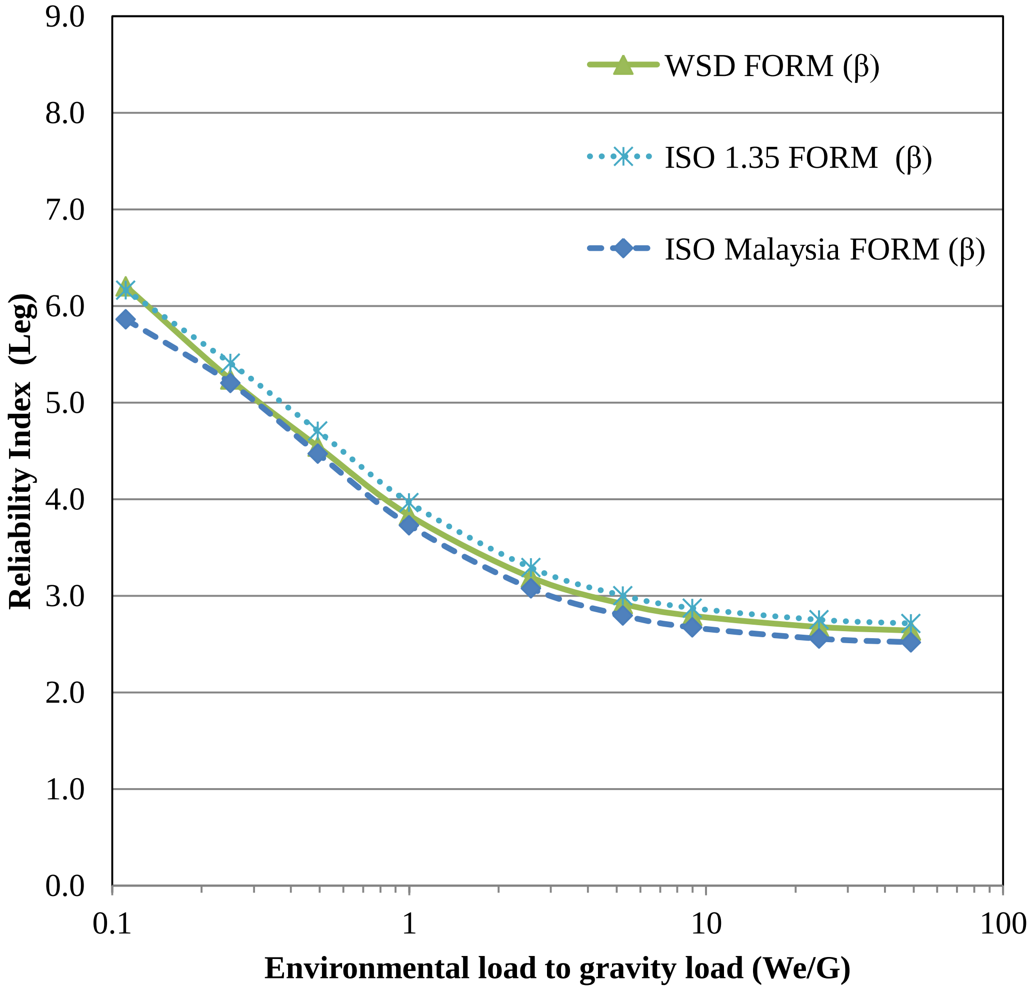

Figure 4.1.4.9 Graph of reliability index Vs environmental load to gravity load ratio for component under compression and bending for leg member using FORM

According to Figure 4.1.4.10, by using SORM, the value of reliability index when environmental load to gravity load ratio is equal to 1.0 using ISO code with load factor of 1.35 is 3.784, while reliability index of ISO Malaysia with load factor of 1.23 is 3.5416. On the other hand, value of reliability index of WSD is 3.6564.

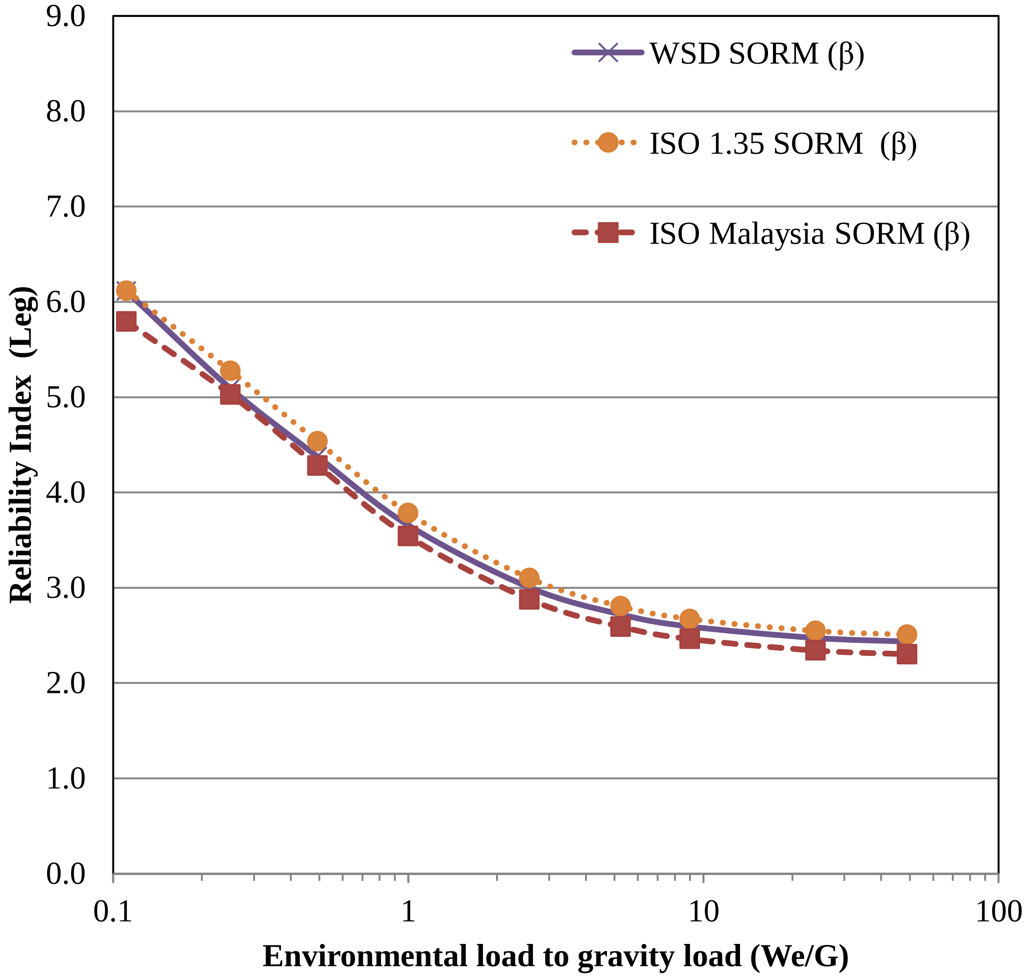

Figure 4.1.4.10 Graph of reliability index Vs environmental load to gravity load ratio for component under compression and bending for leg member using SORM

4.1.4.6 Tension, Bending and Hydrostatic Pressure

According to Figure 4.1.4.11, by using FORM, the value of reliability index when environmental load to gravity load ratio is equal to 1.0 using ISO code with load factor of 1.35 is 4.4286, while reliability index of ISO Malaysia with load factor of 1.23 is 4.2244. On the other hand, value of reliability index of WSD is 3.8175.

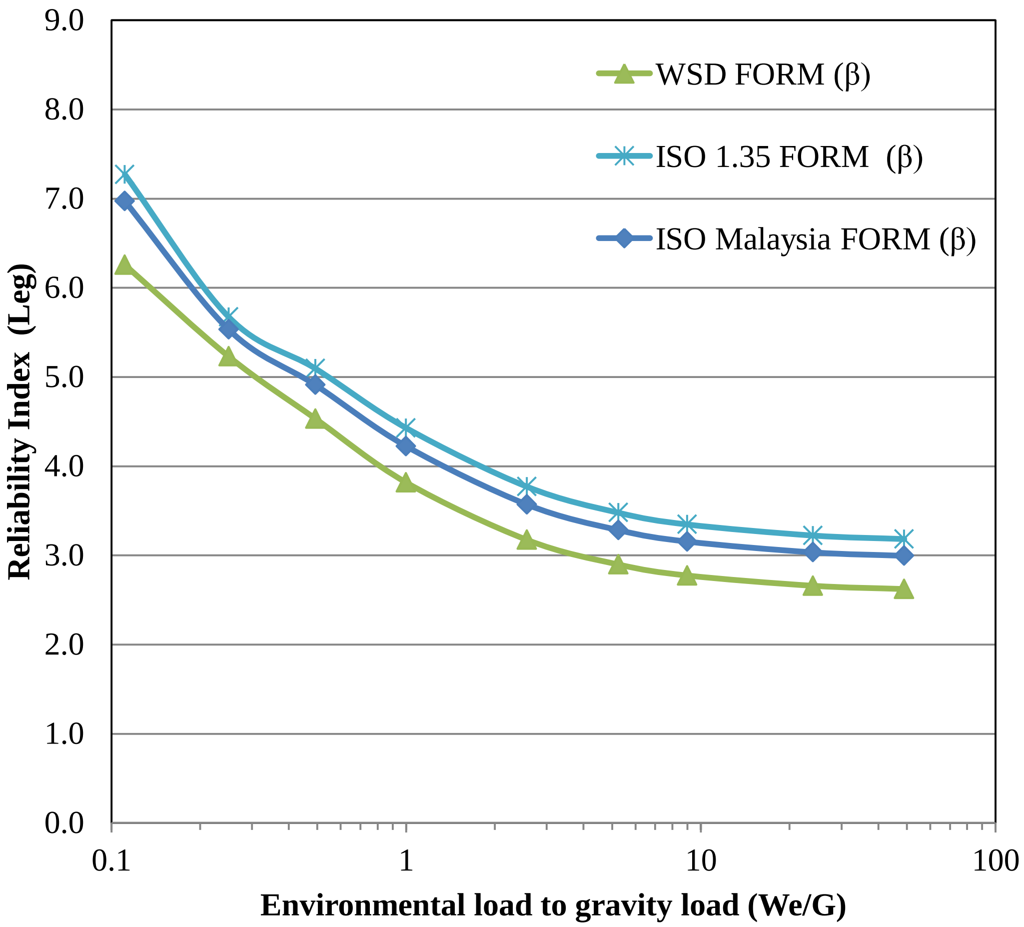

Figure 4.1.4.11 Graph of reliability index Vs environmental load to gravity load ratio for component under tension, bending and hydrostatic pressure for leg member using FORM

According to Figure 4.1.4.12, by using SORM, the value of reliability index when environmental load to gravity load ratio is equal to 1.0 using ISO code with load factor of 1.35 is 4.2763, while reliability index of ISO Malaysia with load factor of 1.23 is 4.0636. On the other hand, value of reliability index of WSD is 3.6429.

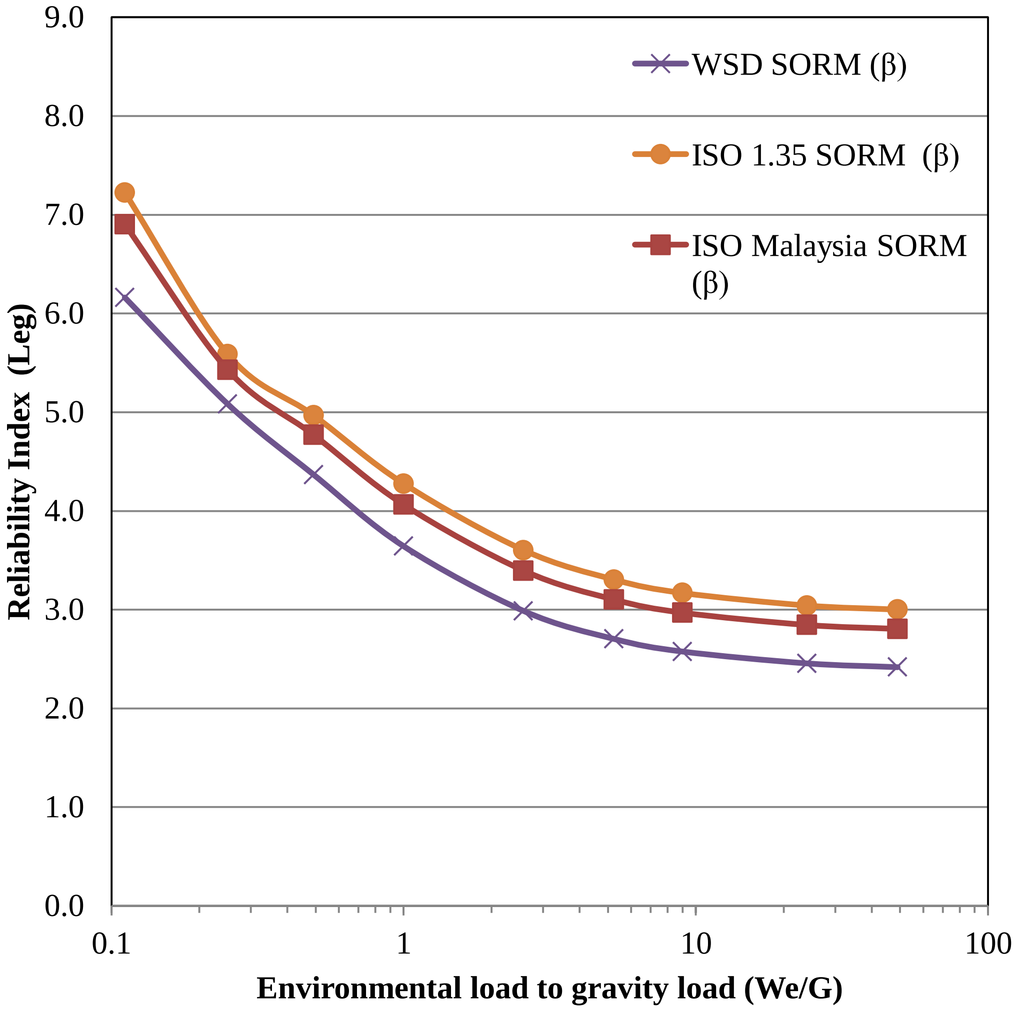

Figure 4.1.4.12 Graph of reliability index Vs environmental load to gravity load ratio for component under tension, bending and hydrostatic pressure for leg member using SORM

4.1.4.7 Compression, Bending and Hydrostatic Pressure

According to Figure 4.1.4.13, by using FORM, the value of reliability index when environmental load to gravity load ratio is equal to 1.0 using ISO code with load factor of 1.35 is 4.6489, while reliability index of ISO Malaysia with load factor of 1.23 is 4.4626. On the other hand, value of reliability index of WSD is 4.537.

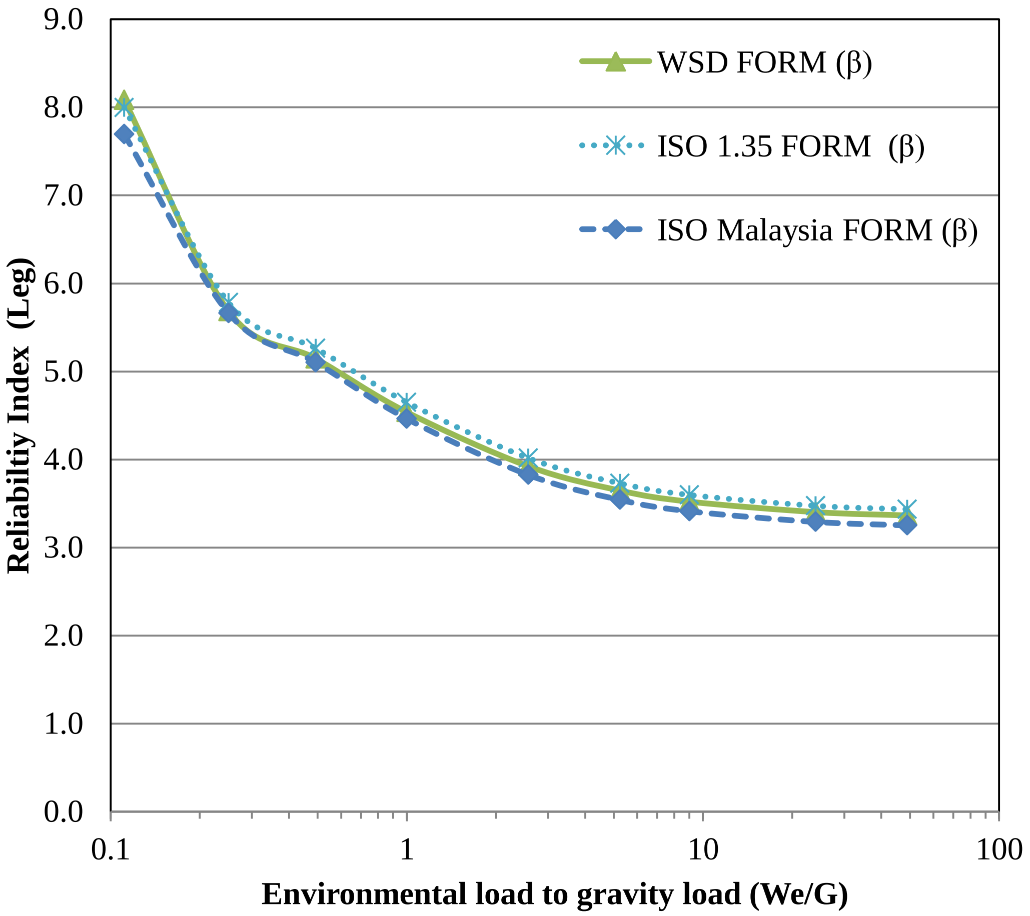

Figure 4.1.4.13 Graph of reliability index Vs environmental load to gravity load ratio for component under compression, bending and hydrostatic pressure for leg member using FORM

According to Figure 4.1.4.14, by using SORM, the value of reliability index when environmental load to gravity load ratio is equal to 1.0 using ISO code with load factor of 1.35 is 4.5114, while reliability index of ISO Malaysia with load factor of 1.23 is 4.3166. On the other hand, value of reliability index of WSD is 4.4002.

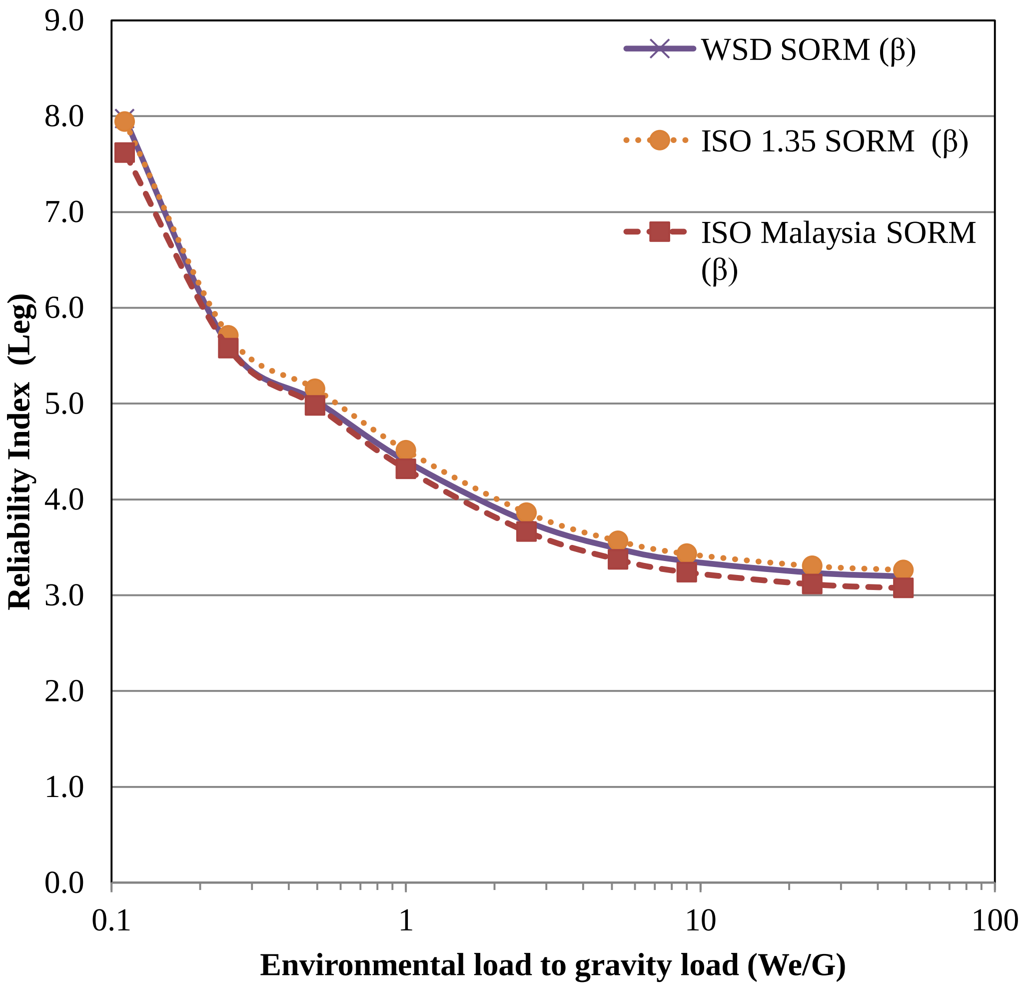

Figure 4.1.4.14 Graph of reliability index Vs environmental load to gravity load ratio for component under compression, bending and hydrostatic pressure for leg member using SORM

4.2 Environmental load factor

Environmental load factor can be determined by plotting the curve of reliability index for WSD and reliability index for ISO with different environmental load factor values. At the point of intersection between the two curves is the environmental load factor. The intersection point is the point where the ISO standard gives the same safety index as WSD standard. The condition of environmental load to gravity load ratio of 1.0 is chosen. Figure 4.2.1 and Figure 4.2.2 shows the environmental load factors found using FORM and SORM.

According to Figure 4.2.1, the environmental load factor found using FORM is 1.23.

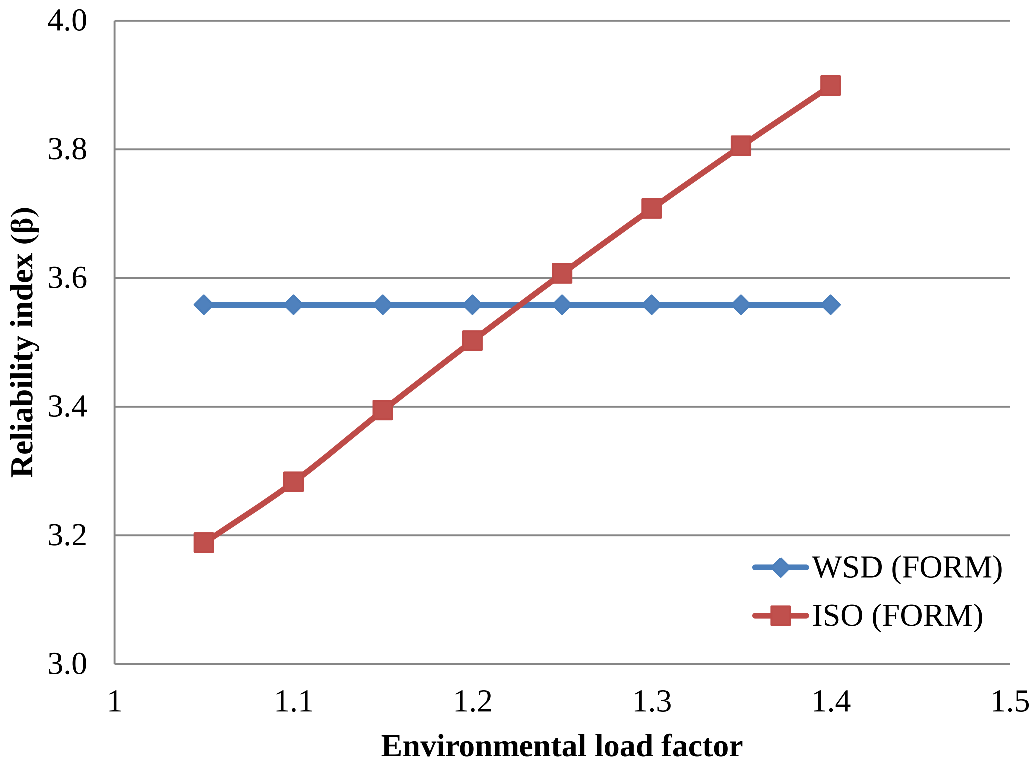

Figure 4.2.1 Environmental load factor using FORM

According to Figure 4.2.2, the environmental load factor found using SORM is 1.23.

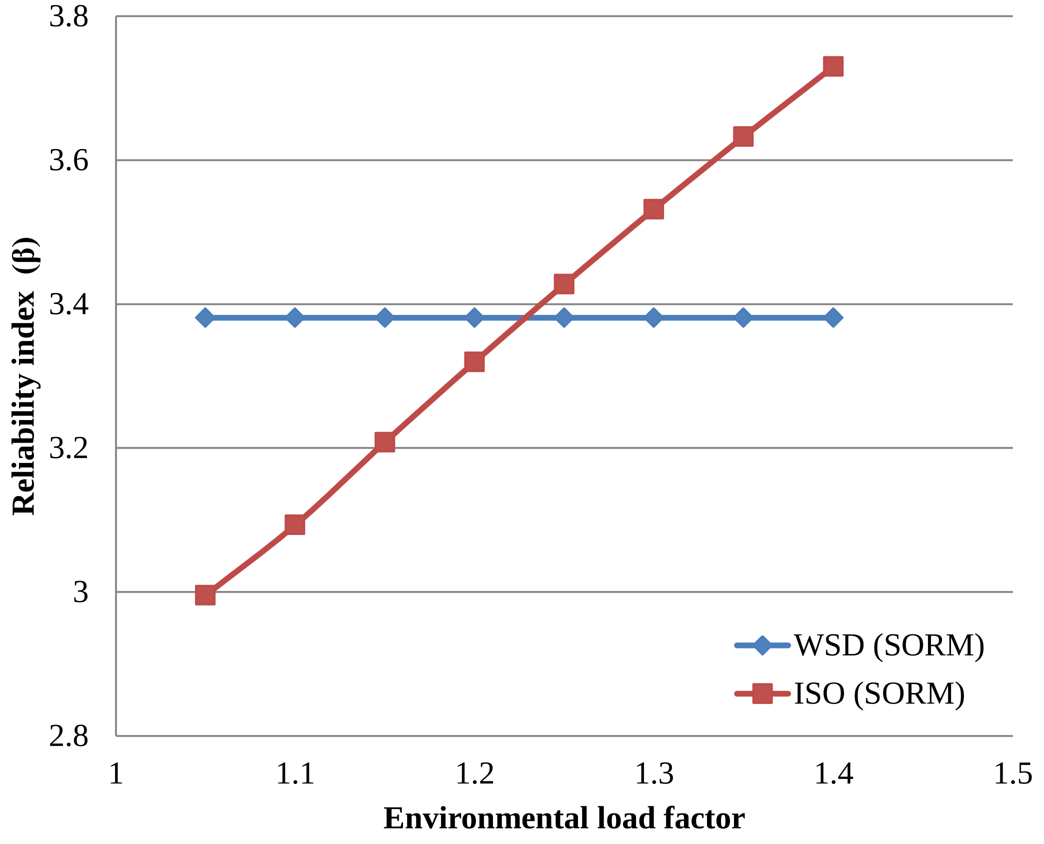

Figure 4.2.2 Environmental load factor using SORM

4.3 Sensitivity Analysis of Random Variables

Sensitivity analysis identifies the relationship between the change in reliability and the change in characteristics of uncertain variables, in which most of the current sensitivity analysis methods are applicable for only random variables. In other words, sensitivity analysis provides information about the relationship between reliability and the distribution parameters of random variables. Hence, sensitivity analysis can be used to identify the most significant random variables that have the highest contributions to reliability. In this study, sensitivity indices are defined for the sensitivity of reliability with respect to parameters of random variables for vertical diagonal, horizontal diagonal, horizontal periphery and leg members.

According to the Table 4.3.1.1 to Table 4.3.1.7, for every member and all of the isolated and combined stresses, environmental load uncertainty model is the most significant random variable which has highest contribution to reliability. It can also be said that among all of the random variables listed, random variables that have the significant contributions to reliability are environmental load uncertainty model, stress model uncertainty, yield strength, current and significant wave height.

Table 4.3.1 shows the optimum values of variables which were found from the FORM reliability analysis.

Table 4.3.1 Table of values of parameters of variability

	Parameters of Variability	
Basic Variable	Mean	Standard Deviation
Yield strength (N/mm^2)	424.35	17.25
Diameter (mm)	711.00	1.28
Thickness (mm)	15.36	0.24
Young's modulus (Gpa)	210,000	10,500
Significant wave height (m)	4.22	0.57
Current (m)	0.79	0.15
Environmental load uncertainty model	1.00	0.15
Dead load (kN)	1.00	0.06
Live load (kN)	1.00	0.10
Stress model uncertainty	1.27	0.05

4.3.1 Axial Tension

According to Table 4.3.1.1, the top three most significant random variables that have the highest contributions to reliability are defined in which, for vertical diagonal member are environmental load uncertainty model, followed by significant wave height, and yield strength. For horizontal diagonal member are environmental load uncertainty model, followed by yield strength, and stress model uncertainty. In the case of horizontal periphery and leg members are environmental load uncertainty model, followed by significant wave height, and yield strength.

Table 4.3.1.1 Table of sensitivity analysis of random variables under axial tension

	Sensitivity factor (α)			
Basic variable	Vertical Diagonal	Horizontal Diagonal	Horizontal Periphery	Leg
Yield strength	-0.1683	-0.0782	-0.1597	-0.1646
Diameter	-0.0075	-0.0035	-0.0072	-0.0056
Thickness	-0.0622	-0.0290	-0.0578	-0.0617
Significant wave height	0.1953	-0.0148	0.2832	0.2963
Current	-0.0655	-0.0493	-0.0477	-0.0559
Environmental load uncertainty model	-0.9476	-0.9909	-0.9297	-0.9232
Dead Load	0.0102	0.0267	0.0012	0.0012
Live Load	0.0171	0.0446	0.0020	0.0021
Stress model uncertainty	-0.0641	-0.0763	-0.1557	-0.1606

4.3.2 Axial Compression

According to Table 4.3.1.2, the top three most significant random variables that have the highest contributions to reliability are defined in which, for vertical diagonal member are environmental load uncertainty model, followed by yield strength, and stress model uncertainty. For horizontal diagonal member are environmental load uncertainty model, followed by effective length ratio, and current. In the case of horizontal periphery member are environmental load uncertainty model, followed by yield strength, and stress model uncertainty. Lastly, for leg members are environmental load uncertainty model, followed by significant wave height, and yield strength.

Table 4.3.1.2 Table of sensitivity analysis of random variables under axial compression

	Sensitivity factor (α)			
Basic variable	Vertical Diagonal	Horizontal Diagonal	Horizontal Periphery	Leg
Yield strength	-0.1265	-0.0815	-0.1508	-0.1439
Diameter	-0.0067	-0.0191	-0.0090	-0.0053
Thickness	-0.0463	-0.0678	-0.0547	-0.0550
Young’s modulus	-0.0149	-0.1344	-0.0280	-0.0038
Effective length factor	0.0638	0.5848	0.1192	0.0146
Length	0.0015	0.0140	0.0028	0.0004
Significant wave height	0.0961	-0.0637	0.2748	0.2749
Current	-0.0335	-0.2106	-0.0462	-0.0513
Environmental load uncertainty model	-0.9739	-0.7379	-0.9270	-0.9366
Dead Load	0.0305	0.0087	0.0011	0.0010
Live Load	0.0508	0.0145	0.0019	0.0016
Stress model uncertainty	-0.1232	-0.1867	-0.1493	-0.1435

4.3.3 Bending

According to Table 4.3.1.3, the top three most significant random variables that have the highest contributions to reliability are defined in which, for vertical diagonal member are environmental load uncertainty model, followed by stress model uncertainty, and yield strength. For horizontal diagonal member are environmental load uncertainty model, followed by stress model uncertainty, and current. In the case of horizontal periphery member are environmental load uncertainty model, followed by yield strength, and stress model uncertainty. Lastly, for leg members are environmental load uncertainty model, followed by significant wave height, and stress model uncertainty.

Table 4.3.1.3 Table of sensitivity analysis of random variables under bending

	Sensitivity factor (α)			
Basic variable	Vertical Diagonal	Horizontal Diagonal	Horizontal Periphery	Leg
Yield strength	-0.2112	-0.2245	-0.1237	-0.1248
Diameter	-0.0194	-0.0208	-0.0112	-0.0097
Thickness	-0.0891	-0.0981	-0.0427	-0.0713
Young’s modulus	-0.0219	-0.0273	0	-0.0401
Significant wave height	0.0386	-0.0670	0.2116	0.3346
Current	-0.1454	-0.2300	-0.0355	-0.0356
Environmental load uncertainty model	-0.9180	-0.8912	-0.9602	-0.9135
Dead Load	0.0683	0.0602	0.0058	0.0012
Live Load	0.1138	0.1003	0.0097	0.0020
Stress model uncertainty	-0.2522	-0.2711	-0.1206	-0.1729

4.3.4 Tension and Bending

According to Table 4.3.1.4, the top three most significant random variables that have the highest contributions to reliability are defined in which, for vertical diagonal member are environmental load uncertainty model, followed by stress model uncertainty, and yield strength. For horizontal diagonal member are environmental load uncertainty model, followed by stress model uncertainty, and current. In the case of horizontal periphery member are environmental load uncertainty model, followed by significant wave height, and stress model uncertainty. Lastly, for leg members are environmental load uncertainty model, followed by stress model uncertainty, and significant wave height.

Table 4.3.1.4 Table of sensitivity analysis of random variables under tension and bending

	Sensitivity factor (α)			
Basic variable	Vertical Diagonal	Horizontal Diagonal	Horizontal Periphery	Leg
Yield strength	-0.1907	-0.1961	-0.1540	-0.1462
Diameter	-0.0122	-0.0126	-0.0101	-0.0070
Thickness	-0.0743	-0.0789	-0.0546	-0.0642
Young’s modulus	-0.0084	-0.0098	0	-0.0152
Significant wave height	0.0914	-0.0726	0.2717	0.3017
Current	-0.0814	-0.2404	-0.0564	-0.0467
Environmental load uncertainty model	-0.8645	-0.8428	-0.9198	-0.8766
Dead Load	0.0587	0.0016	0.0012	0.0012
Live Load	0.0978	0.0027	0.0019	0.0021
Stress model uncertainty	-0.4273	-0.4262	-0.1680	-0.3355

4.3.5 Compression and Bending

According to Table 4.3.1.5, the top three most significant random variables that have the highest contributions to reliability are defined in which, for vertical diagonal member are environmental load uncertainty model, followed by stress model uncertainty, and yield strength. For horizontal diagonal member are environmental load uncertainty model, followed by stress model uncertainty, and current. In the case of horizontal periphery member are environmental load uncertainty model, followed by significant wave height, and yield strength. Lastly, for leg members are environmental load uncertainty model, followed by stress model uncertainty, and significant wave height.

Table 4.3.1.5 Table of sensitivity analysis of random variables under compression and bending

	Sensitivity factor (α)			
Basic variable	Vertical Diagonal	Horizontal Diagonal	Horizontal Periphery	Leg
Yield strength	-0.1494	-0.1779	-0.1660	-0.1462
Diameter	-0.0121	-0.0178	-0.0138	-0.0088
Thickness	-0.0761	-0.0771	-0.0613	-0.0649
Young's modulus	-0.0438	-0.0641	-0.0109	-0.0216
Effective length factor	0.0335	0.2288	0.0477	0.0063
Length	0.0008	0.0053	0.0011	0.0002
Significant wave height	0.0674	-0.0711	0.2817	0.2963
Current	-0.0898	-0.2355	-0.0646	-0.0475
Environmental load uncertainty model	-0.8988	-0.8254	-0.8982	-0.8791
Dead Load	0.0501	0.0016	0.0085	0.0079
Live Load	0.0835	0.0027	0.0141	0.0132
Stress model uncertainty	-0.3724	-0.4047	-0.1231	-0.3352

4.3.6 Tension, Bending and Hydrostatic Pressure

According to Table 4.3.1.6, the top three most significant random variables that have the highest contributions to reliability are defined in which, for vertical diagonal member are environmental load uncertainty model, followed by stress model uncertainty, and yield strength. For horizontal diagonal member are environmental load uncertainty model, followed by stress model uncertainty, and current. In the case of horizontal periphery member are environmental load uncertainty model, followed by significant wave height, and yield strength. Lastly, for leg members are environmental load uncertainty model, followed by stress model uncertainty, and significant wave height.

Table 4.3.1.6 Table of sensitivity analysis of random variables under tension, bending and hydrostatic pressure

	Sensitivity factor (α)			
Basic variable	Vertical Diagonal	Horizontal Diagonal	Horizontal Periphery	Leg
Yield strength	-0.1592	-0.1874	-0.1512	-0.1460
Diameter	-0.0116	-0.0137	-0.0108	-0.0080
Thickness	-0.0638	-0.0775	-0.0533	-0.0555
Young's modulus	-0.0101	-0.0135	0	-0.0052
Significant wave height	0.0639	-0.0733	0.2568	0.2772
Current	-0.0848	-0.2444	-0.0493	-0.0456
Environmental load uncertainty model	-0.9162	-0.8617	-0.9240	-0.8992
Dead Load	0.0451	0.0015	0.0071	0.0061
Live Load	0.0752	0.0025	0.0118	0.0102
Stress model uncertainty	-0.3345	-0.3883	-0.1257	-0.2966

4.3.7 Compression, Bending and Hydrostatic Pressure

According to Table 4.3.1.7, the top three most significant random variables that have the highest contributions to reliability are defined in which, for vertical diagonal member are environmental load uncertainty model, followed by stress model uncertainty, and yield strength. For horizontal diagonal member are environmental load uncertainty model, followed by stress model uncertainty, and current. In the case of horizontal periphery member are environmental load uncertainty model, followed by significant wave height, and stress model uncertainty. Lastly, for leg members are environmental load uncertainty model, followed by significant wave height, and stress model uncertainty.

Table 4.3.1.7 Table of sensitivity analysis of random variables under compression, bending and hydrostatic pressure

	Sensitivity factor (α)			
Basic variable	Vertical Diagonal	Horizontal Diagonal	Horizontal Periphery	Leg
Yield strength	-0.0918	-0.1401	-0.1480	-0.1235
Diameter	-0.0078	-0.0167	-0.0124	-0.0074
Thickness	-0.0485	-0.0722	-0.0545	-0.0543
Young’s modulus	-0.0289	-0.0580	-0.0094	-0.0185
Effective length factor	0.0181	0.1964	0.0412	0.0050
Length	0.0004	0.0046	0.0009	0.0001
Significant wave height	0.0398	-0.0698	0.2632	0.2834
Current	-0.0616	-0.2364	-0.0515	-0.0375
Environmental load uncertainty model	-0.9660	-0.8612	-0.9199	-0.9111
Dead Load	0.0246	0.0093	0.0073	0.0009
Live Load	0.0410	0.0156	0.0122	0.0015
Stress model uncertainty	-0.2170	-0.3608	-0.2071	-0.2637

CHAPTER 5

CONCLUSION AND RECOMMENDATION

5.1 Conclusion

Structural reliability is evaluated for selected different types of members of offshore jacket platform using FORM and SORM methods by varying the environmental load to gravity load ratio ranging from 0.1 to 50.0. As environmental to gravity load ratio increases, the environmental loads govern over the gravity loads, which are summation of dead load and live load. According to the results obtained, as environmental to gravity load ratio, W_e/G ratio increases, the steepness of the curve decreases. Besides that, reliability decreases as W_e/G ratio increases, and the value of reliability indices are higher when gravity load governs compared to when environmental load governs.

5.1.1 Target Reliability

API WSD target reliability is used in this study. The target reliability for WSD using FORM is 3.6 while the value of target reliability for WSD using SORM is 3.4 in this study by averaging the reliability index values found from all of the stresses for every member.

5.1.2 Sensitivity Analysis

Sensitivity analysis of random variables is carried out for isolated and combined stresses and random variables that have the significant contributions to reliability are environmental load uncertainty model, stress model uncertainty, yield strength, current and significant wave height but environmental load uncertainty model has the highest contribution to reliability.

5.1.3 Environmental Load Factor

The environmental load factor recommended is 1.23 for offshore regions of Malaysia, compared to this ISO load factor is 1.35. The reduction of load factor will cause reduced ultimate load and thus smaller section size could be used and this will produce less weight for Jacket. The reduced weight will affect ultimately on cost savings as well as it will help our environment by using less amount of dead weight of steel.

5.2 Recommendation

Following are the main recommendations which are based on current study.

Since this study depends on data on the gravity and environmental loads. The database can be upgraded so that if there is any discrepancy, it should be removed by collecting more data.

Besides that, one jacket platform was used for SORM analysis in this study. More jacket platforms should be used to determine the reliability.

It is also recommended to select representative members in the range of twenty to thirty for each group of members as only ten elements were selected for each group of members.

Other than that, other methods of reliability analysis such as the Monte Carlo importance sampling may be used to verify the results.

REFERENCES

Abayomi, E. O., 2012. *Uncertainty Quantification and Risk Assessment of Offshore Structures.* Master Dissertation. University of Aberdeen.

Achintya, H. & Sankaran, M., 2000. *Probability, Reliability and Statistical Methods in Engineering Design.* United States of America: John Wiley & Sons, Inc.

API (WSD), 2008. RP 2A-WSD. American Petroleum Institute.

BOMEL Ltd, 2003. *System-based calibration of North West European annex environmental load factors for the ISO fixed steel offshore structures code 19902,* Fifield: HSE BOOKS.

Bucher, C. G. and Bourgund, U., 1990. A fast and efficient response surface approach for structural reliability problems. *Structural Safety,* 7(1), pp. 57-66.

Bulleit, W. M., 2008. Uncertainty in Structural Engineering. *PRACTICE PERIODICAL ON STRUCTURAL DESIGN AND CONSTRUCTION,* February, pp. 24-30.

Choi, S. K., Grandhi, R. V. and Canfield, R. A., 2006. *Reliability-based Structural Design.* 1st ed. London: Springer.

Choi, S. K., Ramana, V. G. and Robert, A. C., 2007. *Reliability-based Structural Design.* 1st ed. London: Springer.

Ferguson, M. C., 1990. *A Comparative Study Using API RP2A-LRFD.*. Houston, Offshore Technology Conference.

Fugro GEOS, 2001. *Wind and wave frequency distributions for sites around the British Isles,* Southampton: HSE Books.

Gudfinnur , S., Espen , C., Inge, L. & Bent , B., 1996. *Guideline for Offshore Structural Reliability Analysis: Application to Jacket Platforms,* Norway: Det Norske Veritas.

Graff, J. W., Tromans, P. S., Efthymiou, M.: *The reliability of offshore structures and its dependence on design code and environment*. Presented at the Offshore Technology Conference, OTC 7382, Houston.

Grant, C. K., 1995. *Development of a New Metocean Design Basis for the NW Shelf of Europe.* Texas, Offshore Technology Conference.

Haldar, A. & Mahadevan, S., 2000. *Probability, Reliability abd Statistical Methods in Engineering Design.* New York: John Wiley & Sons, Inc.

Heideman, J. C., Hagen, O., Cooper, C. & Dahl, F. E., 1989. Joint probability of extreme waves and currents on Norwegian Shelf. J. Waterw.. *Ocean Eng.,* Volume 115, pp. 534-546.

Idrus, B. A., Potty, N. S. and Nizamani, Z., 2011. TUBULAR STRENGTH COMPARISON OF OFFSHORE JACKET STRUCTURES UNDER API RP2A AND ISO 19902. *The Institutions of Engineers,* 72(3), pp. 41-50

ISO 19902, 2007. International Standard Organization 19902.

Johannessen, K., Meling, T. S. & Haver, S., 2002. Joint distribution for wind and waves in the northern north sea. *Int. J. Offshore Polar Eng.,* 12(1), pp. 1-8.

Kurian, V. J., Nizamani, Z., Liew, M. S.and Wahab and M. M. A., 2014. *System Reliability for Jacket Platform Subjected to Wave and Current Loads.* Kuala Lumpur, ESTCON - ICCOEE 2012.

Lee, O. S. and Kim, D. H., 2007. *Reliability of Fatigue Damaged Structure Using FORM, SORM and Fatigue Model.* London, WCE 2007.

Mangiavacchi, A., Rodenbusch, G., Radford, A., Wisch, D., 2005. *API offshore structures and standards: RP2A and much more.* Presented at Offshore Technology Conference, Houston.

Marley, M., Etterdal, E. and Grigorian, H., 2001. Structural Reliability Assessment of Ekofisk Jacket Under Extreme Loading, OTC 13190. Houston.

Missouri University of Science and Technology, 2008. *Uncertainty Analysis and Sensitivity Analysis for Multidisciplinary Systems Design.* Eisenhower Parkway: ProQuest.

Moses, F., 1981. *Reliability Based Design of Offshore Structures.* s.l., American Petroleum Institute.

MSL Engineering Limited, 2001. *Load factor calibration for ISO 13819 Regional Annex: Component resistance,* Norwich: HSE BOOKS.

Nizamani, Z., 2015. *Ocean Engineering & Oceanography: Environmental Load Factors and System Strength Evaluation of Offshore Jacket Platforms*. Kampar: Springer.

Nizamani, Z., Kurian, V. J. and Liew, M. S., 2014. Determination of environmental load factors for ISO 19902 code in offshore Malaysia using FORM structural reliability method. *Ocean Engineering,* Volume 92, pp. 31-43.

Pradnyana, G., Surahman, A. and Dasbi, S., 2000. *Review on the original annex of ISO-13819 standard for planning, designing and constructing fixed offshore platforms in Indonesia.* Bali, sixth AEESEAP Triennial Conference Kuta.

Petrauskas, C. , Botelho, D. L. R. , Krieger, W. F. , Griffin, J. J., 1994. A Reliability Model for Offshore Platforms and Its Application to ST151 "H" and "K" Platforms During Hurricane Andrew (1992). *BOSS -CONFERENCE-,* Volume 3, p. 17.

Raheem, S. E. A., 2013. Nonlinear response of fixed jacket offshore platform under structural and wave loads. *Coupled System Mechanics*, 2(1), pp. 111-126.

Sadeghi, K., 2007. An Overview of Design, Analysis, Construction and Installation of Offshore Petroleum Platforms Suitable for Cyprus Oil/ Gas Fields. *GAU Journal,* 2(4), pp. 1-16.

Sahoo, T., 2012. *Mathematical Techniques for Wave Interaction with Flexible Structure.* 3rd ed. USA: CRC Press.

Salau, M. A., Esezobor, D. E. and Omotoso, M. F., 2011. Reliability Assessment of Offshore Jacket Structures in Niger Delta. *Petroleum and Coal,* 53(4), pp. 291-301.

Speight, J. G., 2014. *Handbook for Offshore Oil and Gas Operations.* 1st ed. Waltham: Elsevier.

Theophanatos, A. and Wickham, A. H. S., 1993. Modelling of environmental loading for adaptation of API RP 2A - load and resistance factor design in UK offshore structural design practice. *Proceedings of the ICE,* 101(4), pp. 195-204.

Thomas, R., Wartelle, R. & Griff, C. L., 1976. *Fixed platform design for South East Asia.* s.l., Society of Engineering.

Tzyy, S. L. and Andrzej S. N., 1984. *Proof Loading and Structural Reliability.* 8th ed. Great Britain: Elsevier Applied Science .

University of Surrey, 2000. *A Review of Reliability Considerations for Fixed Offshore Platforms,* Surrey: Health & Safety Executive.

Yan-Gang, Z. & Tetsuro Ono, 1999. A general procedure for first/second-order reliability method (FORM/SORM). *Structural Safety* , Issue 21, pp. 95-112.

Yan-Gang, Z. & Tetsuro, O., 1999. New Approximations for SORM: Part 2. *Journal of Engineering Mechanics*, pp. 86-93.

Yusuke, H. et al., 2002. *Foundation Design Codes and Soil Investigation in View of International Harmonization and Performance Based Design.* Tokyo: Swets and Zeitlinger .

APPENDIX A: Table of result for reliability indices and probability of failure using ISO code with load factor of 1.40, 1.35 and 1.23, and API WSD code under axial tension for vertical diagonal, horizontal diagonal, horizontal periphery and leg members

Axial Tension	ISO (Load factor = 1.40)				ISO (Load factor = 1.35)				ISO (Load factor = 1.23)				API WSD			
	FORM β	FORM P_f	SORM β	SORM P_f	FORM P_f	SORM β	SORM P_f	FORM β	FORM P_f	SORM β	SORM P_f	FORM β	FORM P_f	SORM β	SORM P_f	FORM β
Vertical Diagonal																
0.9 GL+ 0.1 EL	8.4923	8.4000	8.4000	8.3600	8.3217	5.5511×10^{-17}	8.2100	8.8169×10^{-17}	7.8764	1.6653×10^{-15}	7.7397	4.9155×10^{-15}	5.9867	1.0707×10^{-9}	5.9397	1.4276×10^{-9}
0.8 GL+ 0.2 EL	5.5043	1.8534×10^{-8}	5.4259	2.8826×10^{-8}	5.4414	2.6430×10^{-8}	5.3579	4.2094×10^{-8}	5.2655	6.9919×10^{-8}	5.1674	1.1867×10^{-7}	5.2580	7.2827×10^{-8}	5.1624	1.2191×10^{-7}
0.67 GL+ 0.33 EL	4.8583	5.9202×10^{-7}	4.7433	1.0514×10^{-6}	4.7779	8.8581×10^{-7}	4.6578	1.5977×10^{-6}	4.5634	2.5166×10^{-6}	4.4305	4.7001×10^{-6}	4.5857	2.2629×10^{-6}	4.4574	4.1489×10^{-6}
0.5 GL+ 0.5 EL	4.1317	1.8003×10^{-5}	3.9848	3.3768×10^{-5}	4.0424	2.6455×10^{-5}	3.8911	4.9887×10^{-5}	3.8126	6.8765×10^{-5}	3.6504	1.3093×10^{-4}	3.8684	5.4784×10^{-5}	3.7112	1.0312×10^{-4}
0.28 GL+ 0.72 EL	3.4227	3.0997×10^{-4}	3.2490	5.7908×10^{-4}	3.3344	4.2735×10^{-4}	3.1565	7.9830×10^{-4}	3.1123	9.2818×10^{-4}	2.9236	1.7301×10^{-3}	3.1929	7.0427×10^{-4}	3.0094	1.3087×10^{-3}
0.16 GL+ 0.84 EL	3.1106	9.3369×10^{-4}	2.9241	1.7275×10^{-3}	3.0245	1.2452×10^{-3}	2.8337	2.3006×10^{-3}	2.8095	2.4807×10^{-3}	2.6075	4.5603×10^{-3}	2.8985	1.8747×10^{-3}	2.7020	3.4459×10^{-3}

0.1 GL+ 0.9 EL	2.9699	1.4896×10^{-3}	2.7772	2.7414×10^{-3}	2.8851	1.9562×10^{-3}	2.6881	3.5934×10^{-3}	2.6739	3.7483×10^{-3}	2.4654	6.8434×10^{-3}	2.7662	2.8358×10^{-3}	2.5634	5.1829×10^{-3}
0.04 GL+ 0.96 EL	2.8382	2.2687×10^{-3}	2.6394	4.1525×10^{-3}	2.7548	2.9368×10^{-3}	2.5515	5.3630×10^{-3}	2.5474	5.4267×10^{-3}	2.3324	9.8406×10^{-3}	2.6424	4.1160×10^{-3}	2.4334	7.4796×10^{-3}
0.02 GL+ 0.98 EL	2.7961	2.5862×10^{-3}	2.5953	4.7250×10^{-3}	2.7131	3.3324×10^{-3}	2.5078	6.0736×10^{-3}	2.5070	6.0872×10^{-3}	2.2899	1.1014×10^{-2}	2.6029	4.6221×10^{-3}	2.3918	8.3831×10^{-3}
Horizontal Diagonal																
0.9 GL+ 0.1 EL	5.9373	1.4487×10^{-9}	5.9034	1.7799×10^{-9}	5.8919	1.9093×10^{-9}	5.8548	2.3877×10^{-9}	5.7578	4.2610×10^{-9}	5.7104	5.6358×10^{-9}	5.7279	5.0850×10^{-9}	5.6795	6.7546×10^{-9}
0.8 GL+ 0.2 EL	5.0561	2.1392×10^{-7}	4.9723	3.3089×10^{-7}	4.9674	3.3928×10^{-7}	4.8769	5.3887×10^{-7}	4.7192	1.1841×10^{-6}	4.6099	2.0147×10^{-6}	4.7115	1.2295×10^{-6}	4.6064	2.0482×10^{-6}
0.67 GL+ 0.33 EL	4.1645	1.5602×10^{-5}	4.0380	2.6956×10^{-5}	4.0541	2.5167×10^{-5}	3.9218	4.3946×10^{-5}	3.7621	8.4249×10^{-5}	3.6160	1.4961×10^{-4}	3.7943	7.4037×10^{-5}	3.6535	1.2933×10^{-4}
0.5 GL+ 0.5 EL	3.1876	7.1734×10^{-4}	3.0298	1.2237×10^{-3}	3.0693	1.0728×10^{-3}	2.9079	1.8194×10^{-3}	2.7673	2.8257×10^{-3}	2.5978	4.6911×10^{-3}	2.8397	2.2579×10^{-3}	2.6741	3.7470×10^{-3}
0.28 GL+ 0.72 EL	2.2555	1.2049×10^{-2}	2.0807	1.8731×10^{-2}	2.1409	1.6140×10^{-2}	1.9640	2.4767×10^{-2}	1.8537	3.1892×10^{-2}	1.6719	4.7271×10^{-2}	1.9550	2.5293×10^{-2}	1.7755	3.7911×10^{-2}
0.16 GL+ 0.84 EL	1.8482	3.2288×10^{-2}	1.6682	4.7643×10^{-2}	1.7369	4.1200×10^{-2}	1.5552	5.9949×10^{-2}	1.4597	7.2191×10^{-2}	1.2741	1.0132×10^{-1}	1.5711	5.8085×10^{-2}	1.3872	8.2693×10^{-2}
0.1 GL+ 0.9 EL	1.6649	4.7971×10^{-2}	1.4828	6.9062×10^{-2}	1.5554	5.9928×10^{-2}	1.3718	8.5064×10^{-2}	1.2832	9.9716×10^{-2}	1.0960	1.3654×10^{-1}	1.3986	8.0968×10^{-2}	1.2130	1.1257×10^{-1}
0.04 GL+ 0.96 EL	1.4932	6.7688×10^{-2}	1.3095	9.5191×10^{-2}	1.3856	8.2939×10^{-2}	1.2004	1.1500×10^{-1}	1.1184	1.3170×10^{-1}	9.2983×10^{-1}	1.7623×10^{-1}	1.2373	1.0799×10^{-1}	1.0501	1.4683×10^{-1}
0.02 GL+ 0.98 EL	1.4384	7.5156×10^{-2}	1.2541	1.0490×10^{-1}	1.3314	9.1533×10^{-2}	1.1457	1.2597×10^{-1}	1.0658	1.4325×10^{-1}	8.7686×10^{-1}	1.9028×10^{-1}	1.1858	1.1786×10^{-1}	9.9816×10^{-1}	1.5910×10^{-1}
Horizontal Periphery																
0.9 GL+ 0.1 EL	8.5118	8.4600	8.4000	8.3700	8.3471	8.3000	8.3000	8.2600	7.9178	1.2212×10^{-15}	7.7933	3.2711×10^{-15}	6.0170	8.8818×10^{-10}	5.9661	1.2148×10^{-9}

0.8 GL+ 0.2 EL	5.5550	1.3881×10^{-8}	5.4713	2.2341×10^{-8}	5.4947	1.9566×10^{-8}	5.4059	3.2244×10^{-8}	5.3259	5.0232×10^{-8}	5.2229	8.8093×10^{-8}	5.3185	5.2307×10^{-8}	5.2178	9.0527×10^{-8}
0.67 GL+ 0.33 EL	4.9332	4.0447×10^{-7}	4.8141	7.3941×10^{-7}	4.8556	6.0016×10^{-7}	4.7318	1.1126×10^{-6}	4.6483	1.6730×10^{-6}	4.5127	3.1997×10^{-6}	4.6697	1.5079×10^{-6}	4.5384	2.8336×10^{-6}
0.5 GL+ 0.5 EL	4.2303	1.1669×10^{-5}	4.0822	2.2304×10^{-5}	4.1438	1.7080×10^{-5}	3.9918	3.2792×10^{-5}	3.9213	4.4042×10^{-5}	3.7592	8.5219×10^{-5}	3.9753	3.5148×10^{-5}	3.8180	6.7270×10^{-5}
0.28 GL+ 0.72 EL	3.5443	1.9682×10^{-4}	3.3720	3.7312×10^{-4}	3.4590	2.7106×10^{-4}	3.2829	5.1374×10^{-4}	3.2447	5.8787×10^{-4}	3.0586	1.1118×10^{-3}	3.3225	4.4603×10^{-4}	3.1413	8.4095×10^{-4}
0.16 GL+ 0.84 EL	3.2431	5.9109×10^{-4}	3.0592	1.1097×10^{-3}	3.1603	7.8816×10^{-4}	2.9723	1.4779×10^{-3}	2.9534	1.5715×10^{-3}	2.7550	2.9348×10^{-3}	3.0391	1.1864×10^{-3}	2.8459	2.2143×10^{-3}
0.1 GL+ 0.9 EL	3.1077	9.4271×10^{-4}	2.9181	1.7611×10^{-3}	3.0262	1.2384×10^{-3}	2.8324	2.3099×10^{-3}	2.8232	2.3771×10^{-3}	2.6187	4.4134×10^{-3}	2.9120	1.7958×10^{-3}	2.7129	3.3350×10^{-3}
0.04 GL+ 0.96 EL	2.9811	1.4363×10^{-3}	2.7858	2.6700×10^{-3}	2.9009	1.8604×10^{-3}	2.7014	3.4524×10^{-3}	2.7019	3.4469×10^{-3}	2.4913	6.3645×10^{-3}	2.7932	2.6093×10^{-3}	2.5883	4.8230×10^{-3}
0.02 GL+ 0.98 EL	2.9407	1.6376×10^{-3}	2.7435	3.0395×10^{-3}	2.8610	2.1117×10^{-3}	2.6595	3.9123×10^{-3}	2.6633	3.8688×10^{-3}	2.4506	7.1311×10^{-3}	2.7553	2.9315×10^{-3}	2.5484	5.4102×10^{-3}
Leg																
0.9 GL+ 0.1 EL	8.5069	8.4700	8.4000	8.3600	8.3367	8.3000	8.30000	8.2700	7.8906	1.4988×10^{-15}	7.7455	4.7894×10^{-15}	5.9916	1.0389×10^{-9}	5.9392	1.4317×10^{-9}
0.8 GL+ 0.2 EL	5.5104	1.7904×10^{-8}	5.4251	2.8964×10^{-8}	5.4475	2.5535×10^{-8}	5.3572	4.2270×10^{-8}	5.2715	6.7669×10^{-8}	5.1670	1.1892×10^{-7}	5.2639	7.0533×10^{-8}	5.1619	1.2224×10^{-7}
0.67 GL+ 0.33 EL	4.8623	5.8022×10^{-7}	4.7431	1.0522×10^{-6}	4.7814	8.7044×10^{-7}	4.6578	1.5979×10^{-6}	4.5655	2.4910×10^{-6}	4.4308	4.6946×10^{-6}	4.5878	2.2393×10^{-6}	4.4574	4.1482×10^{-6}
0.5 GL+ 0.5 EL	4.1307	1.8081×10^{-5}	3.9848	3.3763×10^{-5}	4.0409	2.6625×10^{-5}	3.8913	4.9862×10^{-5}	3.8100	6.9482×10^{-5}	3.6509	1.3068×10^{-4}	3.8658	5.5356×10^{-5}	3.7113	1.0309×10^{-4}
0.28 GL+ 0.72 EL	3.4188	3.1446×10^{-4}	3.2499	5.7725×10^{-4}	3.3306	4.3336×10^{-4}	3.1578	7.9477×10^{-4}	3.1089	9.3898×10^{-4}	2.9261	1.7161×10^{-3}	3.1890	7.1390×10^{-4}	3.0111	1.3015×10^{-3}

0.16 GL+ 0.84 EL	3.1068	9.4549 $\times10^{-4}$	2.9262	1.7157 $\times10^{-3}$	3.0211	1.2591 $\times10^{-3}$	2.8364	2.2812 $\times10^{-3}$	2.8074	2.4973 $\times10^{-3}$	2.6118	4.5036 $\times10^{-3}$	2.8955	1.8927 $\times10^{-3}$	2.7053	3.4121 $\times10^{-3}$
0.1 GL+ 0.9 EL	2.9666	1.5054 $\times10^{-3}$	2.7801	2.7169 $\times10^{-3}$	2.8823	1.9736 $\times10^{-3}$	2.6916	3.5557 $\times10^{-3}$	2.6727	3.7620 $\times10^{-3}$	2.4706	6.7449 $\times10^{-3}$	2.7639	2.8554 $\times10^{-3}$	2.5675	5.1217 $\times10^{-3}$
0.04 GL+ 0.96 EL	2.8355	2.2874 $\times10^{-3}$	2.6431	4.1072 $\times10^{-3}$	2.7527	2.9550 $\times10^{-3}$	2.5559	5.2962 $\times10^{-3}$	2.5472	5.4291 $\times10^{-3}$	2.3384	9.6823 $\times10^{-3}$	2.6411	4.1325 $\times10^{-3}$	2.4383	7.3774 $\times10^{-3}$
0.02 GL+ 0.98 EL	2.7937	2.6053 $\times10^{-3}$	2.5993	4.6704 $\times10^{-3}$	2.7114	3.3499 $\times10^{-3}$	2.5125	5.9941 $\times10^{-3}$	2.5073	6.0833 $\times10^{-3}$	2.2962	1.0831 $\times10^{-2}$	2.6019	4.6359 $\times10^{-3}$	2.3971	8.2638 $\times10^{-3}$

APPENDIX B: Table of result for reliability indices and probability of failure using ISO code with load factor of 1.40, 1.35 and 1.23, and API WSD code under axial compression for vertical diagonal, horizontal diagonal, horizontal periphery and leg members

Axial Compression	ISO (Load factor = 1.40)				ISO (Load factor = 1.35)				ISO (Load factor = 1.23)				API WSD			
	FORM β	FORM P_f	SORM β	SORM P_f	FORM P_f	SORM β	SORM P_f	FORM β	FORM P_f	SORM β	SORM P_f	FORM β	FORM P_f	SORM β	SORM P_f	FORM β
Vertical Diagonal																
0.9 GL+ 0.1 EL	9.5084	8.4600	9.4000	8.3700	9.3381	9.3000	9.3000	9.2600	6.1082	5.0384 $\times10^{-10}$	6.0698	6.4024 $\times10^{-10}$	6.0481	7.3289 $\times10^{-10}$	6.0040	9.6236 $\times10^{-10}$
0.8 GL+ 0.2 EL	5.6668	7.2760 $\times10^{-9}$	5.5993	1.0759 $\times10^{-8}$	5.6153	9.8137 $\times10^{-9}$	5.5437	1.4807 $\times10^{-8}$	5.4717	2.2291 $\times10^{-8}$	5.3885	3.5520 $\times10^{-8}$	5.3752	3.8243 $\times10^{-8}$	5.2841	6.3178 $\times10^{-8}$
0.67 GL+ 0.33 EL	5.0950	1.7437 $\times10^{-7}$	4.9924	2.9814 $\times10^{-7}$	5.0264	2.4989 $\times10^{-7}$	4.9193	4.3431 $\times10^{-7}$	4.8427	6.4042 $\times10^{-7}$	4.7238	1.1573 $\times10^{-6}$	4.7380	1.0791 $\times10^{-6}$	4.6126	1.9882 $\times10^{-6}$
0.5 GL+ 0.5 EL	4.4318	4.6717 $\times10^{-6}$	4.2960	8.6939 $\times10^{-6}$	4.3521	6.7429 $\times10^{-6}$	4.2121	1.2650 $\times10^{-5}$	4.1455	1.6952 $\times10^{-5}$	3.9950	3.2341 $\times10^{-5}$	4.0471	2.5930 $\times10^{-5}$	3.8917	4.9774 $\times10^{-5}$
0.28 GL+ 0.72 EL	3.7551	8.6644 $\times10^{-5}$	3.5915	1.6439 $\times10^{-4}$	3.6729	1.1988 $\times10^{-4}$	3.5055	2.2789 $\times10^{-4}$	3.4652	2.6489 $\times10^{-4}$	3.2879	5.0478 $\times10^{-4}$	3.3829	3.5858 $\times10^{-4}$	3.2015	6.8358 $\times10^{-4}$
0.16 GL+ 0.84 EL	3.4494	2.8092 $\times10^{-4}$	3.2734	5.3130 $\times10^{-4}$	3.3682	3.7837 $\times10^{-4}$	3.1883	7.1567 $\times10^{-4}$	3.1643	7.7739 $\times10^{-4}$	2.9743	1.4683 $\times10^{-3}$	3.0904	9.9956 $\times10^{-4}$	2.8966	1.8864 $\times10^{-3}$
0.1 GL+ 0.9 EL	3.3103	4.6605 $\times10^{-4}$	3.1284	8.7871 $\times10^{-4}$	3.2297	6.1953 $\times10^{-4}$	3.0440	1.1675 $\times10^{-3}$	3.0283	1.2298 $\times10^{-3}$	2.8323	2.3109 $\times10^{-3}$	2.9583	1.5468 $\times10^{-3}$	2.7585	2.9031 $\times10^{-3}$
0.04 GL+ 0.96 EL	3.1792	7.3838 $\times10^{-4}$	2.9917	1.3871 $\times10^{-3}$	3.0995	9.6915 $\times10^{-4}$	2.9080	1.8186 $\times10^{-3}$	2.9007	1.8618 $\times10^{-3}$	2.6988	3.4796 $\times10^{-3}$	2.8344	2.2957 $\times10^{-3}$	2.6288	4.2842 $\times10^{-3}$

0.02 GL+ 0.98 EL	3.1372	8.5282×10^{-4}	2.9479	1.5999×10^{-3}	3.0578	1.1148×10^{-3}	2.8644	2.0888×10^{-3}	2.8599	2.1191×10^{-3}	2.6560	3.9531×10^{-3}	2.7948	2.5968×10^{-3}	2.5873	4.8368×10^{-3}
Horizontal Diagonal																
0.9 GL+ 0.1 EL	3.7264	9.7128×10^{-5}	3.7027	1.0667×10^{-4}	3.6275	1.4308×10^{-4}	3.6016	1.5814×10^{-4}	3.3836	3.5771×10^{-4}	3.3520	4.0109×10^{-4}	3.7234	9.8277×10^{-5}	3.6828	1.1532×10^{-4}
0.8 GL+ 0.2 EL	3.3138	4.6015×10^{-4}	3.2378	6.0222×10^{-4}	3.2139	6.5462×10^{-4}	3.1366	8.5468×10^{-4}	2.9689	1.4944×10^{-3}	2.8882	1.9371×10^{-3}	3.2817	5.1586×10^{-4}	3.1881	7.1614×10^{-4}
0.67 GL+ 0.33 EL	2.9012	1.8589×10^{-3}	2.7825	2.6969×10^{-3}	2.8052	2.5147×10^{-3}	2.6870	3.6051×10^{-3}	2.5703	5.0806×10^{-3}	2.4530	7.0840×10^{-3}	2.8512	2.1775×10^{-3}	2.7225	3.2397×10^{-3}
0.5 GL+ 0.5 EL	2.3287	9.9380×10^{-3}	2.1124	1.7326×10^{-2}	2.2379	1.2615×10^{-2}	2.0177	2.1813×10^{-2}	2.0062	2.2416×10^{-2}	1.7785	3.7664×10^{-2}	2.2763	1.1413×10^{-2}	2.0339	2.0980×10^{-2}
0.28 GL+ 0.72 EL	1.7073	4.3883×10^{-2}	1.4632	7.1703×10^{-2}	1.6134	5.3332×10^{-2}	1.3694	8.5441×10^{-2}	1.3781	8.4083×10^{-2}	1.1342	1.2835×10^{-1}	1.6535	4.9114×10^{-2}	1.4032	8.0283×10^{-2}
0.16 GL+ 0.84 EL	1.4026	8.0362×10^{-2}	1.1589	1.2325×10^{-1}	1.3099	9.5122×10^{-2}	1.0663	1.4315×10^{-1}	1.0786	1.4038×10^{-1}	8.3505×10^{-1}	2.0185×10^{-1}	1.3570	8.7393×10^{-2}	1.1097	1.3356×10^{-1}
0.1 GL+ 0.9 EL	1.2609	1.0367×10^{-1}	1.0179	1.5437×10^{-1}	1.1690	1.2121×10^{-1}	9.2601×10^{-1}	1.7722×10^{-1}	9.4025×10^{-1}	1.7354×10^{-1}	6.9712×10^{-1}	2.4286×10^{-1}	1.2200	1.1123×10^{-1}	9.7411×10^{-1}	1.6500×10^{-1}
0.04 GL+ 0.96 EL	1.1260	1.3009×10^{-1}	8.8369×10^{-1}	1.8843×10^{-1}	1.0350	1.5034×10^{-1}	7.9268×10^{-1}	2.1398×10^{-1}	8.0897×10^{-1}	2.0927×10^{-1}	5.6625×10^{-1}	2.8561×10^{-1}	1.0900	1.3787×10^{-1}	8.4529×10^{-1}	1.9897×10^{-1}
0.02 GL+ 0.98 EL	1.0824	1.3953×10^{-1}	8.4040×10^{-1}	2.0034×10^{-1}	9.9178×10^{-1}	1.6065×10^{-1}	7.4969×10^{-1}	2.2672×10^{-1}	7.6671×10^{-1}	2.2163×10^{-1}	5.2411×10^{-1}	3.0010×10^{-1}	1.0481	1.4730×10^{-1}	8.0378×10^{-1}	2.1076×10^{-1}
Horizontal Periphery																

0.9 GL+ 0.1 EL	8.6870	8.6000	8.6000	8.5600	8.5675	8.5000	8.5000	8.4600	8.2394	1.1102×10^{-16}	8.0992	2.9921×10^{-16}	6.0749	6.2032×10^{-10}	6.0249	8.4627×10^{-10}
0.8 GL+ 0.2 EL	5.6832	6.6110×10^{-9}	5.6048	1.0426×10^{-8}	5.6317	8.9209×10^{-9}	5.5486	1.4397×10^{-8}	5.4879	2.0331×10^{-8}	5.3917	3.4901×10^{-8}	5.4263	2.8759×10^{-8}	5.3245	5.0605×10^{-8}
0.67 GL+ 0.33 EL	5.1186	1.5388×10^{-7}	5.0031	2.8203×10^{-7}	5.0501	2.2078×10^{-7}	4.9299	4.1138×10^{-7}	4.8665	5.6801×10^{-7}	4.7342	1.0998×10^{-6}	4.8087	7.5969×10^{-7}	4.6731	1.4835×10^{-6}
0.5 GL+ 0.5 EL	4.4642	4.0177×10^{-6}	4.3171	7.9040×10^{-6}	4.3850	5.7986×10^{-6}	4.2339	1.1486×10^{-5}	4.1802	1.4564×10^{-5}	4.0188	2.9242×10^{-5}	4.1381	1.7512×10^{-5}	3.9752	3.5166×10^{-5}
0.28 GL+ 0.72 EL	3.8026	7.1586×10^{-5}	3.6306	1.4138×10^{-4}	3.7220	9.8820×10^{-5}	3.5463	1.9533×10^{-4}	3.5186	2.1691×10^{-4}	3.3335	4.2878×10^{-4}	3.4967	2.3556×10^{-4}	3.3108	4.6512×10^{-4}
0.16 GL+ 0.84 EL	3.5063	2.2719×10^{-4}	3.3232	4.4498×10^{-4}	3.4270	3.0511×10^{-4}	3.2402	5.9719×10^{-4}	3.2286	6.2205×10^{-4}	3.0322	1.2138×10^{-3}	3.2155	6.5106×10^{-4}	3.0187	1.2693×10^{-3}
0.1 GL+ 0.9 EL	3.3720	3.7316×10^{-4}	3.1836	7.2725×10^{-4}	3.2936	4.9453×10^{-4}	3.1015	9.6266×10^{-4}	3.0981	9.7399×10^{-4}	2.8962	1.8883×10^{-3}	3.0889	1.0045×10^{-3}	2.8868	1.9461×10^{-3}
0.04 GL+ 0.96 EL	3.2458	5.8565×10^{-4}	3.0523	1.1355×10^{-3}	3.1684	7.6628×10^{-4}	2.9712	1.4834×10^{-3}	2.9759	1.4606×10^{-3}	2.7687	2.8139×10^{-3}	2.9703	1.4875×10^{-3}	2.7629	2.8641×10^{-3}
0.02 GL+ 0.98 EL	3.2054	6.7438×10^{-4}	3.0102	1.3052×10^{-3}	3.1284	8.7875×10^{-4}	2.9294	1.6980×10^{-3}	2.9369	1.6575×10^{-3}	2.7279	3.1866×10^{-3}	2.9324	1.6816×10^{-3}	2.7233	3.2314×10^{-3}
Leg																
0.9 GL+ 0.1 EL	10.227	10.000	9.0000	8.7000	10.061	9.7000	9.0000	8.6000	6.1657	3.5091×10^{-10}	6.1295	4.4077×10^{-10}	6.1386	4.1627×10^{-10}	6.1004	5.2905×10^{-10}
0.8 GL+ 0.2 EL	5.7623	4.1497×10^{-9}	5.6984	6.0460×10^{-9}	5.7169	5.4246×10^{-9}	5.6496	8.0415×10^{-9}	5.5906	1.1312×10^{-8}	5.5138	1.7558×10^{-8}	5.5558	1.3818×10^{-8}	5.4774	2.1579×10^{-8}
0.67 GL+ 0.33 EL	5.2353	8.2360×10^{-8}	5.1402	1.3725×10^{-7}	5.1733	1.1501×10^{-7}	5.0745	1.9423×10^{-7}	5.0067	2.7683×10^{-7}	4.8987	4.8231×10^{-7}	4.9806	3.1697×10^{-7}	4.8726	5.5065×10^{-7}
0.5 GL+ 0.5 EL	4.6110	2.0040×10^{-6}	4.4883	3.5902×10^{-6}	4.5367	2.8577×10^{-6}	4.4107	5.1512×10^{-6}	4.3434	7.0134×10^{-6}	4.2094	1.2805×10^{-5}	4.3360	7.2552×10^{-6}	4.2030	1.3172×10^{-5}
0.28 GL+ 0.72 EL	3.9554	3.8210×10^{-5}	3.8097	6.9571×10^{-5}	3.8769	5.2900×10^{-5}	3.7281	9.6458×10^{-5}	3.6779	1.1759×10^{-4}	3.5211	2.1484×10^{-4}	3.6915	1.1149×10^{-4}	3.5362	2.0300×10^{-4}

0.16 GL+ 0.84 EL	3.6547	1.2873 $\times10^{-4}$	3.4986	2.3389 $\times10^{-4}$	3.5765	1.7413 $\times10^{-4}$	3.4171	3.1644 $\times10^{-4}$	3.3797	3.6283 $\times10^{-4}$	3.2121	6.5894 $\times10^{-4}$	3.4021	3.3433 $\times10^{-4}$	3.2361	6.0587 $\times10^{-4}$
0.1 GL+ 0.9 EL	3.5172	2.1810 $\times10^{-4}$	3.3560	3.9541 $\times10^{-4}$	3.4394	2.9155 $\times10^{-4}$	3.2749	5.2845 $\times10^{-4}$	3.2444	5.8853 $\times10^{-4}$	3.0714	1.0651 $\times10^{-3}$	3.2706	5.3659 $\times10^{-4}$	3.0994	9.6958 $\times10^{-4}$
0.04 GL+ 0.96 EL	3.3872	3.5301 $\times10^{-4}$	3.2212	6.3838 $\times10^{-4}$	3.3100	4.6642 $\times10^{-4}$	3.1406	8.4299 $\times10^{-4}$	3.1172	9.1302 $\times10^{-4}$	2.9390	1.6466 $\times10^{-3}$	3.1468	8.2529 $\times10^{-4}$	2.9705	1.4867 $\times10^{-3}$
0.02 GL+ 0.98 EL	3.3455	4.1065 $\times10^{-4}$	3.1778	7.4194 $\times10^{-4}$	3.2686	5.4049 $\times10^{-4}$	3.0975	9.7590 $\times10^{-4}$	3.0764	1.0475 $\times10^{-3}$	2.8965	1.8869 $\times10^{-3}$	3.1072	9.4450 $\times10^{-4}$	2.9291	1.6997 $\times10^{-3}$

APPENDIX C: Table of result for reliability indices and probability of failure using ISO code with load factor of 1.40, 1.35 and 1.23, and API WSD code under bending for vertical diagonal, horizontal diagonal, horizontal periphery and leg members

Bending	ISO (Load factor = 1.40)				ISO (Load factor = 1.35)				ISO (Load factor = 1.23)				API WSD			
	FORM β	FORM P_f	SORM β	SORM P_f	FORM P_f	SORM β	SORM P_f	FORM β	FORM P_f	SORM β	SORM P_f	FORM β	FORM P_f	SORM β	SORM P_f	FORM β
Vertical Diagonal																
0.9 GL+ 0.1 EL	6.9681	1.6063×10^{-12}	6.8883	2.8223×10^{-12}	6.7772	6.1260×10^{-12}	6.6824	1.1757×10^{-11}	6.2851	1.6379×10^{-10}	6.1378	4.1847×10^{-10}	5.5593	1.3542×10^{-8}	5.4606	2.3723×10^{-8}
0.8 GL+ 0.2 EL	4.9780	3.2124×10^{-7}	4.8424	6.4148×10^{-7}	4.8772	5.3810×10^{-7}	4.7290	1.1281×10^{-6}	4.5930	2.1841×10^{-6}	4.4090	5.1932×10^{-6}	4.4296	4.7201×10^{-6}	4.2344	1.1456×10^{-5}
0.67 GL+ 0.33 EL	4.1010	2.0570×10^{-5}	3.9063	4.6855×10^{-5}	3.9851	3.3726×10^{-5}	3.7812	7.8025×10^{-5}	3.6807	1.1629×10^{-4}	3.4552	2.7491×10^{-4}	3.5414	1.9902×10^{-4}	3.3110	4.6488×10^{-4}
0.5 GL+ 0.5 EL	3.1834	7.2775×10^{-4}	2.9449	1.6153×10^{-3}	3.0663	1.0835×10^{-3}	2.8219	2.3870×10^{-3}	2.7691	2.8103×10^{-3}	2.5111	6.0184×10^{-3}	2.6576	3.9348×10^{-3}	2.3962	8.2835×10^{-3}
0.28 GL+ 0.72 EL	2.3510	9.3622×10^{-3}	2.0835	1.8603×10^{-2}	2.2418	1.2486×10^{-2}	1.9702	2.4409×10^{-2}	1.9692	2.4463×10^{-2}	1.6877	4.5738×10^{-2}	1.8839	2.9787×10^{-2}	1.5996	5.4849×10^{-2}
0.16 GL+ 0.84 EL	1.9951	2.3013×10^{-2}	1.7165	4.3031×10^{-2}	1.8906	2.9337×10^{-2}	1.6083	5.3884×10^{-2}	1.6308	5.1463×10^{-2}	1.3396	9.0182×10^{-2}	1.5563	5.9824×10^{-2}	1.2625	1.0339×10^{-1}
0.1 GL+ 0.9 EL	1.8364	3.3147×10^{-2}	1.5530	6.0211×10^{-2}	1.7342	4.1444×10^{-2}	1.4472	7.3921×10^{-2}	1.4805	6.9374×10^{-2}	1.1850	1.1801×10^{-1}	1.4106	7.9187×10^{-2}	1.1126	1.3294×10^{-1}
0.04 GL+ 0.96 EL	1.6886	4.5645×10^{-2}	1.4008	8.0642×10^{-2}	1.5886	5.6079×10^{-2}	1.2973	9.7263×10^{-2}	1.3408	8.9997×10^{-2}	1.0413	1.4887×10^{-1}	1.2752	1.0113×10^{-1}	9.7325×10^{-1}	1.6521×10^{-1}

0.02 GL+ 0.98 EL	1.6416	5.0338 $\times10^{-2}$	1.3523	8.8137 $\times10^{-2}$	1.5422	6.1507 $\times10^{-2}$	1.2496	1.0572 $\times10^{-1}$	1.2964	9.7423 $\times10^{-2}$	9.9563 $\times10^{-1}$	1.5971 $\times10^{-1}$	1.2321	1.0896 $\times10^{-1}$	9.2895 $\times10^{-1}$	1.7646 $\times10^{-1}$
Horizontal Diagonal																
0.9 GL+ 0.1 EL	6.8369	4.0471 $\times10^{-12}$	6.7259	8.7229 $\times10^{-12}$	6.6185	1.8146 $\times10^{-11}$	6.4787	4.6243 $\times10^{-11}$	5.5000	1.8990 $\times10^{-8}$	5.4176	3.0198 $\times10^{-8}$	5.3900	3.5234 ×10-8	5.2961	5.9138 $\times10^{-8}$
0.8 GL+ 0.2 EL	4.6544	1.6247 $\times10^{-6}$	4.5262	3.0027 $\times10^{-6}$	4.5330	2.9082 $\times10^{-6}$	4.3933	5.5823 $\times10^{-6}$	4.1936	1.3726 $\times10^{-5}$	4.0250	2.8491 $\times10^{-5}$	4.0835	2.2183 $\times10^{-5}$	3.9174	4.4751 $\times10^{-5}$
0.67 GL+ 0.33 EL	3.6276	1.4302e $\times10^{-4}$	3.4645	2.6565 $\times10^{-4}$	3.4935	2.3834 $\times10^{-4}$	3.3250	4.4216 $\times10^{-4}$	3.1448	8.3108 $\times10^{-4}$	2.9648	1.5143 $\times10^{-3}$	3.0704	1.0687 $\times10^{-3}$	2.8924	1.9114 $\times10^{-3}$
0.5 GL+ 0.5 EL	2.5767	4.9870 $\times10^{-3}$	2.3960	8.2881 $\times10^{-3}$	2.4444	7.2543 $\times10^{-3}$	2.2611	1.1878 $\times10^{-2}$	2.1102	1.7421 $\times10^{-2}$	1.9212	2.7352 $\times10^{-2}$	2.0693	1.9257 $\times10^{-2}$	1.8812	2.9975 $\times10^{-2}$
0.28 GL+ 0.72 EL	1.6316	5.1387 $\times10^{-2}$	1.4426	7.4564 $\times10^{-2}$	1.5091	6.5636 $\times10^{-2}$	1.3186	9.3648 $\times10^{-2}$	1.2040	1.1430 $\times10^{-1}$	1.0099	1.5627 $\times10^{-1}$	1.1899	1.1705 $\times10^{-1}$	9.9595 $\times10^{-1}$	1.5964 $\times10^{-1}$
0.16 GL+ 0.84 EL	1.2283	1.0967 $\times10^{-1}$	1.0366	1.4996 $\times10^{-1}$	1.1112	1.3325 $\times10^{-1}$	9.1816 $\times10^{-1}$	1.7927 $\times10^{-1}$	8.2056 $\times10^{-1}$	2.0595 $\times10^{-1}$	6.2437 $\times10^{-1}$	2.6619 $\times10^{-1}$	8.1674 $\times10^{-1}$	2.0704 $\times10^{-1}$	6.2049 $\times10^{-1}$	2.6747 $\times10^{-1}$
0.1 GL+ 0.9 EL	1.0485	1.4721 $\times10^{-1}$	8.5562 $\times10^{-1}$	1.9610 $\times10^{-1}$	9.3391 $\times10^{-1}$	1.7517 $\times10^{-1}$	7.3980 $\times10^{-1}$	2.2971 $\times10^{-1}$	6.5020 $\times10^{-1}$	2.5778 $\times10^{-1}$	4.5298 $\times10^{-1}$	3.2528 $\times10^{-1}$	6.5071 $\times10^{-1}$	2.5762 $\times10^{-1}$	4.5337 $\times10^{-1}$	3.2514 $\times10^{-1}$
0.04 GL+ 0.96 EL	8.8106 $\times10^{-1}$	1.8914 $\times10^{-1}$	6.8712 $\times10^{-1}$	2.4600 $\times10^{-1}$	7.6901 $\times10^{-1}$	2.2094 $\times10^{-1}$	5.7384 $\times10^{-1}$	2.8304 $\times10^{-1}$	4.9195 $\times10^{-1}$	3.1138 $\times10^{-1}$	2.9369 $\times10^{-1}$	3.8450 $\times10^{-1}$	4.9634 $\times10^{-1}$	3.0983 $\times10^{-1}$	2.9792 $\times10^{-1}$	3.8288 $\times10^{-1}$
0.02 GL+ 0.98 EL	8.2778 $\times10^{-1}$	2.0390 $\times10^{-1}$	6.3349 $\times10^{-1}$	2.6321 $\times10^{-1}$	7.1655 $\times10^{-1}$	2.3683 $\times10^{-1}$	5.2103 $\times10^{-1}$	3.0117 $\times10^{-1}$	4.4166 $\times10^{-1}$	3.2937 $\times10^{-1}$	2.4305 $\times10^{-1}$	4.0398 $\times10^{-1}$	4.4725 $\times10^{-1}$	3.2735 $\times10^{-1}$	2.4847 $\times10^{-1}$	4.0188 $\times10^{-1}$
Horizontal Periphery																
0.9 GL+ 0.1 EL	11.720	11.0000	11.0000	10.6000	11.567	11.000	11.000	10.600	6.2821	1.6703 $\times10^{-10}$	6.2554	1.9826 $\times10^{-10}$	6.0848	5.8327 $\times10^{-10}$	6.0408	7.6669 $\times10^{-10}$
0.8 GL+ 0.2 EL	5.9629	1.2391 $\times10^{-9}$	5.9142	1.6676 $\times10^{-9}$	5.9295	1.5196 $\times10^{-9}$	5.8783	2.0731 $\times10^{-9}$	5.8369	2.6596 $\times10^{-9}$	5.7787	3.7643 $\times10^{-9}$	5.4518	2.4926 $\times10^{-8}$	5.3628	4.0963 $\times10^{-8}$
0.67 GL+ 0.33 EL	5.5438	1.4802 $\times10^{-8}$	5.4676	2.2812 $\times10^{-8}$	5.4964	1.9376 $\times10^{-8}$	5.4172	3.0278 $\times10^{-8}$	5.3690	3.9587 $\times10^{-8}$	5.2816	6.4026 $\times10^{-8}$	4.8463	6.2907 $\times10^{-7}$	4.7262	1.1439 $\times10^{-6}$

0.5 GL+ 0.5 EL	5.0340	2.4017×10^{-7}	4.9299	4.1144×10^{-7}	4.9745	3.2701×10^{-7}	4.8673	5.6558×10^{-7}	4.8187	7.2256×10^{-7}	4.7037	1.2774×10^{-6}	4.1835	1.4351×10^{-5}	4.0369	2.7079×10^{-5}
0.28 GL+ 0.72 EL	4.4702	3.9076×10^{-6}	4.3416	7.0716×10^{-6}	4.4037	5.3219×10^{-6}	4.2722	9.6766×10^{-6}	4.2334	1.1509×10^{-5}	4.0947	2.1138×10^{-5}	3.5422	1.9843×10^{-4}	3.3718	3.7335×10^{-4}
0.16 GL+ 0.84 EL	4.2015	1.3257×10^{-5}	4.0624	2.4284×10^{-5}	4.1335	1.7865×10^{-5}	3.9915	3.2825×10^{-5}	3.9609	3.7330×10^{-5}	3.8117	6.9012×10^{-5}	3.2594	5.5823×10^{-4}	3.0776	1.0432×10^{-3}
0.1 GL+ 0.9 EL	4.0764	2.2865×10^{-5}	3.9325	4.2034×10^{-5}	4.0081	3.0610×10^{-5}	3.8612	5.6406×10^{-5}	3.8353	6.2717×10^{-5}	3.6811	1.1611×10^{-4}	3.1318	8.6864×10^{-4}	2.9445	1.6173×10^{-3}
0.04 GL+ 0.96 EL	3.9571	3.7932×10^{-5}	3.8085	6.9898×10^{-5}	3.8886	5.0418×10^{-5}	3.7371	9.3076×10^{-5}	3.7160	1.0121×10^{-4}	3.5571	1.8747×10^{-4}	3.0122	1.2967×10^{-3}	2.8195	2.4052×10^{-3}
0.02 GL+ 0.98 EL	3.9185	4.4543×10^{-5}	3.7685	8.2127×10^{-5}	3.8500	5.9058×10^{-5}	3.6970	1.0907×10^{-4}	3.6776	1.1774×10^{-4}	3.5172	2.1809×10^{-4}	2.9740	1.4697×10^{-3}	2.7794	2.7226×10^{-3}
Leg																
0.9 GL+ 0.1 EL	6.9954	1.3221×10^{-12}	6.9242	2.1920×10^{-12}	6.8258	4.3707×10^{-12}	6.7419	7.8173×10^{-12}	6.3902	8.2843×10^{-11}	6.2695	1.8111×10^{-10}	6.0320	8.0993×10^{-10}	5.9807	1.1107×10^{-9}
0.8 GL+ 0.2 EL	5.2265	8.6351×10^{-8}	5.1092	1.6173×10^{-7}	5.1392	1.3793×10^{-7}	5.0138	2.6689×10^{-7}	4.8916	5.0003×10^{-7}	4.7431	1.0525×10^{-6}	5.3436	4.5564×10^{-8}	5.2456	7.7868×10^{-8}
0.67 GL+ 0.33 EL	4.4660	3.9845×10^{-6}	4.3205	7.7842×10^{-6}	4.3639	6.3878×10^{-6}	4.2133	1.2584×10^{-5}	4.0948	2.113×10^{-5}	3.9317	4.2180×10^{-5}	4.6951	1.3321×10^{-6}	4.5715	2.4215×10^{-6}
0.5 GL+ 0.5 EL	3.6661	1.2314×10^{-4}	3.5012	2.3156×10^{-4}	3.5632	1.8318×10^{-4}	3.3943	3.4398×10^{-4}	3.3023	4.7943×10^{-4}	3.1230	8.9499×10^{-4}	3.9964	3.2156×10^{-5}	3.8519	5.8609×10^{-5}
0.28 GL+ 0.72 EL	2.9518	1.5795×10^{-3}	2.7671	2.8278×10^{-3}	2.8577	2.1338×10^{-3}	2.6685	3.8099×10^{-3}	2.6233	4.3544×10^{-3}	2.4219	7.7204×10^{-3}	3.3367	4.2395×10^{-4}	3.1726	7.5544×10^{-4}
0.16 GL+ 0.84 EL	2.6517	4.0045×10^{-3}	2.4550	7.0442×10^{-3}	2.5624	5.1970×10^{-3}	2.3607	9.1192×10^{-3}	2.3414	9.6056×10^{-3}	2.1260	1.6752×10^{-2}	3.0501	1.1437×10^{-3}	2.8758	2.0148×10^{-3}
0.1 GL+ 0.9 EL	2.5189	5.8855×10^{-3}	2.3160	1.0280×10^{-2}	2.4320	7.5072×10^{-3}	2.2237	1.3083×10^{-2}	2.2172	1.3304×10^{-2}	1.9944	2.3054×10^{-2}	2.9216	1.7409×10^{-3}	2.7422	3.0512×10^{-3}

0.04 GL+ 0.96 EL	2.3960	8.2885×10^{-3}	2.1865	1.4391×10^{-2}	2.3113	1.0408×10^{-2}	2.0962	1.8032×10^{-2}	2.1024	1.7759×10^{-2}	1.8720	3.0606×10^{-2}	2.8017	2.5421×10^{-3}	2.6171	4.4345×10^{-3}
0.02 GL+ 0.98 EL	2.3569	9.2130×10^{-3}	2.1453	1.5966×10^{-2}	2.2730	1.1513×10^{-2}	2.0556	1.9910×10^{-2}	2.0660	1.9413×10^{-2}	1.8330	3.3401×10^{-2}	2.7634	2.8602×10^{-3}	2.5771	4.9822×10^{-3}

APPENDIX D: Table of result for reliability indices and probability of failure using ISO code with load factor of 1.40, 1.35 and 1.23, and API WSD code under tension and bending for vertical diagonal, horizontal diagonal, horizontal periphery and leg members

Tension and Bending	ISO (Load factor = 1.40)				ISO (Load factor = 1.35)				ISO (Load factor = 1.23)				API WSD			
	FORM β	FORM P_f	SORM β	SORM P_f	FORM P_f	SORM β	SORM P_f	FORM β	FORM P_f	SORM β	SORM P_f	FORM β	FORM P_f	SORM β	SORM P_f	FORM β
Vertical Diagonal																
0.9 GL+ 0.1 EL	5.9890	1.0559×10^{-9}	5.9511	1.3313×10^{-9}	5.8675	2.2119×10^{-9}	5.8242	2.8691×10^{-9}	5.5611	1.3402×10^{-8}	5.5029	1.8678×10^{-8}	5.5239	1.6575×10^{-8}	5.4372	2.7068×10^{-8}
0.8 GL+ 0.2 EL	5.6320	8.9051×10^{-9}	5.3058	5.6086×10^{-8}	5.3246	5.0582×10^{-8}	5.1684	1.1803×10^{-7}	5.0861	1.8276×10^{-7}	4.8292	6.8535×10^{-7}	4.8673	5.6565×10^{-7}	4.5939	2.1749×10^{-6}
0.67 GL+ 0.33 EL	4.6465	1.6881×10^{-6}	4.4567	4.1615×10^{-6}	4.5464	2.7290×10^{-6}	4.3471	6.8985×10^{-6}	4.2812	9.2964×10^{-6}	4.0628	2.4241×10^{-5}	4.0983	2.0811×10^{-5}	3.8684	5.4780×10^{-5}
0.5 GL+ 0.5 EL	3.8429	6.0790×10^{-5}	3.6399	1.3637×10^{-4}	3.7422	9.1202×10^{-5}	3.5349	2.0395×10^{-4}	3.4872	2.4409×10^{-4}	3.2697	5.3830×10^{-4}	3.3369	4.2363×10^{-4}	3.1012	9.6355×10^{-4}
0.28 GL+ 0.72 EL	3.1117	9.3006×10^{-4}	2.8939	1.9027×10^{-3}	3.0181	1.2720×10^{-3}	2.7960	2.5868×10^{-3}	2.7845	2.6808×10^{-3}	2.5517	5.3597×10^{-3}	2.6618	3.8861×10^{-3}	2.4113	7.9472×10^{-3}
0.16 GL+ 0.84 EL	2.7965	2.5833×10^{-3}	2.5684	5.1079×10^{-3}	2.7065	3.3995×10^{-3}	2.4741	6.6777×10^{-3}	2.4832	6.5112×10^{-3}	2.2396	1.2558×10^{-2}	2.3716	8.8551×10^{-3}	2.1119	1.7347×10^{-2}
0.1 GL+ 0.9 EL	2.6550	3.9655×10^{-3}	2.4217	7.7241×10^{-3}	2.5668	5.1316×10^{-3}	2.3291	9.9270×10^{-3}	2.3482	9.4320×10^{-3}	2.0991	1.7903×10^{-2}	2.2415	1.2496×10^{-2}	1.9772	2.4009×10^{-2}
0.04 GL+ 0.96 EL	2.5227	5.8229×10^{-3}	2.2841	1.1183×10^{-2}	2.4362	7.4204×10^{-3}	2.1931	1.4149×10^{-2}	2.2222	1.3137×10^{-2}	1.9675	2.4560×10^{-2}	2.1199	1.7005×10^{-2}	1.8511	3.2080×10^{-2}

0.02 GL+ 0.98 EL	2.4805	6.5605 $\times10^{-3}$	2.2401	1.2543 $\times10^{-2}$	2.3946	8.3201 $\times10^{-3}$	2.1496	1.5792 $\times10^{-2}$	2.1819	1.4557 $\times10^{-2}$	1.9255	2.7083 $\times10^{-2}$	2.0811	1.8711 $\times10^{-2}$	1.8108	3.5089 $\times10^{-2}$
Horizontal Diagonal																
0.9 GL+ 0.1 EL	5.6857	6.5128 $\times10^{-9}$	5.6341	8.7989 $\times10^{-9}$	5.5400	1.5124 $\times10^{-8}$	5.4827	2.0943 $\times10^{-8}$	5.1707	1.1662 $\times10^{-7}$	5.0980	1.7163 $\times10^{-7}$	5.3040	5.6655 $\times10^{-8}$	5.2063	9.6342 $\times10^{-8}$
0.8 GL+ 0.2 EL	4.7958	8.0998 $\times10^{-7}$	4.5386	2.8313 $\times10^{-6}$	4.6624	1.5629 $\times10^{-6}$	4.3541	6.6793 $\times10^{-6}$	4.2914	8.8759 $\times10^{-6}$	4.0125	3.0042 $\times10^{-5}$	4.3022	8.4551 $\times10^{-6}$	4.0502	2.5583 $\times10^{-5}$
0.67 GL+ 0.33 EL	3.8194	6.6888 $\times10^{-5}$	3.6179	1.4849 $\times10^{-4}$	3.6924	1.1109 $\times10^{-4}$	3.4891	2.4235 $\times10^{-4}$	3.3681	3.7851 $\times10^{-4}$	3.1636	7.7918 $\times10^{-4}$	3.3909	3.4836 $\times10^{-4}$	3.1935	7.0278 $\times10^{-4}$
0.5 GL+ 0.5 EL	2.8586	2.1275 $\times10^{-3}$	2.6686	3.8083 $\times10^{-3}$	2.7390	3.0811 $\times10^{-3}$	2.5481	5.4148 $\times10^{-3}$	2.4393	7.3571 $\times10^{-3}$	2.2468	1.2325 $\times10^{-2}$	2.4846	6.4845 $\times10^{-3}$	2.2943	1.0888 $\times10^{-2}$
0.28 GL+ 0.72 EL	1.9949	2.3027 $\times10^{-2}$	1.8074	3.5353 $\times10^{-2}$	1.8849	2.9723 $\times10^{-2}$	1.6966	4.4890 $\times10^{-2}$	1.6115	5.3532 $\times10^{-2}$	1.4214	7.7597 $\times10^{-2}$	1.6736	4.7106 $\times10^{-2}$	1.4840	6.8903 $\times10^{-2}$
0.16 GL+ 0.84 EL	1.6216	5.2442 $\times10^{-2}$	1.4339	7.5799 $\times10^{-2}$	1.5161	6.4753 $\times10^{-2}$	1.3276	9.2158 $\times10^{-2}$	1.2545	1.0483 $\times10^{-1}$	1.0642	1.4361 $\times10^{-1}$	1.3230	9.2922 $\times10^{-2}$	1.1329	1.2863 $\times10^{-1}$
0.1 GL+ 0.9 EL	1.4539	7.2993 $\times10^{-2}$	1.2659	1.0277 $\times10^{-1}$	1.3503	8.8453 $\times10^{-2}$	1.1617	1.2269 $\times10^{-1}$	1.0942	1.3693 $\times10^{-1}$	9.0371 $\times10^{-1}$	1.8308 $\times10^{-1}$	1.1654	1.2193 $\times10^{-1}$	9.7495 $\times10^{-1}$	1.6479 $\times10^{-1}$
0.04 GL+ 0.96 EL	1.2968	9.7352 $\times10^{-2}$	1.1086	1.3381 $\times10^{-1}$	1.1953	1.1599 $\times10^{-1}$	1.0063	1.5714 $\times10^{-1}$	9.4433 $\times10^{-1}$	1.7250 $\times10^{-1}$	7.5348 $\times10^{-1}$	2.2558 $\times10^{-1}$	1.0179	1.5437 $\times10^{-1}$	8.2704 $\times10^{-1}$	2.0411 $\times10^{-1}$
0.02 GL+ 0.98 EL	1.2466	1.0627 $\times10^{-1}$	1.0583	1.4497 $\times10^{-1}$	1.1457	1.2596 $\times10^{-1}$	9.5663 $\times10^{-1}$	1.6938 $\times10^{-1}$	8.9647 $\times10^{-1}$	1.8500 $\times10^{-1}$	7.0550 $\times10^{-1}$	2.4025 $\times10^{-1}$	9.7076 $\times10^{-1}$	1.6583 $\times10^{-1}$	7.7978 $\times10^{-1}$	2.1776 $\times10^{-1}$
Horizontal Periphery																
0.9 GL+ 0.1 EL	8.6005	8.5700	8.5000	8.4600	8.4629	8.4000	8.4000	8.3600	8.1088	2.2204 $\times10^{-16}$	7.9010	1.4053 $\times10^{-15}$	7.6129	1.3434 $\times10^{-14}$	7.4015	6.7367 $\times10^{-14}$
0.8 GL+ 0.2 EL	5.7578	4.2601 $\times10^{-9}$	5.6795	6.7536 $\times10^{-9}$	5.7109	5.6183 $\times10^{-9}$	5.6278	9.1268 $\times10^{-9}$	5.5798	1.2038 $\times10^{-8}$	5.4832	2.0888 $\times10^{-8}$	5.3903	3.5165 $\times10^{-8}$	5.2998	5.7954 $\times10^{-8}$

0.67 GL+ 0.33 EL	5.2288	8.5326×10^{-8}	5.1154	1.5652×10^{-7}	5.1652	1.2007×10^{-7}	5.0473	2.2406×10^{-7}	4.9947	2.9467×10^{-7}	4.8651	5.7211×10^{-7}	4.7601	9.6751×10^{-7}	4.6458	1.6940×10^{-6}
0.5 GL+ 0.5 EL	4.6087	2.0257×10^{-6}	4.4691	3.9278×10^{-6}	4.5342	2.8917×10^{-6}	4.3911	5.6393×10^{-6}	4.3409	7.0945×10^{-6}	4.1895	1.3977×10^{-5}	4.0851	2.2028×10^{-5}	3.9547	3.8316×10^{-5}
0.28 GL+ 0.72 EL	3.9730	3.5489×10^{-5}	3.8177	6.7349×10^{-5}	3.8961	4.8868×10^{-5}	3.7382	9.2654×10^{-5}	3.7019	1.0698×10^{-4}	3.5375	2.0197×10^{-4}	3.4504	2.7987×10^{-4}	3.3080	4.6990×10^{-4}
0.16 GL+ 0.84 EL	3.6858	1.1397×10^{-4}	3.5246	2.1209×10^{-4}	3.6099	1.5315×10^{-4}	3.4461	2.8433×10^{-4}	3.4195	3.1365×10^{-4}	3.2494	5.7829×10^{-4}	3.1743	7.5098×10^{-4}	3.0256	1.2405×10^{-3}
0.1 GL+ 0.9 EL	3.5552	1.8884×10^{-4}	3.3912	3.4799×10^{-4}	3.4800	2.5072×10^{-4}	3.3135	4.6076×10^{-4}	3.2920	4.9743×10^{-4}	3.1190	9.0718×10^{-4}	3.0503	1.1432×10^{-3}	2.8985	1.8748×10^{-3}
0.04 GL+ 0.96 EL	3.4322	2.9936×10^{-4}	3.2655	5.4642×10^{-4}	3.3578	3.9283×10^{-4}	3.1886	7.1490×10^{-4}	3.1723	7.5607×10^{-4}	2.9966	1.3648×10^{-3}	2.9343	1.6715×10^{-3}	2.7794	2.7234×10^{-3}
0.02 GL+ 0.98 EL	3.3928	3.4594×10^{-4}	3.2252	6.2951×10^{-4}	3.3187	4.5224×10^{-4}	3.1485	8.2043×10^{-4}	3.1341	8.6193×10^{-4}	2.9575	1.5509×10^{-3}	2.8973	1.8821×10^{-3}	2.7413	3.0600×10^{-3}
Leg																
0.9 GL+ 0.1 EL	5.7705	3.9518×10^{-9}	5.7303	5.0138×10^{-9}	5.6521	7.9235×10^{-9}	5.6050	1.0414×10^{-8}	5.3538	4.3052×10^{-8}	5.2881	6.1780×10^{-8}	6.1490	3.8995×10^{-10}	6.0593	6.8376×10^{-10}
0.8 GL+ 0.2 EL	5.4801	2.1256×10^{-8}	5.1927	1.0362×10^{-7}	5.3381	4.6951×10^{-8}	4.9898	3.0221×10^{-7}	4.9829	3.1320×10^{-7}	4.5939	2.1756×10^{-6}	5.2578	7.2883×10^{-8}	5.1042	1.6614×10^{-7}
0.67 GL+ 0.33 EL	4.6029	2.0835×10^{-6}	4.4050	5.2884×10^{-6}	4.5019	3.3669×10^{-6}	4.2965	8.6744×10^{-6}	4.2373	1.1310×10^{-5}	4.0186	2.9272×10^{-5}	4.5635	2.5154e $\times10^{-6}$	4.3904	5.6568×10^{-6}
0.5 GL+ 0.5 EL	3.8392	6.1722×10^{-5}	3.6447	1.3387×10^{-4}	3.7416	9.1438×10^{-5}	3.5439	1.9710×10^{-4}	3.4956	2.3652×10^{-4}	3.2904	5.0024×10^{-4}	3.8525	5.8470×10^{-5}	3.6722	1.2022×10^{-4}
0.28 GL+ 0.72 EL	3.1607	7.8706×10^{-4}	2.9612	1.5324×10^{-3}	3.0719	1.0634×10^{-3}	2.8689	2.0592×10^{-3}	2.8514	2.1763×10^{-3}	2.6391	4.1566×10^{-3}	3.2104	6.6280×10^{-4}	3.0200	1.2638×10^{-3}
0.16 GL+ 0.84 EL	2.8717	2.0413×10^{-3}	2.6654	3.8446×10^{-3}	2.7873	2.6577×10^{-3}	2.5771	4.9820×10^{-3}	2.5783	4.9648×10^{-3}	2.3575	9.1992×10^{-3}	2.9345	1.6705×10^{-3}	2.7365	3.1047×10^{-3}
0.1 GL+ 0.9 EL	2.7428	3.0460×10^{-3}	2.5325	5.6627×10^{-3}	2.6603	3.9030×10^{-3}	2.4459	7.2241×10^{-3}	2.4566	7.0127×10^{-3}	2.2310	1.2841×10^{-2}	2.8109	2.4701×10^{-3}	2.6088	4.5436×10^{-3}

0.04 GL+ 0.96 EL	2.6227	4.3624 $\times 10^{-3}$	2.4080	8.0194 $\times 10^{-3}$	2.5421	5.5091 $\times 10^{-3}$	2.3231	1.0086 $\times 10^{-2}$	2.3434	9.5555 $\times 10^{-3}$	2.1125	1.7320 $\times 10^{-2}$	2.6955	3.5142 $\times 10^{-3}$	2.4889	6.4062 $\times 10^{-3}$
0.02 GL+ 0.98 EL	2.5844	4.8775 $\times 10^{-3}$	2.3683	8.9359 $\times 10^{-3}$	2.5045	6.1316 $\times 10^{-3}$	2.2839	1.1189 $\times 10^{-2}$	2.3073	1.0519 $\times 10^{-2}$	2.0747	1.9007 $\times 10^{-2}$	2.6587	3.9224 $\times 10^{-3}$	2.4506	7.1306 $\times 10^{-3}$

APPENDIX E: Table of result for reliability indices and probability of failure using ISO code with load factor of 1.40, 1.35 and 1.23, and API WSD code under compression and bending for vertical diagonal, horizontal diagonal, horizontal periphery and leg members

Compression and Bending	ISO (Load factor = 1.40)				ISO (Load factor = 1.35)				ISO (Load factor = 1.23)				API WSD			
	FORM β	FORM P_f	SORM β	SORM P_f	FORM P_f	SORM β	SORM P_f	FORM β	FORM P_f	SORM β	SORM P_f	FORM β	FORM P_f	SORM β	SORM P_f	FORM β
Vertical Diagonal																
0.9 GL+ 0.1 EL	6.4372	6.0862 $\times10^{-11}$	6.3893	8.3322 $\times10^{-11}$	6.3111	1.3852 $\times10^{-10}$	6.2577	1.9530 $\times10^{-10}$	5.9924	1.0341 $\times10^{-9}$	5.9239	1.5721 $\times10^{-9}$	5.9769	1.1369 $\times10^{-9}$	5.8707	2.1692 $\times10^{-9}$
0.8 GL+ 0.2 EL	5.4820	2.1028 $\times10^{-8}$	5.3691	3.9569 $\times10^{-8}$	5.4117	3.1217 $\times10^{-8}$	5.2873	6.2079 $\times10^{-8}$	5.2079	9.5502 $\times10^{-8}$	5.0439	2.2807 $\times10^{-7}$	4.9988	2.8838 $\times10^{-7}$	4.8083	7.6114 $\times10^{-7}$
0.67 GL+ 0.33 EL	4.7542	9.9609 $\times10^{-7}$	4.5860	2.2594 $\times10^{-6}$	4.6608	1.5748 $\times10^{-6}$	4.4836	3.6694 $\times10^{-6}$	4.4110	5.1451 $\times10^{-6}$	4.2129	1.2607 $\times10^{-5}$	4.2272	1.1831 $\times10^{-5}$	4.0106	3.0287 $\times10^{-5}$
0.5 GL+ 0.5 EL	3.9475	3.9484 $\times10^{-5}$	3.7499	8.8437 $\times10^{-5}$	3.8482	5.9496 $\times10^{-5}$	3.6456	1.3341 $\times10^{-4}$	3.5950	1.6220 $\times10^{-4}$	3.3802	3.6214 $\times10^{-4}$	3.4501	2.8017 $\times10^{-4}$	3.2130	6.5669 $\times10^{-4}$
0.28 GL+ 0.72 EL	3.1900	7.1144 $\times10^{-4}$	2.9697	1.4905 $\times10^{-3}$	3.0953	9.8312 $\times10^{-4}$	2.8704	2.0499 $\times10^{-3}$	2.8583	2.1293 $\times10^{-3}$	2.6218	4.3737 $\times10^{-3}$	2.7493	2.9860 $\times10^{-3}$	2.4931	6.3314 $\times10^{-3}$
0.16 GL+ 0.84 EL	2.8604	2.1157 $\times10^{-3}$	2.6277	4.2978 $\times10^{-3}$	2.7688	2.8130 $\times10^{-3}$	2.5315	5.6786 $\times10^{-3}$	2.5409	5.5289 $\times10^{-3}$	2.2918	1.0960 $\times10^{-2}$	2.4466	7.2109 $\times10^{-3}$	2.1807	1.4602 $\times10^{-2}$
0.1 GL+ 0.9 EL	2.7120	3.3436 $\times10^{-3}$	2.4733	6.6935 $\times10^{-3}$	2.6220	4.3703 $\times10^{-3}$	2.3786	8.6887 $\times10^{-3}$	2.3984	8.2332 $\times10^{-3}$	2.1432	1.6050 $\times10^{-2}$	2.3106	1.0428 $\times10^{-2}$	2.0401	2.0668 $\times10^{-2}$
0.04 GL+ 0.96 EL	2.5731	5.0398 $\times10^{-3}$	2.3284	9.9460 $\times10^{-3}$	2.4846	6.4843 $\times10^{-3}$	2.2352	1.2701 $\times10^{-2}$	2.2652	1.1750 $\times10^{-2}$	2.0039	2.2538 $\times10^{-2}$	2.1833	1.4506 $\times10^{-2}$	1.9084	2.8167 $\times10^{-2}$

0.02 GL+ 0.98 EL	2.5287	5.7245 $\times10^{-3}$	2.2820	1.1244 $\times10^{-2}$	2.4407	7.3287 $\times10^{-3}$	2.1894	1.4285 $\times10^{-2}$	2.2227	1.3119 $\times10^{-2}$	1.9595	2.5030 $\times10^{-2}$	2.1427	1.6069 $\times10^{-2}$	1.8664	3.0995 $\times10^{-2}$
Horizontal Diagonal																
0.9 GL+ 0.1 EL	4.8607	5.8497 $\times10^{-7}$	4.8117	7.4825 $\times10^{-7}$	4.7334	1.1041 $\times10^{-6}$	4.6804	1.4313 $\times10^{-6}$	4.4140	5.0738 $\times10^{-6}$	4.3507	6.7845 $\times10^{-6}$	4.7758	8.9505 $\times10^{-7}$	4.6984	1.3113 $\times10^{-6}$
0.8 GL+ 0.2 EL	4.2652	9.9861 $\times10^{-6}$	4.1000	2.0655 $\times10^{-5}$	4.1282	1.8277 $\times10^{-5}$	3.9618	3.7198 $\times10^{-5}$	3.7887	7.5720 $\times10^{-5}$	3.6203	1.4716 $\times10^{-4}$	4.0879	2.1768 $\times10^{-5}$	3.8858	5.0991 $\times10^{-5}$
0.67 GL+ 0.33 EL	3.5194	2.1628 $\times10^{-4}$	3.1880	7.1630 $\times10^{-4}$	3.3889	3.5089 $\times10^{-4}$	3.0684	1.0760 $\times10^{-3}$	3.0618	1.1002 $\times10^{-3}$	2.7621	2.8713 $\times10^{-3}$	3.3058	4.7361 $\times10^{-4}$	3.0194	1.2666 $\times10^{-3}$
0.5 GL+ 0.5 EL	2.6045	4.6001 $\times10^{-3}$	2.3444	9.5290 $\times10^{-3}$	2.4846	6.4851 $\times10^{-3}$	2.2257	1.3018 $\times10^{-2}$	2.1855	1.4426 $\times10^{-2}$	1.9295	2.6835 $\times10^{-2}$	2.4375	7.3953 $\times10^{-3}$	2.1883	1.4324 $\times10^{-2}$
0.28 GL+ 0.72 EL	1.7730	3.8113 $\times10^{-2}$	1.5324	6.2707 $\times10^{-2}$	1.6635	4.8107 $\times10^{-2}$	1.4229	7.7386 $\times10^{-2}$	1.3919	8.1980 $\times10^{-2}$	1.1511	1.2485 $\times10^{-1}$	1.6521	4.9260 $\times10^{-2}$	1.4157	7.8432 $\times10^{-2}$
0.16 GL+ 0.84 EL	1.4119	7.8993 $\times10^{-2}$	1.1756	1.1988 $\times10^{-1}$	1.3070	9.5611 $\times10^{-2}$	1.0704	1.4222 $\times10^{-1}$	1.0474	1.4745 $\times10^{-1}$	8.1007 $\times10^{-1}$	2.0895 $\times10^{-1}$	1.3105	9.5007 $\times10^{-2}$	1.0771	1.4072 $\times10^{-1}$
0.1 GL+ 0.9 EL	1.2494	1.0577 $\times10^{-1}$	1.0145	1.5517 $\times10^{-1}$	1.1466	1.2578 $\times10^{-1}$	9.1138 $\times10^{-1}$	1.8105 $\times10^{-1}$	8.9256 $\times10^{-1}$	1.8605 $\times10^{-1}$	6.5633 $\times10^{-1}$	2.5581 $\times10^{-1}$	1.1567	1.2370 $\times10^{-1}$	9.2421 $\times10^{-1}$	1.7769 $\times10^{-1}$
0.04 GL+ 0.96 EL	1.0971	1.3629 $\times10^{-1}$	8.6341 $\times10^{-1}$	1.9395 $\times10^{-1}$	9.9638 $\times10^{-1}$	1.5953 $\times10^{-1}$	7.6222 $\times10^{-1}$	2.2296 $\times10^{-1}$	7.4762 $\times10^{-1}$	2.2734 $\times10^{-1}$	5.1222 $\times10^{-1}$	3.0425 $\times10^{-1}$	1.0125	1.5565 $\times10^{-1}$	7.8076 $\times10^{-1}$	2.1747 $\times10^{-1}$
0.02 GL+ 0.98 EL	1.0485	1.4721 $\times10^{-1}$	8.1509 $\times10^{-1}$	2.0751 $\times10^{-1}$	9.4840 $\times10^{-1}$	1.7146 $\times10^{-1}$	7.1453 $\times10^{-1}$	2.3745 $\times10^{-1}$	7.0133 $\times10^{-1}$	2.4155 $\times10^{-1}$	4.6615 $\times10^{-1}$	3.2055 $\times10^{-1}$	9.6640 $\times10^{-1}$	1.6692 $\times10^{-1}$	7.3487 $\times10^{-1}$	2.3121 $\times10^{-1}$
Horizontal Periphery																
0.9 GL+ 0.1 EL	5.9468	1.3670 $\times10^{-9}$	5.8004	3.3075 $\times10^{-9}$	5.8121	3.0840 $\times10^{-9}$	5.6567	7.7177 $\times10^{-9}$	5.4707	2.2413 $\times10^{-8}$	5.2920	6.0479 $\times10^{-8}$	6.5226	3.4553 $\times10^{-11}$	6.4040	7.5683 $\times10^{-11}$
0.8 GL+ 0.2 EL	5.2462	7.7640 $\times10^{-8}$	5.0910	1.7813 $\times10^{-7}$	5.1540	1.2752 $\times10^{-7}$	4.9796	3.1855 $\times10^{-7}$	4.8852	5.1666 $\times10^{-7}$	4.6432	1.7153 $\times10^{-6}$	5.2015	9.8837 $\times10^{-8}$	5.0897	1.7932 $\times10^{-7}$
0.67 GL+ 0.33 EL	4.5044	3.3275 $\times10^{-6}$	4.3368	7.2291 $\times10^{-6}$	4.4016	5.3736 $\times10^{-6}$	4.2274	1.1821 $\times10^{-5}$	4.1315	1.8016 $\times10^{-5}$	3.9435	4.0155 $\times10^{-5}$	4.5181	3.1198 $\times10^{-6}$	4.3917	5.6233 $\times10^{-6}$

0.5 GL+ 0.5 EL	3.7473	8.9358 $\times10^{-5}$	3.5891	1.6590 $\times10^{-4}$	3.6475	1.3240 $\times10^{-4}$	3.4865	2.4473 $\times10^{-4}$	3.3952	3.4295 $\times10^{-4}$	3.2273	6.2474 $\times10^{-4}$	3.8156	6.7938 $\times10^{-5}$	3.6823	1.1559 $\times10^{-4}$
0.28 GL+ 0.72 EL	3.0831	1.0243 $\times10^{-3}$	2.9340	1.6732 $\times10^{-3}$	2.9929	1.3818 $\times10^{-3}$	2.8414	2.2461 $\times10^{-3}$	2.7684	2.8163 $\times10^{-3}$	2.6105	4.5208 $\times10^{-3}$	3.1830	7.2889 $\times10^{-4}$	3.0438	1.1681 $\times10^{-3}$
0.16 GL+ 0.84 EL	2.8035	2.5275 $\times10^{-3}$	2.6558	3.9561 $\times10^{-3}$	2.7181	3.2831 $\times10^{-3}$	2.5679	5.1164 $\times10^{-3}$	2.5066	6.0956 $\times10^{-3}$	2.3496	9.3970 $\times10^{-3}$	2.9126	1.7920 $\times10^{-3}$	2.7692	2.8101 $\times10^{-3}$
0.1 GL+ 0.9 EL	2.6795	3.6862 $\times10^{-3}$	2.5319	5.6720 $\times10^{-3}$	2.5964	4.7110 $\times10^{-3}$	2.4462	7.2191 $\times10^{-3}$	2.3908	8.4066 $\times10^{-3}$	2.2336	1.2753 $\times10^{-2}$	2.7920	2.6194 $\times10^{-3}$	2.6461	4.0707 $\times10^{-3}$
0.04 GL+ 0.96 EL	2.5645	5.1664 $\times10^{-3}$	2.4167	7.8318 $\times10^{-3}$	2.4834	6.5059 $\times10^{-3}$	2.3330	9.8246 $\times10^{-3}$	2.2835	1.1201 $\times10^{-2}$	2.1259	1.6756 $\times10^{-2}$	2.6796	3.6860 $\times10^{-3}$	2.5312	5.6830 $\times10^{-3}$
0.02 GL+ 0.98 EL	2.5279	5.7366 $\times10^{-3}$	2.3800	8.6566 $\times10^{-3}$	2.4476	7.1907 $\times10^{-3}$	2.2970	1.0810 $\times10^{-2}$	2.2494	1.2243 $\times10^{-2}$	2.0916	1.8236 $\times10^{-2}$	2.6438	4.0996 $\times10^{-3}$	2.4946	6.3051 $\times10^{-3}$
Leg																
0.9 GL+ 0.1 EL	6.2849	1.6407 $\times10^{-10}$	6.2437	2.1371 $\times10^{-10}$	6.1651	3.5209 $\times10^{-10}$	6.1166	4.7800 $\times10^{-10}$	5.8628	2.2750 $\times10^{-9}$	5.7943	3.4310 $\times10^{-9}$	6.2056	2.7248 $\times10^{-10}$	6.1111	4.9471 $\times10^{-10}$
0.8 GL+ 0.2 EL	5.4801	2.1252 $\times10^{-8}$	5.3579	4.2106 $\times10^{-8}$	5.4093	3.1642 $\times10^{-8}$	5.2748	6.6446 $\times10^{-8}$	5.2046	9.7218 $\times10^{-8}$	5.0286	2.4705 $\times10^{-8}$	5.2421	7.9369 $\times10^{-8}$	5.0915	1.7766 $\times10^{-7}$
0.67 GL+ 0.33 EL	4.7974	8.0352 $\times10^{-7}$	4.6322	1.8087 $\times10^{-6}$	4.7083	1.2488 $\times10^{-6}$	4.5358	2.8691 $\times10^{-6}$	4.4714	3.8854 $\times10^{-6}$	4.2825	9.2383 $\times10^{-6}$	4.5462	2.7312 $\times10^{-6}$	4.3768	6.0213 $\times10^{-6}$
0.5 GL+ 0.5 EL	4.0585	2.4694 $\times10^{-5}$	3.8796	5.2311 $\times10^{-5}$	3.9663	3.6502 $\times10^{-5}$	3.7840	7.7176 $\times10^{-5}$	3.7320	9.4989 $\times10^{-5}$	3.5416	1.9889 $\times10^{-4}$	3.8337	6.3110 $\times10^{-5}$	3.6564	1.2787 $\times10^{-4}$
0.28 GL+ 0.72 EL	3.3779	3.6523 $\times10^{-4}$	3.1906	7.0996 $\times10^{-4}$	3.2916	4.9806 $\times10^{-4}$	3.1011	9.6393 $\times10^{-4}$	3.0765	1.0472 $\times10^{-3}$	2.8776	2.0035 $\times10^{-3}$	3.1916	7.0749 $\times10^{-4}$	3.0037	1.3338 $\times10^{-3}$
0.16 GL+ 0.84 EL	3.0852	1.0170 $\times10^{-3}$	2.8914	1.9177 $\times10^{-3}$	3.0025	1.3387 $\times10^{-3}$	2.8052	2.5140 $\times10^{-3}$	2.7974	2.5762 $\times10^{-3}$	2.5908	4.7877 $\times10^{-3}$	2.9162	1.7717 $\times10^{-3}$	2.7205	3.2592 $\times10^{-3}$

0.1 GL+ 0.9 EL	2.9543	1.5671 $\times10^{-3}$	2.7568	2.9189 $\times10^{-3}$	2.8733	2.0310 $\times10^{-3}$	2.6722	3.7681 $\times10^{-3}$	2.6728	3.7608 $\times10^{-3}$	2.4619	6.9095 $\times10^{-3}$	2.7930	2.6114 $\times10^{-3}$	2.5930	4.7568 $\times10^{-3}$
0.04 GL+ 0.96 EL	2.8320	2.3126 $\times10^{-3}$	2.6306	4.2614 $\times10^{-3}$	2.7528	2.9547 $\times10^{-3}$	2.5475	5.4243 $\times10^{-3}$	2.5568	5.2821 $\times10^{-3}$	2.3413	9.6084 $\times10^{-3}$	2.6779	3.7038 $\times10^{-3}$	2.4736	6.6888 $\times10^{-3}$
0.02 GL+ 0.98 EL	2.7931	2.6104 $\times10^{-3}$	2.5903	4.7945 $\times10^{-3}$	2.7144	3.3202 $\times10^{-3}$	2.5077	6.0758 $\times10^{-3}$	2.5198	5.8704 $\times10^{-3}$	2.3028	1.0646 $\times10^{-2}$	2.6413	4.1298 $\times10^{-3}$	2.4354	7.4385 $\times10^{-3}$

APPENDIX F: Table of result for reliability indices and probability of failure using ISO code with load factor of 1.40, 1.35 and 1.23, and API WSD code under tension, bending and hydrostatic pressure for vertical diagonal, horizontal diagonal, horizontal periphery and leg members

Tension, Bending and Hydrostatic Pressure	ISO (Load factor = 1.40)				ISO (Load factor = 1.35)				ISO (Load factor = 1.23)				API WSD			
	FORM β	FORM P_f	SORM β	SORM P_f	FORM P_f	SORM β	SORM P_f	FORM β	FORM P_f	SORM β	SORM P_f	FORM β	FORM P_f	SORM β	SORM P_f	FORM β
Vertical Diagonal																
0.9 GL+ 0.1 EL	6.9016	2.5706×10^{-12}	6.8629	3.3733×10^{-12}	6.7753	6.2087×10^{-12}	6.7310	8.4266×10^{-12}	6.4553	5.3989×10^{-11}	6.3956	7.9974×10^{-11}	6.2713	1.7902×10^{-10}	6.1692	3.4320×10^{-10}
0.8 GL+ 0.2 EL	5.5846	1.1712×10^{-8}	5.4927	1.9792×10^{-8}	5.5238	1.6591×10^{-8}	5.4241	2.9125×10^{-8}	5.3500	4.3981×10^{-8}	5.2261	8.6538×10^{-8}	5.0898	1.7925×10^{-7}	4.9317	4.0759×10^{-7}
0.67 GL+ 0.33 EL	4.9165	4.4058×10^{-7}	4.7750	8.9859×10^{-7}	4.8330	6.7238×10^{-7}	4.6840	1.4065×10^{-6}	4.6085	2.0278×10^{-6}	4.4407	4.4824×10^{-6}	4.3364	7.2419×10^{-6}	4.1403	1.7341×10^{-5}
0.5 GL+ 0.5 EL	4.1497	1.6647×10^{-5}	3.9732	3.5450×10^{-5}	4.0564	2.4915×10^{-5}	3.8749	5.3325×10^{-5}	3.8170	6.7530×10^{-5}	3.6234	1.4538×10^{-4}	3.5653	1.8170×10^{-4}	3.3427	4.1477×10^{-4}
0.28 GL+ 0.72 EL	3.4040	3.3200×10^{-4}	3.2021	6.8209×10^{-4}	3.3126	4.6217×10^{-4}	3.1062	9.4740×10^{-4}	3.0830	1.0246×10^{-3}	2.8654	2.0823×10^{-3}	2.8617	2.1072×10^{-3}	2.6173	4.4317×10^{-3}
0.16 GL+ 0.84 EL	3.0756	1.0504×10^{-3}	2.8611	2.1111×10^{-3}	2.9865	1.4109×10^{-3}	2.7675	2.8245×10^{-3}	2.7641	2.8538×10^{-3}	2.5337	5.6428×10^{-3}	2.5566	5.2848×10^{-3}	2.3019	1.0672×10^{-2}
0.1 GL+ 0.9 EL	2.9272	1.7100×10^{-3}	2.7065	3.3995×10^{-3}	2.8394	2.2600×10^{-3}	2.6142	4.4720×10^{-3}	2.6206	4.3883×10^{-3}	2.3840	8.5628×10^{-3}	2.4194	7.7725×10^{-3}	2.1598	1.5395×10^{-2}
0.04 GL+ 0.96 EL	2.7879	2.6522×10^{-3}	2.5612	5.2152×10^{-3}	2.7014	3.4526×10^{-3}	2.4701	6.7531×10^{-3}	2.4862	6.4550×10^{-3}	2.2435	1.2432×10^{-3}	2.2910	1.0983×10^{-2}	2.0266	2.1350×10^{-2}

0.02 GL+ 0.98 EL	2.7434	3.0406 $\times10^{-3}$	2.5147	5.9570 $\times10^{-3}$	2.6572	3.9391 $\times10^{-3}$	2.4240	7.6750 $\times10^{-3}$	2.4433	7.2768 $\times10^{-3}$	2.1986	1.3954 $\times10^{-2}$	2.2499	1.2228 $\times10^{-2}$	1.9841	2.3624 $\times10^{-2}$
Horizontal Diagonal																
0.9 GL+ 0.1 EL	6.5212	3.4876 $\times10^{-11}$	6.4640	5.0992 $\times10^{-11}$	6.3695	9.4833 $\times10^{-11}$	6.3051	1.4401 $\times10^{-10}$	5.9831	1.0946 $\times10^{-9}$	5.8980	1.8398 $\times10^{-9}$	6.0769	6.1260 $\times10^{-10}$	5.9477	1.3593 $\times10^{-9}$
0.8 GL+ 0.2 EL	5.0935	1.7578 $\times10^{-7}$	4.9698	3.3511 $\times10^{-7}$	4.9994	2.8751 $\times10^{-7}$	4.8613	5.8306 $\times10^{-7}$	4.7306	1.1195 $\times10^{-6}$	4.5492	2.6922 $\times10^{-6}$	4.6785	1.4446 $\times10^{-6}$	4.5099	3.2436 $\times10^{-6}$
0.67 GL+ 0.33 EL	4.1916	1.3849 $\times10^{-5}$	4.0259	2.8379 $\times10^{-5}$	4.0789	2.2629 $\times10^{-5}$	3.9072	4.6689 $\times10^{-5}$	3.7840	7.7163 $\times10^{-5}$	3.6009	1.5857 $\times10^{-4}$	3.7636	8.3743 $\times10^{-5}$	3.5872	1.6715 $\times10^{-4}$
0.5 GL+ 0.5 EL	3.2439	5.8962 $\times10^{-4}$	3.0662	1.0839 $\times10^{-3}$	3.1298	8.7476 $\times10^{-4}$	2.9499	1.5894 $\times10^{-3}$	2.8412	2.2469 $\times10^{-3}$	2.6568	3.9441 $\times10^{-3}$	2.8490	2.1926 $\times10^{-3}$	2.6673	3.8236 $\times10^{-3}$
0.28 GL+ 0.72 EL	2.3657	8.9990 $\times10^{-3}$	2.1836	1.4494 $\times10^{-2}$	2.2578	1.1978 $\times10^{-2}$	2.0745	1.9016 $\times10^{-2}$	1.9888	2.3360 $\times10^{-2}$	1.8026	3.5725 $\times10^{-2}$	2.0179	2.1802 $\times10^{-2}$	1.8325	3.3437 $\times10^{-2}$
0.16 GL+ 0.84 EL	1.9833	2.3666 $\times10^{-2}$	1.7995	3.5966 $\times10^{-2}$	1.8791	3.0117 $\times10^{-2}$	1.6942	4.5113 $\times10^{-2}$	1.6201	5.2609 $\times10^{-2}$	1.4327	7.5975 $\times10^{-2}$	1.6572	4.8735 $\times10^{-2}$	1.4703	7.0740 $\times10^{-2}$
0.1 GL+ 0.9 EL	1.8110	3.5069 $\times10^{-2}$	1.6265	5.1924 $\times10^{-2}$	1.7085	4.3770 $\times10^{-2}$	1.5230	6.3885 $\times10^{-2}$	1.4543	7.2937 $\times10^{-2}$	1.2663	1.0270 $\times10^{-1}$	1.4949	6.7472 $\times10^{-2}$	1.3072	9.5567 $\times10^{-2}$
0.04 GL+ 0.96 EL	1.6495	4.9526 $\times10^{-2}$	1.4642	7.1567 $\times10^{-2}$	1.5487	6.0729 $\times10^{-2}$	1.3625	8.6526 $\times10^{-2}$	1.2990	9.6969 $\times10^{-2}$	1.1105	1.3339 $\times10^{-1}$	1.3427	8.9678 $\times10^{-2}$	1.1544	1.2417 $\times10^{-1}$
0.02 GL+ 0.98 EL	1.5978	5.5042 $\times10^{-2}$	1.4123	7.8925 $\times10^{-2}$	1.4976	6.7120 $\times10^{-2}$	1.3112	9.4903 $\times10^{-2}$	1.2494	1.0576 $\times10^{-1}$	1.0607	1.4441 $\times10^{-1}$	1.2941	9.7815 $\times10^{-2}$	1.1056	1.3446 $\times10^{-1}$
Horizontal Periphery																
0.9 GL+ 0.1 EL	7.8514	2.0539 $\times10^{-15}$	7.6909	7.2993 $\times10^{-15}$	7.7224	5.7176 $\times10^{-15}$	7.5500	2.1760 $\times10^{-14}$	7.3915	7.2609 $\times10^{-14}$	7.1884	3.2775 $\times10^{-13}$	6.3992	7.8120 $\times10^{-11}$	6.2866	1.6226 $\times10^{-10}$
0.8 GL+ 0.2 EL	5.6755	6.9132 $\times10^{-9}$	5.5842	1.1741 $\times10^{-8}$	5.6227	9.3994 $\times10^{-9}$	5.5253	1.6444 $\times10^{-8}$	5.4746	2.1931 $\times10^{-8}$	5.3601	4.1577 $\times10^{-8}$	5.1449	1.3385 $\times10^{-7}$	5.0298	2.4548 $\times10^{-7}$
0.67 GL+ 0.33 EL	5.1067	1.6395 $\times10^{-7}$	4.9798	3.1819 $\times10^{-7}$	5.0367	2.3675 $\times10^{-7}$	4.9048	4.6753 $\times10^{-7}$	4.8494	6.1911 $\times10^{-7}$	4.7049	1.2702 $\times10^{-6}$	4.4492	4.3092 $\times10^{-6}$	4.3227	7.7072 $\times10^{-6}$

0.5 GL+ 0.5 EL	4.4529	4.2363×10^{-6}	4.3042	8.3795×10^{-6}	4.3733	6.1192×10^{-6}	4.2213	1.2142×10^{-5}	4.1681	1.5361×10^{-5}	4.0083	3.0577×10^{-5}	3.7401	9.1987×10^{-5}	3.6079	1.5435×10^{-4}
0.28 GL+ 0.72 EL	3.8027	7.1575×10^{-5}	3.6445	1.3398×10^{-4}	3.7230	9.8444×10^{-5}	3.5624	1.8371×10^{-4}	3.5223	2.1387×10^{-4}	3.3560	3.9543×10^{-4}	3.1070	9.4512×10^{-4}	2.9688	1.4950×10^{-3}
0.16 GL+ 0.84 EL	3.5140	2.2074×10^{-4}	3.3522	4.0089×10^{-4}	3.4360	2.9518×10^{-4}	3.2720	5.3396×10^{-4}	3.2412	5.9520×10^{-4}	3.0714	1.0652×10^{-3}	2.8374	2.2743×10^{-3}	2.6946	3.5238×10^{-3}
0.1 GL+ 0.9 EL	3.3834	3.5791×10^{-4}	3.2199	6.4115×10^{-4}	3.3065	4.7228×10^{-4}	3.1408	8.4252×10^{-4}	3.1149	9.2013×10^{-4}	2.9433	1.6237×10^{-3}	2.7172	3.2914×10^{-3}	2.5719	5.0571×10^{-3}
0.04 GL+ 0.96 EL	3.2610	5.5511×10^{-4}	3.0957	9.8180×10^{-4}	3.1852	7.2325×10^{-4}	3.0176	1.2738×10^{-3}	2.9968	1.3643×10^{-3}	2.8233	2.3768×10^{-3}	2.6054	4.5884×10^{-3}	2.4574	6.9977×10^{-3}
0.02 GL+ 0.98 EL	3.2218	6.3685×10^{-4}	3.0559	1.1218×10^{-3}	3.1464	8.2638×10^{-4}	2.9782	1.4495×10^{-3}	2.9591	1.5428×10^{-3}	2.7849	2.6770×10^{-3}	2.5698	5.0878×10^{-3}	2.4209	7.7418×10^{-3}
Leg																
0.9 GL+ 0.1 EL	7.3891	7.3941×10^{-14}	7.3497	9.9314×10^{-14}	7.2711	1.7825×10^{-13}	7.2240	2.5227×10^{-13}	6.9720	1.5629×10^{-12}	6.9033	2.5398×10^{-12}	6.2573	1.9579×10^{-10}	6.1622	3.5872×10^{-10}
0.8 GL+ 0.2 EL	5.7237	5.2103×10^{-9}	5.6422	8.3922×10^{-9}	5.6736	6.9897×10^{-9}	5.5865	1.1583×10^{-8}	5.5325	1.5782×10^{-8}	5.4290	2.8334×10^{-8}	5.2301	8.4715×10^{-8}	5.0827	1.8601×10^{-7}
0.67 GL+ 0.33 EL	5.1627	1.2171×10^{-7}	5.0413	2.3114×10^{-7}	5.0943	1.7504×10^{-7}	4.9675	3.3907×10^{-7}	4.9102	4.5496×10^{-7}	4.7698	9.2188×10^{-7}	4.5322	2.9189×10^{-6}	4.3663	6.3190×10^{-6}
0.5 GL+ 0.5 EL	4.5077	3.2772×10^{-6}	4.3590	6.5335×10^{-6}	4.4286	4.7431×10^{-6}	4.2763	9.5014×10^{-6}	4.2244	1.1978×10^{-5}	4.0636	2.4161×10^{-5}	3.8175	6.7401×10^{-5}	3.6429	1.3481×10^{-4}
0.28 GL+ 0.72 EL	3.8497	5.9122×10^{-5}	3.6857	1.1403×10^{-4}	3.7701	8.1576×10^{-5}	3.6033	1.5710×10^{-4}	3.5698	1.7861×10^{-4}	3.3959	3.4206×10^{-4}	3.1737	7.5247×10^{-4}	2.9877	1.4055×10^{-3}
0.16 GL+ 0.84 EL	3.5564	1.8797×10^{-4}	3.3855	3.5521×10^{-4}	3.4784	2.5219×10^{-4}	3.3047	4.7539×10^{-4}	3.2835	5.1256×10^{-4}	3.1025	9.5958×10^{-4}	2.8978	1.8787×10^{-3}	2.7037	3.4284×10^{-3}
0.1 GL+ 0.9 EL	3.4235	3.0905×10^{-4}	3.2492	5.7859×10^{-4}	3.3465	4.0915×10^{-4}	3.1693	7.6398×10^{-4}	3.1546	8.0351×10^{-4}	2.9698	1.4898×10^{-3}	2.7744	2.7648×10^{-3}	2.5759	4.9983×10^{-3}
0.04 GL+ 0.96 EL	3.2987	4.8566×10^{-4}	3.1209	9.0141×10^{-4}	3.2227	6.3487×10^{-4}	3.0420	1.1751×10^{-3}	3.0339	1.2071×10^{-3}	2.8453	2.2186×10^{-3}	2.6593	3.9151×10^{-3}	2.4562	7.0204×10^{-3}

0.02 GL+ 0.98 EL	3.2587	5.5953 $\times 10^{-4}$	3.0798	1.0357 $\times 10^{-3}$	3.1831	7.2845 $\times 10^{-4}$	3.0012	1.3447 $\times 10^{-3}$	2.9953	1.3708 $\times 10^{-3}$	2.8054	2.5126 $\times 10^{-3}$	2.6226	4.3631 $\times 10^{-3}$	2.4179	7.8042 $\times 10^{-3}$

APPENDIX G: Table of result for reliability indices and probability of failure using ISO code with load factor of 1.40, 1.35 and 1.23, and API WSD code under compression, bending and hydrostatic pressure for vertical diagonal, horizontal diagonal, horizontal periphery and leg members

Compression, Bending and Hydrostatic Pressure	ISO (Load factor = 1.40)				ISO (Load factor = 1.35)				ISO (Load factor = 1.23)				API WSD			
	FORM β	FORM P_f	SORM β	SORM P_f	FORM P_f	SORM β	SORM P_f	FORM β	FORM P_f	SORM β	SORM P_f	FORM β	FORM P_f	SORM β	SORM P_f	FORM β
Vertical Diagonal																
0.9 GL+ 0.1 EL	8.2976	5.5511×10^{-17}	8.2929	8.0298×10^{-17}	8.1731	1.1102×10^{-16}	8.1264	2.0507×10^{-16}	7.8562	1.9984×10^{-15}	7.7890	3.4076×10^{-15}	7.8309	2.4425×10^{-15}	7.6870	7.4998×10^{-15}
0.8 GL+ 0.2 EL	5.8221	2.9062×10^{-9}	5.7592	4.2260×10^{-9}	5.7793	3.7501×10^{-9}	5.7124	5.5696×10^{-9}	5.6594	7.5955×10^{-9}	5.5808	1.1969×10^{-8}	5.5105	1.7892×10^{-8}	5.4208	2.9664×10^{-8}
0.67 GL+ 0.33 EL	5.2915	6.0647×10^{-8}	5.1901	1.0510×10^{-7}	5.2295	8.5000×10^{-8}	5.1229	1.5042×10^{-7}	5.0614	2.0813×10^{-7}	4.9413	3.8799×10^{-7}	4.8927	4.9737×10^{-7}	4.7573	9.8115×10^{-7}
0.5 GL+ 0.5 EL	4.6427	1.7192×10^{-6}	4.5020	3.3656×10^{-6}	4.5658	2.4875×10^{-6}	4.4203	4.9290×10^{-6}	4.3652	6.3493×10^{-6}	4.2075	1.2913×10^{-5}	4.2052	1.3044×10^{-5}	4.0268	2.8271×10^{-5}
0.28 GL+ 0.72 EL	3.9493	3.9193×10^{-5}	3.7756	7.9798×10^{-5}	3.8671	5.5078×10^{-5}	3.6890	1.1256×10^{-4}	3.6582	1.2698×10^{-4}	3.4691	2.6111×10^{-4}	3.5237	2.1277×10^{-4}	3.3117	4.6368×10^{-4}
0.16 GL+ 0.84 EL	3.6291	1.4220×10^{-4}	3.4410	2.8978×10^{-4}	3.5467	1.9503×10^{-4}	3.3543	3.9788×10^{-4}	3.3392	4.2011×10^{-4}	3.1358	8.5707×10^{-4}	3.2179	6.4563×10^{-4}	2.9922	1.3849×10^{-3}
0.1 GL+ 0.9 EL	3.4820	2.4880×10^{-4}	3.2872	5.0589×10^{-4}	3.3999	3.3703×10^{-4}	3.2008	6.8533×10^{-4}	3.1937	7.0221×10^{-4}	2.9836	1.4245×10^{-3}	3.0786	1.0398×10^{-3}	2.8468	2.2078×10^{-3}
0.04 GL+ 0.96 EL	3.3428	4.1475×10^{-4}	3.1415	8.4043×10^{-4}	3.2611	5.5497×10^{-4}	3.0554	1.1236×10^{-3}	3.0565	1.1197×10^{-3}	2.8399	2.2565×10^{-3}	2.9472	1.6032×10^{-3}	2.7098	3.3663×10^{-3}

0.02 GL+ 0.98 EL	3.2980	4.8696×10^{-4}	3.0946	9.8540×10^{-4}	3.2164	6.4899×10^{-4}	3.0087	1.3118×10^{-3}	3.0125	1.2957×10^{-3}	2.7937	2.6051×10^{-3}	2.9051	1.8359×10^{-3}	2.6658	3.8400×10^{-3}
Horizontal Diagonal																
0.9 GL+ 0.1 EL	6.6135	1.8772×10^{-11}	6.5575	2.7363×10^{-11}	6.4802	4.5790×10^{-11}	6.4188	6.8689×10^{-11}	6.1434	4.0380×10^{-10}	6.0667	6.5287×10^{-10}	6.4906	4.2755×10^{-11}	6.3858	8.5235×10^{-11}
0.8 GL+ 0.2 EL	5.3299	4.9145×10^{-8}	5.2120	9.3393×10^{-8}	5.2547	7.4118×10^{-8}	5.1238	1.4969×10^{-7}	5.0405	2.3220×10^{-7}	4.8658	5.6990×10^{-7}	5.1056	1.6487×10^{-7}	4.9606	3.5143×10^{-7}
0.67 GL+ 0.33 EL	4.5225	3.0559×10^{-6}	4.3358	7.2599×10^{-6}	4.4239	4.8473×10^{-6}	4.2270	1.1839×10^{-5}	4.1625	1.5736×10^{-5}	3.9434	4.0169×10^{-5}	4.2852	9.1293×10^{-6}	4.0928	2.1311×10^{-5}
0.5 GL+ 0.5 EL	3.6305	1.4146×10^{-4}	3.4173	3.1625×10^{-4}	3.5252	2.1162×10^{-4}	3.3084	4.6916×10^{-4}	3.2572	5.6263×10^{-4}	3.0333	1.2094×10^{-3}	3.4241	3.0842×10^{-4}	3.2144	6.5353×10^{-4}
0.28 GL+ 0.72 EL	2.7758	2.7533×10^{-3}	2.5587	5.2538×10^{-3}	2.6736	3.7520×10^{-3}	2.4548	7.0475×10^{-3}	2.4178	7.8077×10^{-3}	2.1955	1.4063×10^{-2}	2.6123	4.4969×10^{-3}	2.3979	8.2442×10^{-3}
0.16 GL+ 0.84 EL	2.3987	8.2266×10^{-3}	2.1808	1.4598×10^{-2}	2.2990	1.0751×10^{-2}	2.0799	1.8768×10^{-2}	2.0507	2.0148×10^{-2}	1.8288	3.3718×10^{-2}	2.2547	1.2075×10^{-2}	2.0390	2.0723×10^{-2}
0.1 GL+ 0.9 EL	2.2279	1.2945×10^{-2}	2.0097	2.2231×10^{-2}	2.1295	1.6606×10^{-2}	1.9102	2.8053×10^{-2}	1.8849	2.9722×10^{-2}	1.6630	4.8153×10^{-2}	2.0927	1.8187×10^{-2}	1.8766	3.0290×10^{-2}
0.04 GL+ 0.96 EL	2.0672	1.9358×10^{-2}	1.8488	3.2242×10^{-2}	1.9702	2.4410×10^{-2}	1.7507	3.9996×10^{-2}	1.7292	4.1888×10^{-2}	1.5074	6.5856×10^{-2}	1.9403	2.6170×10^{-2}	1.7237	4.2379×10^{-2}
0.02 GL+ 0.98 EL	2.0157	2.1915×10^{-2}	1.7973	3.6147×10^{-2}	1.9191	2.7485×10^{-2}	1.6996	4.4599×10^{-2}	1.6793	4.6542×10^{-2}	1.4576	7.2481×10^{-2}	1.8915	2.9280×10^{-2}	1.6748	4.6991×10^{-2}
Horizontal Periphery																
0.9 GL+ 0.1 EL	7.6487	1.0159×10^{-14}	7.4921	3.3896×10^{-14}	7.5101	2.9532×10^{-14}	7.3403	1.0658×10^{-13}	7.1562	4.1483×10^{-13}	6.9540	1.7750×10^{-12}	7.0670	7.9137×10^{-13}	6.9346	2.0370×10^{-12}
0.8 GL+ 0.2 EL	5.6083	1.0219×10^{-8}	5.5081	1.8135×10^{-8}	5.5505	1.4243×10^{-8}	5.4435	2.6125×10^{-8}	5.3880	3.5618×10^{-8}	5.2616	7.1394×10^{-8}	5.2855	6.2669×10^{-8}	5.1955	1.0207×10^{-7}
0.67 GL+ 0.33 EL	5.0088	2.7384×10^{-7}	4.8743	5.4601×10^{-7}	4.9338	4.0313×10^{-7}	4.7941	8.1713×10^{-7}	4.7334	1.1037×10^{-6}	4.5808	2.3159×10^{-6}	4.6252	1.8714×10^{-6}	4.5190	3.1063×10^{-6}

0.5 GL+ 0.5 EL	4.3309	7.4262 $\times10^{-6}$	4.1782	1.4691 $\times10^{-5}$	4.2475	1.0806 $\times10^{-5}$	4.0918	2.1405 $\times10^{-5}$	4.0334	2.7487 $\times10^{-5}$	3.8702	5.4364 $\times10^{-5}$	3.9338	4.1808 $\times10^{-5}$	3.8189	6.7030 $\times10^{-5}$
0.28 GL+ 0.72 EL	3.6713	1.2066 $\times10^{-4}$	3.5124	2.2204 $\times10^{-4}$	3.5895	1.6566 $\times10^{-4}$	3.4284	3.0362 $\times10^{-4}$	3.3840	3.5719 $\times10^{-4}$	3.2172	6.4716 $\times10^{-4}$	3.2999	4.8353 $\times10^{-4}$	3.1785	7.4029 $\times10^{-4}$
0.16 GL+ 0.84 EL	3.3818	3.6009 $\times10^{-4}$	3.2203	6.4029 $\times10^{-4}$	3.3023	4.7952 $\times10^{-4}$	3.1386	8.4872 $\times10^{-4}$	3.1040	9.5475 $\times10^{-4}$	2.9347	1.6696 $\times10^{-3}$	3.0273	1.2339 $\times10^{-3}$	2.9016	1.8560 $\times10^{-3}$
0.1 GL+ 0.9 EL	3.2515	5.7409 $\times10^{-4}$	3.0886	1.0055 $\times10^{-3}$	3.1732	7.5377 $\times10^{-4}$	3.0082	1.3141 $\times10^{-3}$	2.9786	1.4477 $\times10^{-3}$	2.8078	2.4939 $\times10^{-3}$	2.9053	1.8345 $\times10^{-3}$	2.7774	2.7394 $\times10^{-3}$
0.04 GL+ 0.96 EL	3.1295	8.7561 $\times10^{-4}$	2.9652	1.5126 $\times10^{-3}$	3.0526	1.1345 $\times10^{-3}$	2.8860	1.9507 $\times10^{-3}$	2.8617	2.1070 $\times10^{-3}$	2.6892	3.5808 $\times10^{-3}$	2.7915	2.6231 $\times10^{-3}$	2.6613	3.8915 $\times10^{-3}$
0.02 GL+ 0.98 EL	3.0905	9.9902 $\times10^{-4}$	2.9257	1.7184 $\times10^{-3}$	3.0141	1.2889 $\times10^{-3}$	2.8470	2.2067 $\times10^{-3}$	2.8244	2.3684 $\times10^{-3}$	2.6514	4.0082 $\times10^{-3}$	2.7553	2.9323 $\times10^{-3}$	2.6243	4.3416 $\times10^{-3}$
Leg																
0.9 GL+ 0.1 EL	8.1132	2.2204 $\times10^{-16}$	8.0770	3.2778 $\times10^{-16}$	7.9950	6.6613 $\times10^{-16}$	7.9419	9.8977 $\times10^{-16}$	7.6940	7.1054 $\times10^{-15}$	7.6195	1.2711 $\times10^{-14}$	8.0836	3.3307 $\times10^{-16}$	7.9730	7.6392 $\times10^{-16}$
0.8 GL+ 0.2 EL	5.8254	2.8491 $\times10^{-9}$	5.7568	4.2859 $\times10^{-9}$	5.7827	3.6760 $\times10^{-9}$	5.7099	5.6536 $\times10^{-9}$	5.6632	7.4274 $\times10^{-9}$	5.5783	1.2143 $\times10^{-8}$	5.6831	6.6128 $\times10^{-9}$	5.6011	1.0648 $\times10^{-8}$
0.67 GL+ 0.33 EL	5.3220	5.1326 $\times10^{-8}$	5.2172	9.0805 $\times10^{-8}$	5.2624	7.1086 $\times10^{-8}$	5.1531	1.2808 $\times10^{-7}$	5.1019	1.6810 $\times10^{-7}$	4.9810	3.1625 $\times10^{-7}$	5.1468	1.3251 $\times10^{-7}$	5.0330	2.4143 $\times10^{-7}$
0.5 GL+ 0.5 EL	4.7206	1.1756 $\times10^{-6}$	4.5866	2.2525 $\times10^{-6}$	4.6489	1.6683 $\times10^{-6}$	4.5114	3.2197 $\times10^{-6}$	4.4626	4.0487 $\times10^{-6}$	4.3166	7.9218 $\times10^{-6}$	4.5370	2.8530 $\times10^{-6}$	4.4002	5.4086 $\times10^{-6}$
0.28 GL+ 0.72 EL	4.0909	2.1486 $\times10^{-5}$	3.9383	4.1025 $\times10^{-5}$	4.0157	2.9633 $\times10^{-5}$	3.8604	5.6590 $\times10^{-5}$	3.8254	6.5272 $\times10^{-5}$	3.6634	1.2447 $\times10^{-4}$	3.9232	4.3695 $\times10^{-5}$	3.7701	8.1594 $\times10^{-5}$
0.16 GL+ 0.84 EL	3.8034	7.1374 $\times10^{-5}$	3.6434	1.3454 $\times10^{-4}$	3.7286	9.6257 $\times10^{-5}$	3.5660	1.8122 $\times10^{-4}$	3.5411	1.9925 $\times10^{-4}$	3.3717	3.7353 $\times10^{-4}$	3.6470	1.3266 $\times10^{-4}$	3.4865	2.4465 $\times10^{-4}$
0.1 GL+ 0.9 EL	3.6720	1.2034 $\times10^{-4}$	3.5085	2.2530 $\times10^{-4}$	3.5978	1.6047 $\times10^{-4}$	3.4317	2.9994 $\times10^{-4}$	3.4121	3.2230 $\times10^{-4}$	3.2392	5.9942 $\times10^{-4}$	3.5213	2.1474 $\times10^{-4}$	3.3573	3.9359 $\times10^{-4}$
0.04 GL+ 0.96 EL	3.5479	1.9413 $\times10^{-4}$	3.3811	3.6099 $\times10^{-4}$	3.4744	2.5600 $\times10^{-4}$	3.3048	4.7515 $\times10^{-4}$	3.2909	4.9938 $\times10^{-4}$	3.1143	9.2186 $\times10^{-4}$	3.4028	3.3348 $\times10^{-4}$	3.2353	6.0765 $\times10^{-4}$

0.02 GL+ 0.98 EL	3.5081	2.2564 $\times10^{-4}$	3.3402	4.1866 $\times10^{-4}$	3.4348	2.9647 $\times10^{-4}$	3.2641	5.4901 $\times10^{-4}$	3.2520	5.7289 $\times10^{-4}$	3.0743	1.0550 $\times10^{-3}$	3.3648	3.8296 $\times10^{-4}$	3.1961	6.9651 $\times10^{-4}$

APPENDIX H: gfun file for axial tension for vertical diagonal member

```
function g = gfun_t(Fy,D,T,Hs,Vc,Xw,Dd,Lv,Xm)
%% This function defines the Limit State Function of Simple Tensile
Strength
%  as per ISO / API RP2A WSD (21st (2008) Ed
%%%%%%%%%%%%%%%%%%%%%%%%%%%%%%%%%%%%%%%%%%%%%%%%%%%%%%%%%
%%%  DATA FIELDS IN 'ENVIRONMENTAL LOAD'            %%%
%%%%%%%%%%%%%%%%%%%%%%%%%%%%%%%%%%%%%%%%%%%%%%%%%%%%%%%%%
% Environmental Loads - Surface Response Method used to obtain the
following
% Given as the Output load from SACS on a Particular member!
%%
%%%%%%%%%%%%%%%%%%%%%%%%%%%%%%%%%%%%%%%%%%%%%%%%%%%%%%%%%%%%%%%%%%
%%% DATA FIELDS IN 'REPRESENTATIVE TENSILE STRENGHT' %%%
%%%%%%%%%%%%%%%%%%%%%%%%%%%%%%%%%%%%%%%%%%%%%%%%%%%%%%%%%%%%%%%%%%
A =(pi()./4).*(D.^2 - (D-2.*T).^2);
Resistance =Fy.*A.*Xm;
%%
%%%%%%%%%%%%%%%%%%%%%%%%%%%%%%%%%%%%%%%%%%%%%%%%%%%%%%%%%%%%%%%%%%
%%%DATA FIELDS IN 'NOMINAL STRENGHT FOR SIMPLE JOINT for UC=1'%%%
%%%%%%%%%%%%%%%%%%%%%%%%%%%%%%%%%%%%%%%%%%%%%%%%%%%%%%%%%%%%%%%%%%
%This functions is intented to evaluate the nominal resistance of
typical
%joint using it's nominal geometrical and material properties
% No factor is included.
Fyn = 345;
Dn = 711;
Tn = 15.0;
An = (pi()/4)*(Dn^2-(Dn-2*Tn)^2);
ResISO = Fyn.*An;  %ISO
ResWSD =(0.6.*Fyn).*An;


%%
%%%%%%%%%%%%%%%%%%%%%%%%%%%%%%%%%%%%%%%%%%%%%%%%%%%%%%%%%%%%
%%%  DATA FIELDS IN 'LOAD ACTIONS'                      %%%
%%%%%%%%%%%%%%%%%%%%%%%%%%%%%%%%%%%%%%%%%%%%%%%%%%%%%%%%%%%%
% Environmnetal Load Action Eveluation
Hmx = 2.00.*Hs;
Wn =0.03344.*Hmx.^2-0.5468.*Hmx+0.7487.*Vc.^2-1.295.*Vc+3.976;

% Applied loads on the Joints[Through the BRACE]
%  Lr =(0.45.*Dd+0.45.*Lv+0.09.*Wn./Xw);
% Lr =(0.40.*Dd+0.40.*Lv+0.20.*Wn./Xw);
% Lr =(0.33.*Dd+0.33.*Lv+0.33.*Wn./Xw);
Lr =(0.25.*Dd+0.25.*Lv+0.50.*Wn./Xw);
% Lr =(0.14.*Dd+0.14.*Lv+0.72.*Wn./Xw);
% Lr =(0.08.*Dd+0.08.*Lv+0.84.*Wn./Xw);
% Lr =(0.05.*Dd+0.05.*Lv+0.90.*Wn./Xw);
% Lr =(0.02.*Dd+0.02.*Lv+0.96.*Wn./Xw);
%  Lr =(0.01.*Dd+0.01.*Lv+0.98.*Wn./Xw);
```

```
%  FS =4/(3*1.67); % not used
% FS =1.333; %Used
% Load =Lr.*ResWSD.*FS; %Axial Load [WSD]

 FS =(0.9524.*(Dd+Lv+Wn./Xw))./(1.1.*Dd+1.1.*Lv+1.40.*Wn./Xw);
 Load =Lr.*ResISO.*FS; %Axial Load [ISO]

%%
%%%%%%%%%%%%%%%%%%%%%%%%%%%%%%%%%%%%%%%%%%%%%%%%%%%%%%%%%%
%%%  DATA FIELDS IN 'lIMIT STATE FUCTION'(gfun)        %%%
%%%%%%%%%%%%%%%%%%%%%%%%%%%%%%%%%%%%%%%%%%%%%%%%%%%%%%%%%%
%Limit State Function
 g =Resistance -Load;
```

APPENDIX I: inputfile for axial tension for vertical diagonal member

```
%%%%%%%%%%%%%%%%%%%%%%%%%%%%%%%%%
%%  DATA FIELDS IN 'PROBDATA'  %%
%%%%%%%%%%%%%%%%%%%%%%%%%%%%%%%%%
% Names of random variables. Default names are 'x1', 'x2', ..., if
not explicitely defined.
% probdata.name =  { 'name1' 'name2' ... } or { 'name1'
'name2' ... }'
%>>> Tubular Joint Input Variables <<<<
probdata.name =  { 'Fy'
                   'D'
                   'T'
                   'Hs'
                   'Vc'
                   'Xw'
                   'Dd'
                   'Lv'
                   'Xm'};

% Marginal distributions for each random variable
% probdata.marg =  [ (type) (mean) (stdv) (startpoint) (p1) (p2) (p3)
(p4) (input_type); ... ];
probdata.marg =  [  1   424.350  17.250   345.000    nan    nan
nan   nan 0 ;
                    1   711.000   1.280   711.000    nan    nan
nan   nan 0 ;
                    1    15.360   0.240    15.000    nan    nan
nan   nan 0 ;
                   16     4.220   0.570     4.220    nan    nan
nan   nan 0 ;
                   16     0.790   0.150     0.790    nan    nan
nan   nan 0 ;
                    1     1.000   0.150     1.000    nan    nan
nan   nan 0 ;
                    1     1.000   0.060     1.000    nan    nan
nan   nan 0 ;
                    1     1.000   0.100     1.000    nan    nan
nan   nan 0 ;
                    1     1.260   0.050     1.260    nan    nan
nan   nan 0 ;];

% Correlation matrix
probdata.correlation = eye(9); %Non-Correlated variables, function
eye(n) displays the identitiy matrix
probdata.transf_type = 3;%Natal Joint Distribution - Transformation
matrix
probdata.Ro_method   = 1;%Method for computation of Nataf Corr
Matrix - Solved numerically
```

```
probdata.flag_sens   = 1;%Computation of sensitivities w.r.t - all
sensitivities assessed

%%%%%%%%%%%%%%%%%%%%%%%%%%%%%%%%%%%%
%%  DATA FIELDS IN 'ANALYSISOPT'  %%
%%%%%%%%%%%%%%%%%%%%%%%%%%%%%%%%%%%%
analysisopt.multi_proc           = 1;        % 1: block_size g-calls
sent simultaneously
                                             %    - gfunbasic.m is
used and a vectorized version of gfundata.expression is available.
                                             %      The number of g-
calls sent simultaneously (block_size) depends on the memory
                                             %      available on the
computer running FERUM.
                                             %    - gfunxxx.m user-
specific g-function is used and able to handle block_size
computations
                                             %      sent
simultaneously, on a cluster of PCs or any other multiprocessor
computer platform.
                                             % 0: g-calls sent
sequentially
analysisopt.block_size           = 100;     % Number of g-calls to
be sent simultaneously

% FORM analysis options
analysisopt.i_max                = 1000;     % Maximum number of
iterations allowed in the search algorithm
analysisopt.e1                   = 1e-5;    % Tolerance on how close
design point is to limit-state surface
analysisopt.e2                   = 1e-5;    % Tolerance on how
accurately the gradient points towards the origin
analysisopt.step_code            = 0;        % 0: step size by
Armijo rule, otherwise: given value is the step size
analysisopt.Recorded_u           = 1;        % 0: u-vector not
recorded at all iterations, 1: u-vector recorded at all iterations
analysisopt.Recorded_x           = 1;        % 0: x-vector not
recorded at all iterations, 1: x-vector recorded at all iterations

% FORM, SORM analysis options
analysisopt.grad_flag            = 'ffd';    % 'ddm': direct
differentiation, 'ffd': forward finite difference
analysisopt.ffdpara              = 1000;     % Parameter for
computation of FFD estimates of gradients - Perturbation =
stdv/analysisopt.ffdpara;
                                             % Recommended values:
1000 for basic limit-state functions, 50 for FE-based limit-state
functions
analysisopt.ffdpara_thetag       = 1000;     % Parameter for
computation of FFD estimates of dbeta_dthetag
```

```
                                                % perturbation =
thetag/analysisopt.ffdpara_thetag if thetag ~= 0 or
1/analysisopt.ffdpara_thetag if thetag == 0;
                                                % Recommended values:
1000 for basic limit-state functions, 100 for FE-based limit-state
functions

% Simulation analysis (MC,IS,DS,SS) and distribution analysis
options
analysisopt.num_sim              = 100000;   % Number of samples
(MC,IS), number of samples per subset step (SS) or number of
directions (DS)
analysisopt.rand_generator       = 1;        % 0: default rand
matlab function, 1: Mersenne Twister (to be preferred)

% Simulation analysis (MC, IS) and distribution analysis options
analysisopt.sim_point            = 'origin'; % 'dspt': design point,
'origin': origin in standard normal space (simulation analysis)
analysisopt.stdv_sim             = 1;        % Standard deviation of
sampling distribution in simulation analysis

% Simulation analysis (MC, IS)
analysisopt.target_cov           = 0.05;     % Target coefficient of
variation for failure probability
analysisopt.lowRAM               = 0;        % 1: memory savings
allowed, 0: no memory savings allowed

%%%%%%%%%%%%%%%%%%%%%%%%%%%%%%%%%%%%%%%%%%%%%%%%%%%%%%%%%%
%%  DATA FIELDS IN 'GFUNDATA' (one structure per gfun)  %%
%%%%%%%%%%%%%%%%%%%%%%%%%%%%%%%%%%%%%%%%%%%%%%%%%%%%%%%%%%
% Type of limit-state function evaluator:
% 'basic': the limit-state function is defined by means of an
analytical expression or a Matlab m-function,
%          using gfundata(lsf).expression. The function gfun.m calls
gfunbasic.m, which evaluates gfundata(lsf).expression.
% 'xxx':   the limit-state function evaluation requires a call to an
external code.  The function gfun.m calls gfunxxx.m,
%          which evaluates gfundata(lsf).expression where gext
variable is a result of the external code.
gfundata(1).evaluator  = 'basic';
gfundata(1).type       = 'expression';   % Do no change this field!

% Expression of the limit-state function:
gfundata(1).expression = 'gfun_t(Fy,D,T,Hs,Vc,Xw,Dd,Lv,Xm)';

% Flag for computation of sensitivities w.r.t. thetag parameters of
the limit-state function
% 1: all sensitivities assessed, 0: no sensitivities assessment
gfundata(1).flag_sens  = 0;

%%%%%%%%%%%%%%%%%%%%%%%%%%%%%%%%
```

```
%%  DATA FIELDS IN 'FEMODEL'  %%
%%%%%%%%%%%%%%%%%%%%%%%%%%%%%%%%
femodel = [];

%%%%%%%%%%%%%%%%%%%%%%%%%%%%%%%%%%%%
%%  DATA FIELDS IN 'RANDOMFIELD'  %%
%%%%%%%%%%%%%%%%%%%%%%%%%%%%%%%%%%%%
randomfield = [];
```

APPENDIX J: Finite Element Reliability Using Matlab (FERUM)